Wheat pre-breeding towards disease resistance of fungal pathogens

by

Michaela-Anne White

Thesis presented in partial fulfilment of the requirements for the degree of
Master of Science in Agriculture

at

Stellenbosch University
Department of Genetics, Faculty of AgriSciences

The financial assistance of the National Research Foundation (NRF) towards this research is hereby acknowledged. Opinions expressed and conclusions arrived at are those of the author and are not necessarily to be attributed to the NRF.

Supervisor: Willem Botes
Co-supervisor: Dr Lindy J. Rose

March 2023

Declaration

By submitting this thesis electronically, I declare that the entirety of the work contained therein is my own, original work, that I am the sole author thereof (save to the extent explicitly otherwise stated), that reproduction and publication thereof by Stellenbosch University will not infringe any third-party rights and that I have not previously in its entirety or in part submitted it for obtaining any qualification.

Date: March 2023

Abstract

Bread wheat is an important grain crop cultivated globally, serving as the main source of calories and protein to approximately 4 billion individuals. To sustain increasing consumer demands, the production of wheat is required to increase with 60% by 2050. Wheat production is often threatened by the occurrence of both abiotic and biotic stressors, resulting in reduced yields. The most economically important biotic stressors constraining the production of wheat are fungal diseases. Management strategies have been developed to control disease outbreaks. The integration of disease resistance is highly favoured as it is cost-effective, environmentally friendly and reduces the risk of disease outbreaks.

The aim of the study was to identify crossing parents to introduce into the male-sterility mediated marker-assisted recurrent selection pre-breeding programme. The SU-PBL's 2020 wheat nursery and Fusarium head blight CIMMYT nursery used as male crossing parents, were genotypically and phenotypically assessed for powdery mildew resistance (*Pm37*, *Pm4b*, *MLAG12*, *MLUM15*) and Fusarium head blight resistance (Q*fhs.ifa.5A*, *7AQTL*, *Qfhs.ndsu.3BS*), respectively.

Two superior genotypes with FHB resistance were identified from the FHB CIMMYT nursery. The two wheat lines displayed low disease severity, low DON content and minimal FDK. Five superior wheat lines with powdery mildew resistance were identified from the SU-PBL's 2020 wheat nursery. These superior wheat lines displayed promising genotypic and phenotypic expressions for introduction into the MS-MARS pre-breeding scheme.

Future studies should include additional molecular and phenotypic characterisation of the nurseries. It should also include active powdery mildew resistance breeding. Due to the expected change in climatic conditions worldwide, an increased risk of powdery mildew outbreaks is expected for South Africa. Extensive breeding for powdery mildew disease resistance through the deployment of several viable genes would reduce this threat.

Opsomming

Koring is ’n baie belangrike graangewas wat wêreldwyd gekweek word, en dien as die primêre bron van kalorieë en proteïene vir ongeveer 4 miljard individue. Om aan die toenemende aantal verbruikers se aanvraag te voldoen word daar vereis dat koringproduksie toeneem met ongeveer 60% teen die jaar 2050. Die produksie van koring word dikwels bedreig deur die teenwoordigheid van beide biotiese en abiotiese stressors wat gevolglik lei tot verlaagde opbrengs. Die mees belangrike ekonomiese biotiese stressors wat koringproduksie beperk, is swamsiektes. Beheerstrategieë moet in plek gestel word om die uitbraak van siektes te beperk. Die integrasie van weerstand teen siektes is dus belangrik omdat dit koste-effektief en omgewingsvriendelik is, asook die risiko van die uitbraak van siektes verminder.

Die doelwit van hierdie studie was om kruisings-ouers te identifiseer en tot die manlik steriliteit merkerbemiddelde herhalende seleksie (MS-MBHS) voortelings program toe te voeg. Die Universiteit van Stellenbosch se planteteelt laboratorium (US-PL) se 2020 koring en CIMMYT se aarskroeisiekte kwekerye, is as manlike kruisings-ouers gebruik en is genotipies en fenotipies apart vir witroesweerstand (*Pm37*, *Pm4b*, *MLAG12*, *MLUM15*) en aarskroeiweerstand (*Qfhs.ifa.5A*, *7AQTL*, *Qfhs.ndsu.3BS*) getoets.

Twee hoofgenotipes met aarskroeiweerstand is geïdentifiseer uit die CIMMYT aarskroeisiekteweerstand kwekery. Die twee koringlyne het lae infeksievlakke, lae DON-inhoud en minimale FDK getoon. Vyf hoofkoringlyne met witroesweerstand is geïndentifiseer uit die US-PL se 2020 kwekery. Dié koringlyne het belowende genotipiese en fenotipiese uitdrukking getoon vir toevoeging tot die MS-MBHS voortelingskema.

Toekomstige navorsing moet daarop fokus om addisionele molekulêre en fenotipiese karakterisering van die kwekery in te sluit, asook aktiewe witroesweerstandsteling. As gevolg van die verwagde wêreldwye verandering in klimaatstoestande, word ’n verhoogde risiko vir witroesuitbraak vir Suid-Afrika voorspel. Uitgebreide witroessiekteweerstandsteling deur die vrystelling van weerstandsgene, sal hierdie bedreiging verminder.

Acknowledgements

I would like to acknowledge and give my sincere gratitude to:

- The Almighty, for granting me the strength and discipline to complete my master's degree.
- My supervisor Willem Botes and co-supervisor Dr Lindy Rose for their guidance and continuous support.
- The SU-PBL staff and students for their support and friendship.
- The NRF and SANSOR for their financial support towards the completion of my research project.
- My parents and sister for their unconditional love and support.

List of abbreviations

%	Percentage
°C	Degrees Celsius
µl	Microlitre
µm	Micrometre
15-ADON	15- acetyldeoxynivalenol
3-DON	3-acetyldeoxynivalenol
4-ANIV	4-acetylnivalenol
$AgNO_3$	Silver nitrate
ANOVA	Analysis of variance
APR	Adult plant resistance
ARC-SG	Agricultural Research Council – Small Grains
ASR	All-stage resistance
Avr	Avirulence gene
BAC	Bacterial artificial chromosome
Bgt	*Blumeria graminis* f. sp. *tritici*
bp	Base pairs
Btr	Brittle rachis gene
CAF	Central Analytical Facility
CIMMYT	The International Maize and Wheat Improvement Centre
cm	Centimetre
cM	Centimorgan
CNL	Coiled coil-nucleotide binding-leucine rich repeat
CTAB	Cetyl trimethylammonium bromide
CV	Coefficient of variation
df	Degrees of freedom
DH	Double haploid
DMI	Demethylation inhibitors

DNA	Deoxyribonucleic Acid
DON	Deoxynivalenol
DON-3-Glc	Deoxynivalenol-3-glucoside
dpi	Days post inoculation
f. sp.	*Formae speciales*
FAO	Food and Agricultural Organisation
FDK	Fusarium damaged kernel
FHB	Fusarium head blight
g	Grams
Gb	Gigabase
GEBV	Genomic estimated breeding values
GWAS	Genome-wide association mapping
HSD	Honest significant difference
IARC	International Agency for Research on Cancer
IWGSC	International Wheat Genome Sequencing Consortium
kg/person	Kilogram per person
L	Litre
LCMS/MS	Liquid chromatography tandem mass spectrometry
Lr	Leaf rust resistance gene
LSD	Least significant difference
MAS	Marker assisted selection
Mat	Mating types
Mb	Megabase
mg/µl	Milligram per microlitre
min	Minute
ml	Millilitre
mm	Millimetre
mM	Millimolar
Ms	Male-sterility gene

MS-MARS	Male-sterility mediated marker-assisted recurrent selection
MT	Million tonnes
MTP	Minimal tilling pathway
MY	Market year
MYA	Million years ago
NaOH	Sodium hydroxide
ng/µl	Nanogram per microlitre
NIV	Nivalenol
PAGE	Polyacrylamide gel electrophoresis
PCR	Polymerase chain reaction
PDA	Potato dextrose agar
Pgt	*Puccinia graminis* f. sp. *tritici*
Pm	Powdery mildew resistance gene
pmol/µl	Picomole per microlitre
ppb	Parts per billion
Pst	*Puccinia striiformis* f. sp. *tritici*
Pt	*Puccinia triticina*
QTL	Quantitative trait loci
R^2	Coefficient of determination
RAPD	Random amplified polymorphic DNA
rcf	Relative centrifugal force
roH_2O	Reverse osmosis water
rpm	Revolutions per minute
sec	Second
Sr	Stem rust resistance gene
SSD	Single seed descent
SSR	Simple sequence repeat
SU-PBL	Stellenbosch University Plant Breeding Laboratory
t/ha	Tons per hectare

TCT-B	Type-B trichothecenes
TEMED	Tetramethylethylenediamine
Tg	Tenacious glume gene
TKW	Thousand kernel weight
Vrn	Vernalisation genes
X^2	Chi-squared
ZEA	Zearalenone

List of Figures

List of Tables

Preface

This thesis was presented at three local conferences:

1. 14th Southern African Breeder's Association Symposium

White, M and Botes, W.C. (2022) 'Wheat pre-breeding towards disease resistance of fungal pathogens'. Stellenbosch, March 2022. (Poster presentation) (Awarded best poster presentation)

2. 1st Annual Grain Research Conference (Grain SA)

White, M and Botes, W. C. (2022) 'Wheat pre-breeding towards disease resistance of fungal pathogens'. June 2022. (Oral presentation)

3. 33rd SANSOR congress

White, M and Botes, W.C. 'Wheat pre-breeding towards disease resistance of Fusarium head blight'. (Poster presentation) (Awarded best poster presentation)

Table of Contents

Chapter 1. Introduction

Bread wheat is a staple grain crop cultivated globally, serving as the main source of calories and protein to approximately 4 billion individuals. The staple crop supplies daily dietary nutrients to all global regions, with 50 % supply in Africa (FAOSTAT, 2022). The production of wheat is required to increase with 60% by 2050 to sustain increasing consumer demands. South Africa is one of the largest wheat producers in Africa, producing 2.1 million tons (MT) of wheat during the 2020/2021 production season (FAO, 2022). Approximately 50% of consumed wheat in South Africa is obtained through imports to sustain consumer demand. Population expansion along with urbanisation and dietary demands has increased the need to enhance wheat production in South Africa (Tadesse, Bishaw and Assefa, 2019). Food security can be improved and sustained through phenomics and genomics technologies to reduce prevalence of undernourishment in the country (Reynolds and Braun, 2022).

Wheat production is often threatened by the occurrence of both abiotic and biotic stressors, resulting in reduced yields. Climate change is among the most important contributing factors, leading to devastating droughts, floods and even disease outbreaks (Tadesse, Bishaw and Assefa, 2019) The most economically important biotic stressors constraining the production of wheat are fungal diseases such as, wheat rusts (*Puccinia* spp.), Fusarium head blight (FHB) and powdery mildew (*Blumeria graminis* f.sp. *tritici*) (Dean *et al.*, 2012). During heavy infestation, severe disease pressure of these fungal pathogens can cause up to 100% yield loss and eliminate major cultivars once widely cultivated (Jamil *et al.*, 2020).

Several major disease outbreaks have been recorded in Africa, with the stem rust outbreak in 1999 (*Ug99*) causing devastating yield losses. The highly virulent *Ug99* (TTKSK) strain has spread to neighbouring countries in Africa, Middle East and Asia (Bhavani *et al.*, 2019). The rapidly evolving and recombining ability of wheat rust pathogens has resulted in the spread of 13 additional pathotypes of the *Ug99* lineage, causing epidemics in Ethiopia and Europe (Singh *et al.*, 2015). The rapid spread of the *Ug99* strain and the emergence of new variants have overcome several important rust resistance genes, deeming them ineffective (Figueroa, Hammond-Kosack and Solomon, 2018).

The occurrence of FHB, primarily caused by *Fusarium graminearum* is highly destructive to both quantity and quality of wheat (Beukes *et al.*, 2017). The reduction in quality is further compounded by the production of secondary metabolites, such as mycotoxins, by causal fungi. The most prevalent mycotoxins associated with wheat grain are deoxynivalenol (DON) and infrequently DON derivatives, nivalenol (NIV) and zearalenone (ZEA) (Schiro *et al.*, 2018). The consumption of grain with high DON content has caused detrimental health defects in both humans and animals (Khaneghah *et al.*, 2018).

Various management strategies have been developed to control disease outbreaks. The integration of disease resistance is highly favoured as it is cost-effective, environmentally friendly and reduces the risk of disease outbreaks (Tadesse, Bishaw and Assefa, 2019). Several genes conferring resistance towards these fungal pathogens has successfully been deployed into single genotypes through extensive plant breeding (Rutkoski, Krause and Sorrells, 2022). The pyramiding of these genes promotes durable disease resistance, reducing vulnerability against evolving and recombining pathogens (Hasan *et al.*, 2021).

Recurrent mass selection is a complimentary breeding strategy to pyramid desirable genes into a single genotype without reducing genetic diversity and genetic gain. This breeding strategy is commonly used for cross pollinating crops but has been adapted for self-pollinating crops such as wheat through genetic male sterility. The integration of marker-assisted selection through molecular characterisation of wheat lines, has improved selection of desirable genes. An adapted male-sterility mediated marker-assisted recurrent selection (MS-MARS) pre-breeding programme was established at the SU-PBL to facilitate cross pollination of selected wheat lines (Marais, Botes and Louw, 2000).

The aim of the study was to screen for crossing parents containing wheat rust, Fusarium head blight and powdery mildew resistance genes to introduce into the MS-MARS pre-breeding programme at the SU-PBL. To achieve the aim, the study objectives were to:

I. Identify, validate and evaluate novel powdery mildew resistance (*Pm37*, *Pm4b*, *MLAG12*, *MLUM15*) genes using microsatellite markers and seedling assays to assess disease response of the SU-PBL's 2020 wheat nursery;

II. Validate targeted QTLs (Q*fhs.ifa.5A*, *7AQTL*, *Qfhs.ndsu.3BS*) closely linked to FHB resistance genes in an FHB CIMMYT nursery using microsatellite markers and phenotypic assessment to identify superior genotypes;

III. Molecularly characterise the segregating base population for cloned rust resistance genes (*Sr35*, *Sr45*) and gene complexes (*Sr2*/*Yr30*, *Lr34*/*Yr18*/*Sr57*) prior to recurrent mass selection cycles; and

IV. Validate the MS-MARS scheme by selecting suitable donor lines from the SU-PBL's 2020 wheat nursery and FHB CIMMYT nursery to cross pollinate with the highly diverse segregating base population. In addition to, molecular and phenotypic screening for dominant male sterility in the base population.

Chapter 2. Literature review

2.1. Wheat production

2.1.1. Genetic evolution of hexaploid bread wheat

Bread wheat (*Triticum aestivum* L.) is the earliest crop domesticated by ancient civilisation, originating from wild grass in arid conditions. It is an autogamous species classified under the Poaceae family, with a genus *Triticum*. The genus consists of three different ploidy levels, including diploids (Monococcon), tetraploids (Dicoccoidea) and hexaploids (Triticum). The allopolyploidisation of wheat is derived from having sub-genomes of different species (Matsuoka, 2011). The diploid species include *T. urartu* and *T. monococcum*, each containing an AA genome, with *T. urartu* only existing as its wild-type (Matsuoka, 2011). The tetraploid species include *T. timopheevii* and *T. turgidum*, containing an AAGG and an AABB genome, respectively. The hexaploid species include *T. zhukovskyi* and *T. aestivum*, containing an AAAAGG and AABBDD genome, respectively (Allen *et al*., 2017).

A significant discovery during wheat evolution research was the number of chromosomes in wheat. Wheat exists with a series of polyploidism; diploids (*2n=2x=14*), tetraploids (*2n=4x=28*) and hexaploids (*2n=6x=42*). Bread wheat is hexaploid (*2n=6x=42*) with an AABBDD genome, containing seven pairs of chromosomes each belonging to the A, B and D sub-genomes (Matsuoka, 2011).

Common bread wheat has evolved to its current state, because of two allopolyploidisation events. The first event occurred approximately 800 000 years ago, developing tetraploid wild emmer wheat from a hybridisation of two diploid species. The two species involved was a male donor of the A sub-genome that diverged from *T. urartu* approximately 1.3 MYA and a female donor that diverged from *Aegilops speltoides* approximately 4.5 MYA donating the B sub-genome (**Figure 2.1**). The second hybridisation event produced hexaploid wheat by merging the allotetraploid wheat donating the A and B sub-genomes with *Aegilops tauschii* as the progenitor of the D sub-genome. Hulled allohexaploid wheat was formed from the second allopolyploidisation

event, from which modern free-threshing wheat was derived through mutations (Levy and Feldman, 2022).

The sequenced genome of the wild relative *Aegilops tauschii* confirmed that the origin of the D genome was 5.37 MYA from the D-lineage formed by hybridisation of the T and A ancestral genomes approximately 5.5 MYA (**Figure 2.**). The origin of the diploid progenitors for the A sub-genome (*T*. *urartu*) and the D sub-genome (*Ae*. *tauschii*) in *T*. *aestivum* is well described. The identity of the cytoplastic B sub-genome donor of wheat remains difficult to find. There is no diploid species with a high affiliation for the B sub-genome. Moreover, speculating that the species from which it originated is far extinct, simply not identified yet or have polyphyletic origin and evolved through hybridisation with close relatives still existing such as *Ae*. *speltoides* (Levy and Feldman, 2022).

The evolution of wheat under human selection resulted in spontaneous mutations altering spike morphology of wild emmer wheat. Two major morphological changes involved non-brittle rachis and softer glumes. Domestication of wheat with non-brittle rachis, went from fragile spikes shattering at maturity to having seed primarily dispersed by farmers, substantially reducing yield loss. The major gene conferring spike fragility present in modern hexaploid wheat was introduced from wild emmer wheat. *Brittle rachis* (*Btr1* and *Btr2*) genes located on the short arm of chromosomes 3A and 3B confers spike fragility in spp. *dicoccoides*. A recessive mutation in the *Btr1* orthologue of wild emmer loci (*br-A1* and *br-B1*) reduced spike fragility. A single mutation in *br-A1* or *br-B1* only conferred partial fragility. Whereas, a mutation in both alleles yield complete non-brittle rachis. Minor effect QTLs have also been identified and selected to further reinforce rachis strength (Levy and Feldman, 2022).

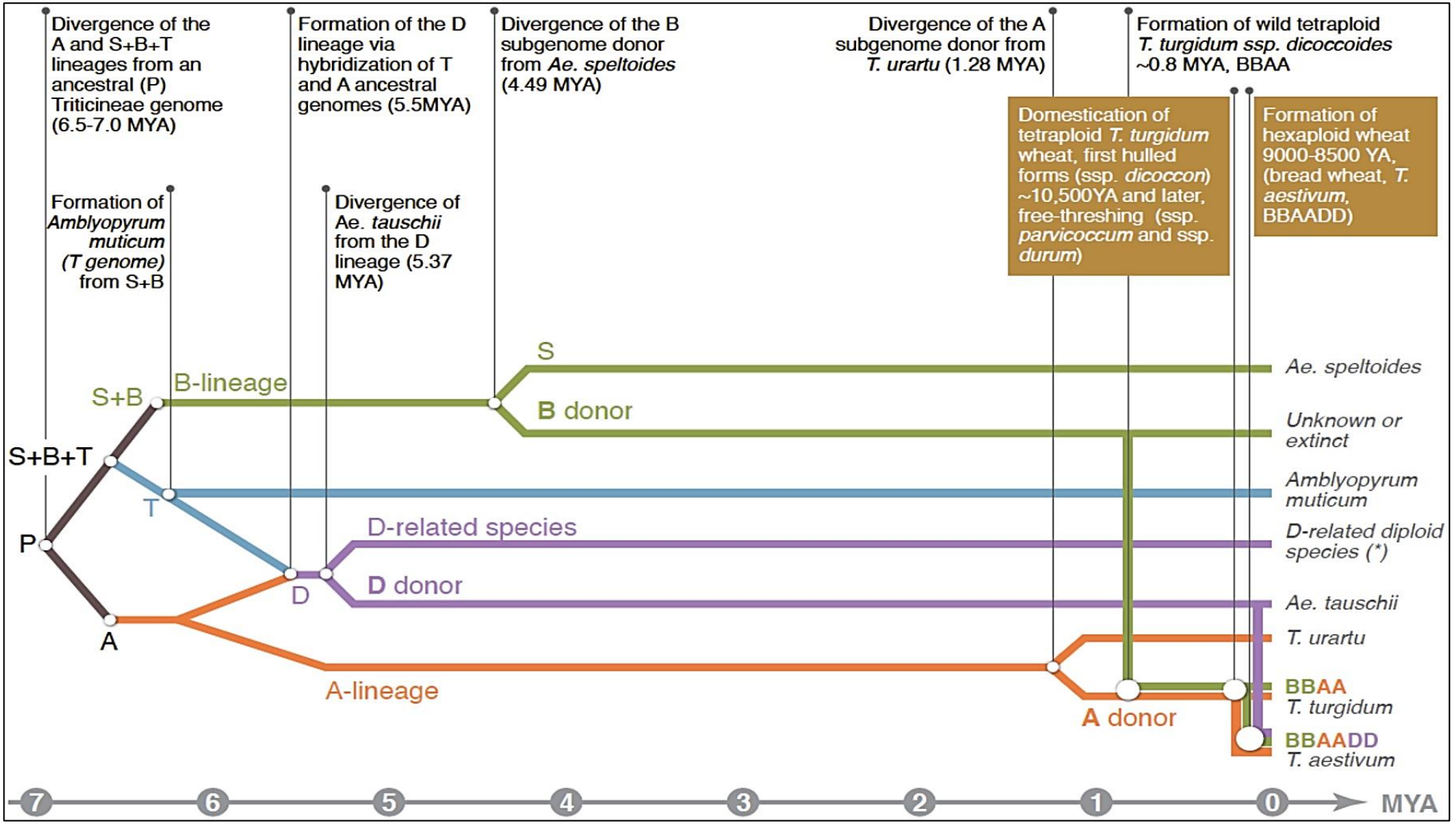

Figure 2.1. Detailed phylogenetic illustration of the evolutionary events involved in the development of modern hexaploid bread wheat. The evolution of wheat is illustrated to initiate 7 MYA from a progenitor donating the A sub-genome of bread wheat (Levy and Feldman, 2022).

The evolution of glume tenacity in wheat is an important domesticated trait for farmers but reduces the fitness of wheat wild types. Wild-type species require tightly packed glumes that are large and hardened to protect grain from birds. Farmers require grain that are free threshing and easily dislodged from the glumes. Free threshing was present during tetraploid domesticated emmer wheat, ssp. *dicoccon*, conferred by a dominant allele, the Q-factor. The Q-allele is located on the long arm of chromosome 5A, encoding an AP2-like transcription factor responsible for the pleiotropic effects observed in wheat. The hybridisation of *Ae. tauschii* and free-threshing tetraploid wheat only produced lines resembling the hulled phenotype of the D sub-genome donor even though the Q-factor inherited was dominant (**Figure 2.2**). This phenomenon is due to a suppressive *Tenacious glume* (*Tg-D1*) gene present in *Ae*. *tauschii*, mapped on chromosome 2D. A single recessive mutation in the *Tg* gene, changing *Tg* to *tg*, producing a free threshing phenotype in *Ae*. *tauschii* (Levy and Feldman, 2022).

Fine mapping of the *Tg* loci revealed that homoeoalleles *Tg-A1* and *Tg-B1* located on chromosomes 2A and 2B, respectively along with the q-allele is responsible for the tenacious glumes. Mutations in all three loci confers complete free threshing, with each mutated loci having an additive effect on glume tenacity. The presence of the dominant Q-allele contributing substantially. Modern hexaploid bread wheat therefore, has a genotype *Q/tg-A1tg-A1/tg-B1tg-B1/tg-D1tg-D1* displaying complete free-threshing (Levy and Feldman, 2022).

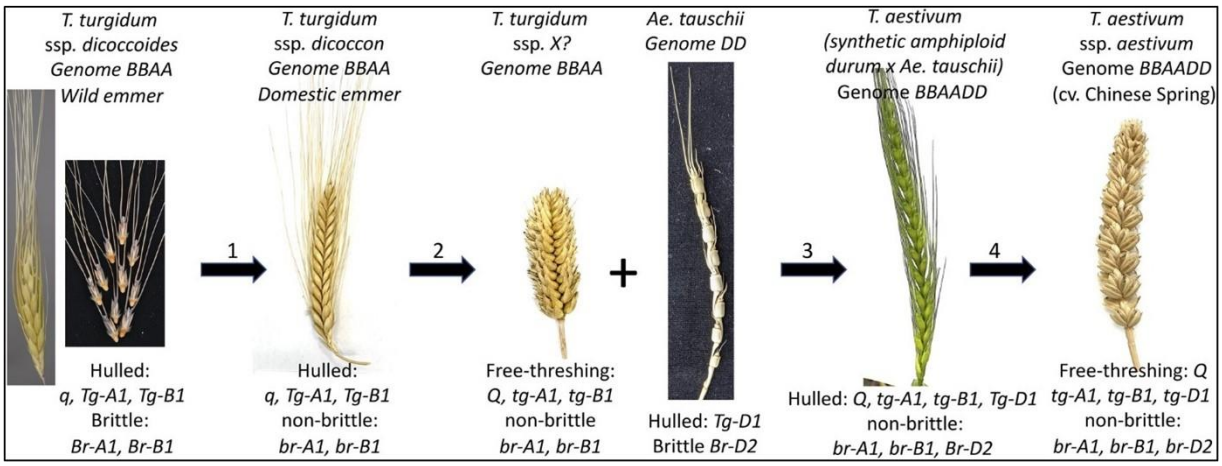

Figure 2.2. Morphological changes observed during the domestication of wheat through major mutational events (Levy and Feldman, 2022).

2.1.2. Advancement in genome sequencing of wheat

Accurate genome sequencing and assembly of wheat and its progenitors has contributed to evolutionary studies and genetic improvements of wheat. In 2005, scientists and breeders established the International Wheat Genome Sequencing Consortium (IWGSC) to initiate wheat genome studies (Shi and Ling, 2018). Initially the IWGSC, sequenced individual chromosome arms using bacterial artificial chromosome (BAC) libraries and physical map constructions. Research groups of different institutions also contributed by generating additional reference sequences of each chromosome or chromosome arm. In 2008, the first chromosome was successfully sequenced (Paux *et al.*, 2008). A physical map of chromosome 3B was assembled through BAC clones, selected using the minimal tilling pathway (MTP) approach. A pseudomolecule of chromosome 3B with a length of 774 megabases (Mb) was generated encoding for 5326 protein-coding genes (Choulet *et al.*, 2014).

In 2012, a whole genome shotgun sequencing technique generated a five-fold coverage sequence of the “Chinese Spring” genome using Roche 454 pyro-sequencing technology. The draft sequence of 5.5 Gb presented between 94 000 and 96 000 genes, representing approximately one-third of the sub-genomes (A, B and D). In 2014, after the publication of the first wheat genome sequence, IWGSC released a chromosome-based draft sequence of “Chinese Spring” using Illumina sequencing technology. They assembled a genome sequence of 10.2 Gb, with a scaffold proportion of only 49% (Shi and Ling, 2018).

Substantial progress was made when an improved reference genome sequence of “Chinese Spring” was published with an assembly representing more than 78% of the genome containing 12.7 Gb (Clavijo *et al.*, 2017). A near-complete “Chinese Spring” genome assembly was generated using short Illumina reads (second generation data) in combination with long Pacific Biosciences reads (third generation data). The sequence length was approximately 17 Gb, representing more than 90% of the “Chinese Spring” genome (Zimin *et al.*, 2017). The IWGSC continued to refine the genome sequence of “Chinese Spring” and recently released the genomic data of the reference sequence (IWGSC v1.0 and v2.1). The newly released reference genome sequence encoded a total of 105 534 high confidence genes (Zhu *et al.*, 2021).

2.1.3. Domestication of bread wheat

Wheat is a widely cultivated grain crop, produced in various geographical regions. The largest wheat producing countries in the world are China, India, Russia, United States, Canada and Pakistan. Wheat cultivation across such a diverse range of environments, requires adaptation in the life cycle and traits affecting plant architecture. Understanding the genes responsible for variation in phenology and their interactions with one another is crucial. It largely determines the successful cultivation of the crop (Hyles *et al.*, 2020).

Major genes responsible for the variations in wheat phenology are the genes expressing vernalisation requirements. Wheat cultivars are categorised into three major groups based on vernalisation, namely, spring wheat, winter wheat and facultative wheat. Vernalisation is the crops chilling requirements (temperature and duration) to accelerate flowering, primarily controlled by allele variants of the *Vrn* genes, namely *Vrn-A1*, *Vrn-B1* and *Vrn-D1*. The vernalisation genes are located on the long arm of chromosome 5 of each sub-genome (A, B and D) (Hyles *et al.*, 2020).

Spring wheat requires little-to-no environmental stimulation to induce flowering due to the presence of the dominant *Vrn-A1* allele. Spring wheat can complete its life cycle from planting to harvest in growing regions where temperatures never reach cold enough for vernalisation. Temperatures required for vernalisation ranges between -1.3°C and 15.7°C, with vernalisation accelerating at 4.9°C. Winter wheat requires vernalisation since it contains the recessive alleles of the *Vrn* gene. It is usually planted in autumn for the wheat to undergo dormancy during the winter season and resumes growth again during the spring season (Hyles *et al.*, 2020).

The life cycle of wheat has distinct phases (**Figure 2.3**). Based on the Feekes scale ranging from stage 1-11, the development of wheat from tillering (stage 1-5), stem elongations (stage 6-10), heading (stage 10.1 - 10.5) and ripening (stage 11). The development of wheat can be described using the comprehensive Zadoks or Haun scale comprising of a two-digit computer-compatible decimal format, ranging from 0 – 100. The most frequent form of measurement used in literature is the Feekes scale method (Hyles *et al.*, 2020).

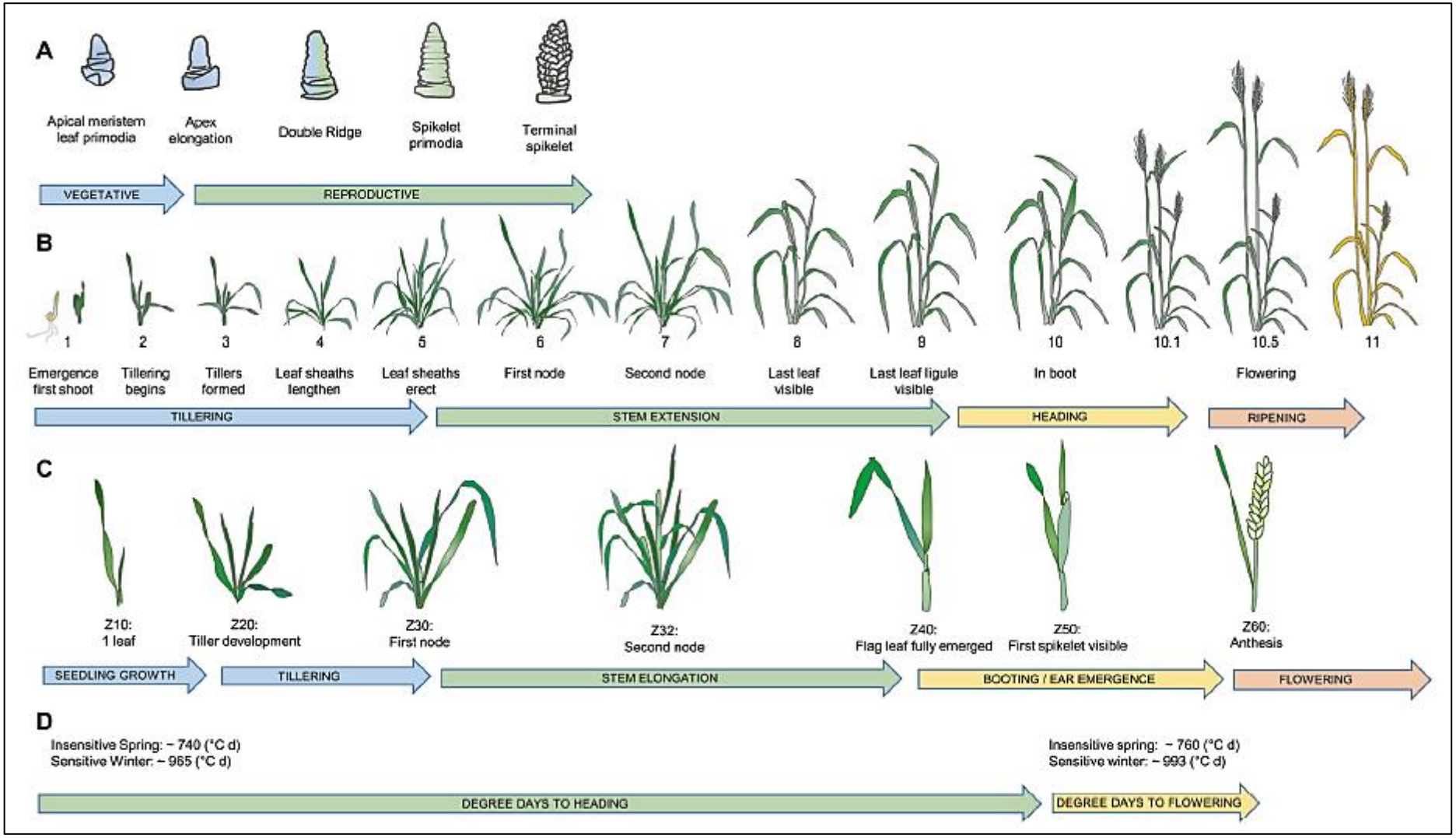

Figure 2.3. Schematic representation of wheat development. **A** The maturation of the apex from the vegetative to reproductive state. **B** Feekes scale ranging from stage 1-11. **C** Zadoks scale **D** Cumulative days to heading (Hyles *et al.*, 2020).

2.1.4. Global production of wheat

Bread wheat is an essential grain crop providing approximately 19% calories and 21% daily protein to 4.5 billion individuals globally. Cultivation of wheat has increased across geographical regions, with adaptation to a range of environments as a result of its complex nature. The sustainable production of wheat varies across different socioeconomic and geographical regions, with production being slightly higher in developed countries as compared to developing countries (Tadesse, Bishaw and Assefa, 2019).

The global production of wheat expects to decline by 0.8% during the 2022 cropping season compared to the 2021 production. Producing an estimated value of only 771 million tonnes (MT), the first decline in production since 2019. The world's largest wheat producing countries are European Union (138.7 MT), Mainland China (136.9 MT), India (105.5 MT), Russia federation (83.5 MT), United States of America (47.0 MT), Canada (31.2 MT), Australia (28.0 MT), Pakistan (26.5 MT), Argentina (21.0 MT) and Ukraine (20.0 MT). South Africa ranking at 40th with a total production of 2.1 MT for the 2022 MY. War-related disruptions of agricultural operations in Ukraine has reduced wheat production for the country by 38%, leaving the country with a forecast of only 20 MT (FAO, 2022).

Exports out of Ukraine is expected to reduce by 50%, equivalent to 9 MT. Consequently, due to restricted movement at their major ports. Based on speculation, Ukraine's exports will commence via railroad at smaller volumes. An overall fall in world trade of 1.7% can occur as a consequence. The largest exporting country forecasted for the 2022/23 MY is the European Union, with a total of 38 million tonnes (FAO, 2022).

Wheat production will marginally exceed wheat utilisation during the 2022/23 MY. Due to the current forecast of 0.4% drop in wheat utilisation to 769 MT during the 2022/23 MY. Wheat utilisation will drop below the ten-year trendline by 1.1% for the first time in three years. Unaffordable prices can be seen dampening the use of wheat for animal feed and industrial use. Particularly in China and European Union, the world's largest market for feed grain (FAO, 2022).

2.1.5. Local production of wheat

The cultivation of small grain cereal in South Africa was established on behalf of the winter season of 1652, two months after Jan van Riebeeck colonised Cape Town. Wheat domestication initiated along the coastline of Cape Town and was short-lived as the coastal conditions were not conducive for wheat production. Along with the failed attempt to cultivate winter wheat in a Mediterranean climate. Successful cultivation was obtained when wheat production migrated inland where winter conditions were less harsh. It was only in 1891, that wheat production became profitable after the initiation of wheat varietal improvement to South African conditions commenced. The production of wheat has ever since increased through continuous wheat improvement practices (**Figure 2.4**) (Nhemachena and Kirsten, 2017).

The three leading organisations responsible for the wheat varietal improvement sector are Bayer established mid 1960s becoming independent in 1999 after collaborating with Monsanto, the Agricultural Research Council - Small Grains (ARC-SG) established in 1976, Corteva entering the sector in the 1990s and lastly Syngenta becoming established late 2000 (Pretorius *et al.*, 2020) .

The production of wheat is ranked the second most important grain crop produced in South Africa following maize production in relation to area planted and total production. The utilisation of wheat in South Africa is primarily allocated for human consumption at 3 500 000 MT (bread making), a portion of it to industrial purposes (alcohol, starch and straw) and the remainder towards animal feed (Esterhuizen, 2022).

Two major wheat types are commercially produced in South Africa, primarily bread wheat (*Triticum aestivum* L.) and less durum wheat (*Triticum turgidum*). They vary in genetic complexity, end-use and adaptability. The end-use of bread wheat and durum wheat comprises of a wide range of products. Bread wheat for production of bread, biscuits and noodles and durum wheat for pasta and in some cases bread-making. In South Africa, *Triticum aestivum* is the primary producing wheat with a very small portion being *Triticum turgidum* production (Nhemachena and Kirsten, 2017).

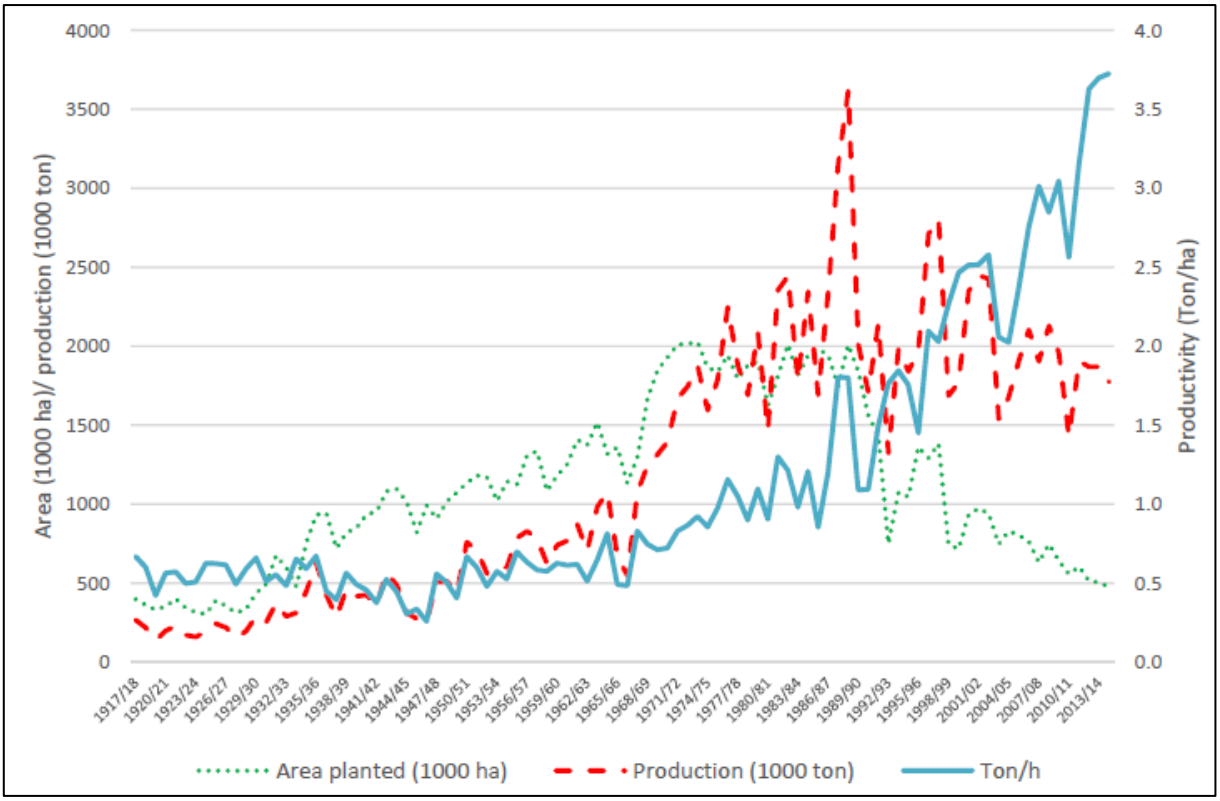

Figure 2.4. Trends in wheat production over the past 100 years (Nhemachena and Kirsten, 2017)

The Sub-Saharan African wheat producing regions accommodates 30% of the total wheat produced in Africa. One of the largest producing countries in Africa is South Africa, with an annual production of 2.1 million tons (MT). Produced across an average area of only 524 000 ha recorded for the 2021 growing season (**Figure 2.5**) (Tadesse, Bishaw and Assefa, 2019).

South Africa has wheat growing under rain-fed and irrigated conditions, the average production under these conditions are 2-4 tons per hectare (t/ha) and 7.9 t/ha, respectively. For dryland conditions, productivity levels have increased from 0.5 t/ha in 1936 to more than 3.5 t/ha recorded in 2015. Of the 36 crop producing regions in South Africa, 32 are used for wheat production (Nhemachena and Kirsten, 2017). The main wheat reproducing regions in South Africa are the South Western part of Western Cape (winter rainfall), Northern Cape (irrigation), North West (mainly irrigation), Free State (summer rainfall), Gauteng, Eastern Cape and the KwaZulu-Natal province (Tadesse, Bishaw and Assefa, 2019). Although a general decrease in production was observed in South Africa it can be argued that the productivity, efficiency, and quality of production has increased. The increase in productivity

is a result of integrated complementary disciplines such as, crop protection, plant breeding, crop physiology and agronomy (Nhemachena and Kirsten, 2017).

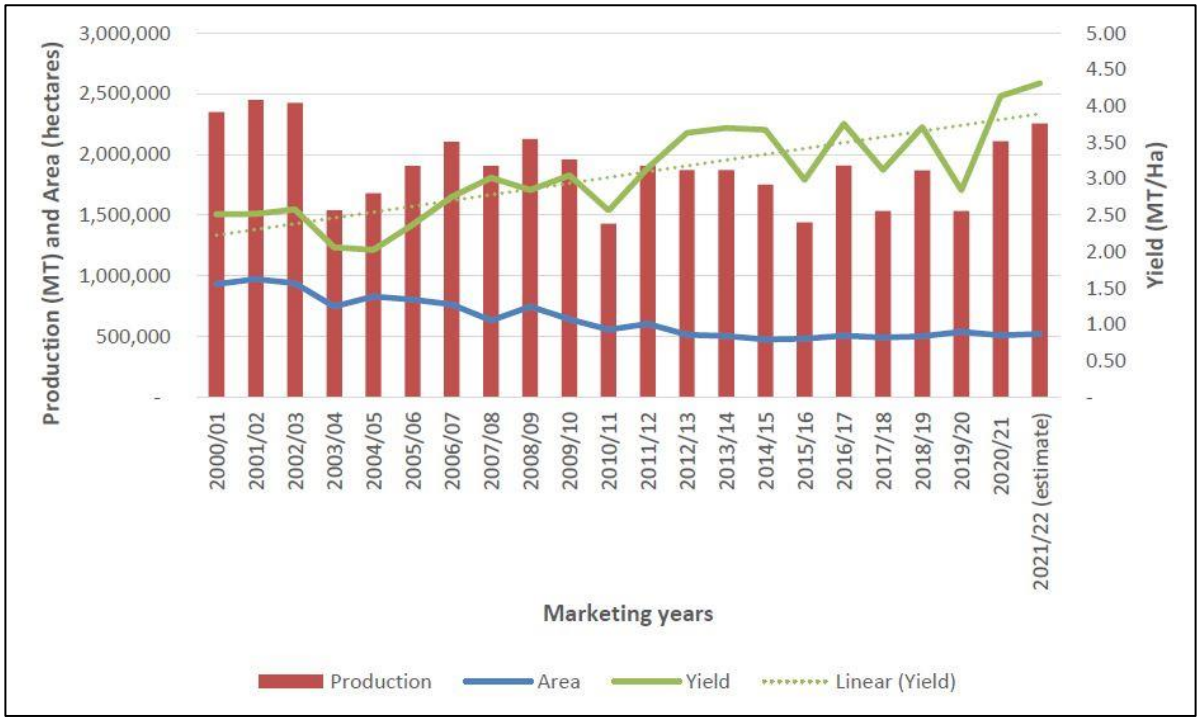

Figure 2.5. South African commercial wheat production, the area utilized during production and the harvest productivity for each production season for the past 20 years (Esterhuizen, 2022)

Two of the major wheat producing provinces in South Africa are in the summer (Free State) and winter (Western Cape) rainfall regions, contributing 346 500 tons and 1 188 000 tons, respectively (SAGIS, 2021). In the summer rainfall regions, wheat can be cultivated under dryland and irrigated conditions, but in the winter rainfall region wheat is only planted under dryland conditions. More than 50% of wheat production occur in the dryland regions, with 30% of irrigated wheat produced under summer rainfall conditions. Unfortunately, the dryland productivity is considerably lower than irrigated regions within South Africa and worldwide (Nhemachena and Kirsten, 2017).

The consumption of wheat in South Africa has increased on average by 2% annually over the past 10 years due to population growth. The annual per capita consumption of wheat in South Africa is 56kg/person, with an average of 2.4 billion loafs of bread consumed annually. Continuous increase in wheat consumption is expected for market year (MY) 2022/23, with an

estimated consumption of 3.7 MMT (**Figure 2.6**). Consumption estimates for the 2021/22 MY is at 3.6 MMT, only slightly higher than the MY 2020/21 recorded at 3.5 MMT wheat consumed (Esterhuizen, 2022).

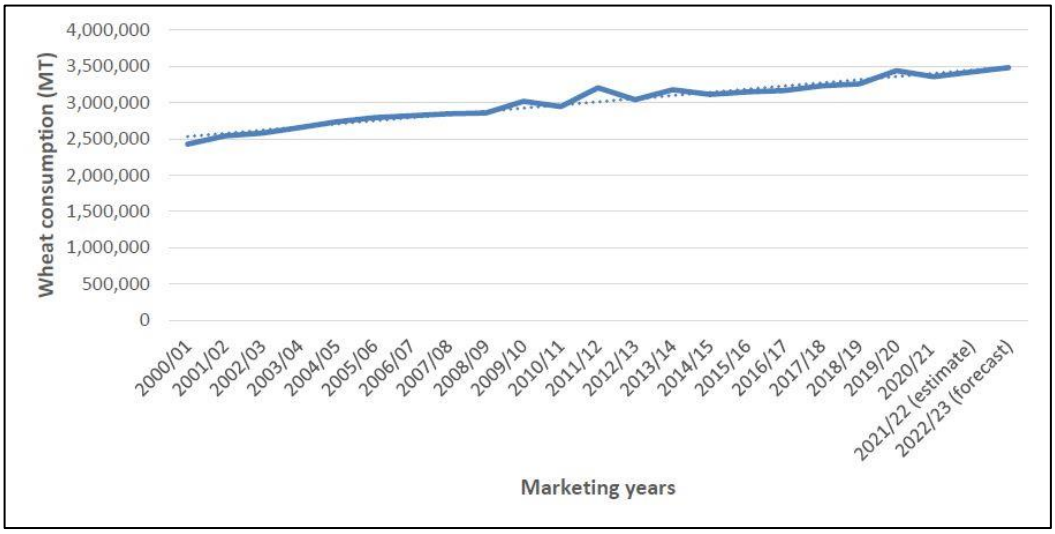

Figure 2.6. Wheat consumption in South Africa over the past 20 years (Esterhuizen, 2022)

The local production of wheat increased to 2 120 000 MT during the 2020/21 MY, resulting in a decrease of 18% in wheat imports for South Africa. During the months of October 2021 – February 2022, South Africa only imported 582 929 MT of wheat, equivalent to the imports for the 2020/21 MY (Esterhuizen, 2022). South Africa currently receives the largest import of wheat from Lithuania, Argentina and Poland and Australia, with the United States ranked at sixth (Nhemachena and Kirsten, 2017).

South Africa exports wheat to neighbouring countries in Africa and provides a pipeline for imports from outside Southern Africa. The local production of wheat in South Africa is expected to increase. Resulting in an average increase of wheat export from South Africa. The quantity of wheat export is expected to reach 200 000 MT in the 2021/22 and 2022/23 MY (Esterhuizen, 2022).

2.1.6. Factors threatening production of wheat

The occurrence of both abiotic and biotic stressors threatens wheat production, with varying intensity across producing regions (Tadesse, Bishaw and Assefa, 2019). The most prevalent limiting factor of wheat productivity and food security is climate change. Climate change has affected wheat production in two ways. The first being increased temperature (heat) and altered rainfall patterns and frequency (flood, droughts). The second being altered soil composition, distribution and frequency of virulent pests and diseases (Qadir *et al.*, 2019). These limiting factors reduces predictability in wheat production, reducing the reliability of pre-planned strategies (Tadesse, Bishaw and Assefa, 2019).

2.1.6.1. Abiotic stressors

In the rain-fed producing environments of South Africa, primarily the mid altitude regions, abiotic stressors such as drought, soil erosion, poor soil fertility and pre-harvest sprouting strongly affect production. The lack of water supply and extreme heat are concerning abiotic stressors for irrigated wheat producing regions (Jha, Bohra and Singh, 2014). Heat stress during the flowering stage of wheat can cause staggering yield loss and reduction in grain quality. Exposure to extreme heat stress initiates physiological changes in wheat by accelerating the developmental stages, ultimately reducing the biomass and inducing early leaf senescence (Jha, Bohra and Singh, 2014; Qadir *et al.*, 2019). An average of 6% reduction is expected for global wheat production with every 1°C increase in surface temperature (Asseng *et al.*, 2017). The future is towards breeding for adapted cultivars to limit factors of abiotic and biotic stressors (Hickey *et al.*, 2019).

2.1.6.2. Biotic stressors

The most economically important biotic stressors constraining the production of wheat in South Africa are pests, weeds and diseases. The occurrence of diseases such as wheat rusts (stem rust, leaf rust and stripe rust), Fusarium head blight and powdery mildew are highly

destructive in major wheat producing regions. Ranked as the most important fungal pathogens to affect wheat production (Dean *et al.*, 2012). The effects of climate change are predicted to drive the emergence of new and highly virulent diseases, with recent epidemics of the *Ug99* stem rust strain rapidly spreading. In Ethiopia, the *Ug99* epidemics eliminated major cultivars such as “Enkoy” with rust resistance gene *Sr36* and “Digalu” with the *SrTmp*$^{+}$ gene. The recently identified “Digula” pathotype (TKTTF) in regions of Ethiopia, becoming an increased threat to wheat production (Figueroa, Hammond-Kosack and Solomon, 2018).

2.2. Wheat rust diseases

Rust fungi are basidiomycetes classified into the *Pucciniales* family, formerly identified as *Urediniales*. This family of fungi is widely distributed and diverse with more than 7 800 species responsible for crop losses worldwide. Three particularly important *Puccinia* spp. causing stem rust, leaf rust and stripe rust include *Puccinia graminis* Pers.:Pers f. sp. *tritici* Eriks. and E. Henn. (*Pgt*), *Puccinia triticina* and *Puccinia striiformis* Westend f. sp. *tritici* Erikss. (*Pst*), respectively (Figueroa, Dodds and Henningsen, 2020).

Rust fungi are obligate biotrophic parasites, producing continuous infection cycles on a living host for survival. The epidemiology and biology of rust fungi is strongly influenced by the co-evolutionary history of their host. Consequently, requiring a high degree of host specificity for pathogen-host interactions and only infects a narrow range of hosts. Their host specificity is reflected in their classification of *formae speciales* (f. sp.) (Figueroa, Hammond-Kosack and Solomon, 2018). Rust fungi are well-known for its complex life cycles and produces specialised haustorium for nutrient gain and secretion of protein effectors for host manipulation (Figueroa, Dodds and Henningsen, 2020).

2.2.1. Stem rust

Stem rust (black rust) is one of the more devastating rust pathogens of wheat caused by *Puccinia graminis* f. sp. *tritici* (*Pgt*). Several major disease outbreaks and massive yield losses

have been recorded for stem rust. Although stem rust is not the most common or widespread of the rust pathogens, it can potentially be the most damaging. Stem rust epidemics have been recorded worldwide in countries such as Canada, India, Australia, and Ethiopia (Singh *et al.*, 2015; Bhavani *et al.*, 2019). The occurrence of stem rust is commonly recorded in regions where warm and moist conditions are prevalent. Symptoms of infection include red brick-like pustules of urediniospores typically on the leaf sheaths, stems, awns, and glumes of susceptible varieties. Yield loss to stem rust can appear as wheat lodging and reduced grain size (Figueroa, Hammond-Kosack and Solomon, 2018).

Stem rust has received significant recognition as several new virulent pathotypes have been identified for the *Pgt* population. The emergence of the most virulent strain of stem rust was reported in Uganda during 1999. Named *Ug99*, after the country and year it was first detected. Rapid spread of the *Ug99* pathotype within Africa and the middle East has increased the concern for wheat production (Figueroa, Hammond-Kosack and Solomon, 2018). Wheat cultivars with widely deployed stem rust resistance genes were compromised by the new *Pgt* pathotype *Ug99* (TTKSK). Over a ten-year period, six new variants of *Ug99 Pgt* pathotypes were identified in regions of Iran, Yemen, and Africa. Approximately 90% of wheat varieties grown worldwide are susceptible to *Ug99* and its related pathotypes (Singh *et al.*, 2015). The “Digalu” virulent pathotype spread to Europe and caused a devastating epidemic (Figueroa, Hammond-Kosack and Solomon, 2018). A similar pathotype was detected in Germany during 2013. However, the pathotype was phenotypically distinct from “Digalu”, displaying virulence to newly identified stem rust resistance gene *Sr45*. (Olivera Firpo *et al.*, 2017). New variants have spread to Sicily causing major outbreaks (Figueroa, Hammond-Kosack and Solomon, 2018).

2.2.2. Stripe rust

Stripe rust (yellow rust) caused by *Puccinia striiformis* Westend f. sp. *tritici* Erikss. (*Pst*) is an important rust disease of wheat. The name stripe rust was derived from the elongated yellow streak symptoms that forms bright yellow uredial pustules arranged in rows on leaf surfaces.

It is an epidemic fungal pathogen of spring wheat with some occurrence on winter wheat (Jamil *et al.*, 2020). Stripe rust is endemic in temperate climatic regions, where cooler and moist weather conditions prevail. (Figueroa, Hammond-Kosack and Solomon, 2018).

Stripe rust occurrence have been reported in over 60 countries worldwide, with evidence of further global expansion. The appearance of highly aggressive *Pst* pathotypes have been recorded in regions unconventional to stripe rust infections (Figueroa, Hammond-Kosack and Solomon, 2018). Stripe rust was first detected in South Africa during 1996 and within two-years from detection had spread to all wheat producing regions within the country (Agenbag *et al.*, 2012; Maree *et al.*, 2019). Over the last few decades, stripe rust has caused susceptibility to 80% of wheat varieties worldwide. A total of 51 major stripe rust epidemics have been reported between 1939 and 2016, with total crop failure reported during severe cases. An annual estimated global loss of 5 million tons was recorded for stripe rust, equating to approximately US$ 1 billion in losses (Jamil *et al.*, 2020).

Substantial progress has been made to manage stripe rust epidemics. Sequencing the genome of stripe rust has provided deep insight into understanding the fungal organism. Several reference genomes have been published for stripe rust. Genomic studies have identified more than 1 000 effector proteins but further annotation of all these proteins is required. Bioinformatics and genomics have contributed substantially to exploring the pathogenicity and evolution of stripe rust. Refined reference sequences of the wheat genome are also publicly available. Bioinformatic tools have identified more than 78 resistance genes for stripe rust (Jamil *et al.*, 2020).

2.2.3. Leaf rust

Leaf rust caused by *Puccinia triticina* Ericks. (*Pt*) is the most frequent and widely dispersed of the three rust diseases. The fungal pathogen infects leave area at all growth stages. During high disease pressure infection can spread to leaf sheaths and glumes causing reduction in grain weight and quantity per spike. Devastating yield losses of 50% has been recorded in susceptible cultivars (Figlan *et al.*, 2020).

Pt populations are highly diverse and exhibit a high degree of adaptability to varying climates resulting in frequent emergence of new virulent pathotypes. Evidence suggests that *Pt* populations originated in the Fertile Crescent region of the Middle East along with wheat (primary host) and meadow rue (alternative host) (Figueroa, Hammond-Kosack and Solomon, 2018).

Leaf rust epidemics have been recorded in southern Africa since early 1980, increasing susceptibility of wheat varieties and yield loss. Leaf rust is prevalent in the winter rainfall regions of Western Cape and in some irrigated regions of other provinces. Recent field surveys have recorded decreasing levels of leaf rust infections across South Africa. Evidence suggests that reduced levels of inoculum is a direct result of routine fungicide applications in these regions (Figlan *et al.*, 2020).

A total of 80 leaf rust resistance genes have been successfully identified across the A, B and D sub-genomes of wheat (Sapkota *et al.*, 2019). Several of these genes sourced from wheat wild relatives such as *Aegilops taushii* (*Lr21*), *Thinopyrum elongatum* Zhuk. (*Lr19*) and *Agropyron elongatum* (*Lr24*) has successfully been translocated into hexaploid wheat. Leaf rust resistance genes with slow rusting resistance (*Lr34*/*Sr57*/*Yr18*/*Pm38* and *Lr67*/*Sr55*/*Yr46*/*Pm46*) has successfully been cloned and deployed into breeding lines (Moore *et al.*, 2015).

2.2.4. Disease cycle of rust pathogens

Wheat rust pathogens are heteroecious and macrocyclic fungi, requiring two taxonomically unrelated hosts to complete their life cycle. Five distinct spore stages occur during a complete life cycle. Teliospores, basidiospores and urediniospores are produced during asexual reproduction primarily on primary host (wheat). Pycniospores and aeciospores are produced during sexual reproduction on alternative hosts (barberry) (**Figure 2.7**) (Kolmer, 2013).

Asexual production is driven by urediniospores mediating infections through haustoria formation essential for nutrient acquisition and effector secretion. Protein effectors facilitate fungal growth and manipulate host defence mechanisms (Figueroa, Hammond-Kosack and

Solomon, 2018). Teliospores are developed directly from uredinial infections and produces basidiospores which are forcibly ejected after meiosis. Basidiospores infect alternative hosts on the adaxial surface. The interaction of two mating types generates a pycnial structure that produces pycniospores, dispersed via insects to interact with opposite mating types for restoration of the dikaryotic nuclear state. The dikaryotic aecium produces aeciospores, and when matured are released by wind dispersal to initiate infection of the wheat host. Urediniospores are produced after infection and cycles continuously or produces teliospores (Kolmer, 2013).

The sexual production of wheat rusts relies on the presence of an alternative host. For stem rust and stripe rust the common alternative hosts is *Berberis vulgaris* (barberry) and less frequent *Mahonia*. The alternative hosts for leaf rust it is *Thalictrum speciosissimum* (meadow rue), *Anchusa*, *Clematis*, and *Isopyrum* (Figueroa, Hammond-Kosack and Solomon, 2018) The alternative host *Berberis* has not been reported or discovered in South Africa yet. Without the alternative host barberry in South Africa, no evidence of sexual production has been reported in the country. The main drivers of variation observed among wheat rust populations within the country are therefore attributed to mutational events and somatic hybridisation (Li *et al.*, 2019; Pretorius *et al.*, 2020).

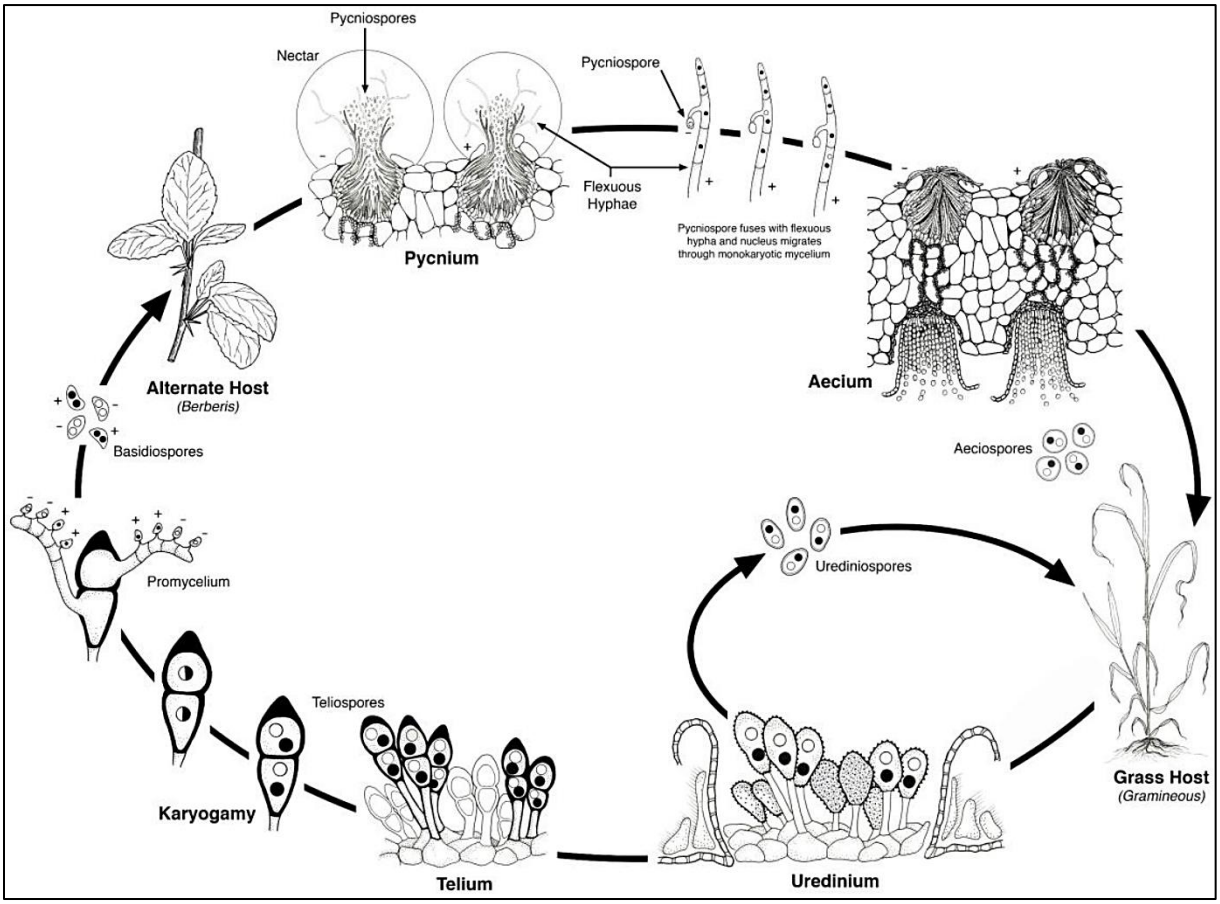

Figure 2.7. Disease cycle of wheat rust pathogens (Kolmer, 2013).

2.2.5. Management strategies for rust diseases

Management strategies to mitigate wheat rust diseases can include cultural control methods, along with chemical applications and genetic resistance. Cultural control practices include the eradication of inter-crops through tillage and the removal of alternative hosts. Genetic resistance has been the preferred method to manage rust disease. The application of fungicides is more frequent when genetic resistance is temporarily unavailable from emergence of new virulent pathotypes. However, in the presence of viable rust resistance, the reliance of chemical control for integrated management can be reduced by 50% (Figueroa, Hammond-Kosack and Solomon, 2018).

2.2.6. Genetic resistance to wheat rust

Disease resistance to wheat rust infections is primarily grouped into two classes, either pathotype-specific (seedling or qualitative resistance) or non-pathotype specific (adult or quantitative resistance). Seedling resistance can usually remain expressive throughout all growth stages of wheat and in some cases are referred to as all-stage resistance (ASR). The qualitative resistance mechanism of ASR is often hypersensitive immunity, through programmed cell death. A large portion of leaf rust resistance genes are pathotype-specific and is conferred by the gene-for-gene model. Major resistance genes of ASR can easily be eliminated by new virulent pathotypes (Figlan *et al.*, 2020).

Adult plant resistance (APR) is usually expressed by minor resistance genes and confers partial or slow rusting resistance in adult plants. It is polygenic with no clear pathotype specificities, but can also be conferred by pathotype-specific resistance, which in most cases are short lived and only effective in the presence of the corresponding avirulence gene. Genes conferring adult plant resistance usually goes undetected during seedling stage, but can remain viable against a broad range of isolates. The partial resistance regulates inoculum availability through less and smaller urediniospores production (Figlan *et al.*, 2020).

By 2018, more than 150 rust resistance genes have been identified in wheat or wheat wild relatives, majority of those genes confer pathotype-specific resistance. Fifty of those genes are designated to stem rust (Sr) resistance genes. One of the most widely cultivated pathotype-specific gene (*Sr31*) against *Pgt* was compromised by the virulent *Ug99* strain. Increasing vulnerability to further spread and emergence of stem rust. “Digula” pathotypes and the *Ug99* lineage has developed virulence to multiple other resistance genes namely, *Sr21*, *Sr24*, *Sr36*, *Sr38*, and *SrTmp*. Resistance genes still capable of protecting wheat against the highly virulent pathotypes of *Pgt* include *Sr2*, *Sr23*, *Sr25*, *Sr33*, *Sr35*, *Sr45* and *Sr50*. More than seventy of those genes are designated to stripe rust (Yr), however, majority of those genes are no longer effective against *Pst* populations. Leaf rust resistance is mediated by 68

resistance genes, with *Lr1*, *Lr3*, *Lr10* and *Lr20* most widely cultivated (Figueroa, Hammond-Kosack and Solomon, 2018).

The ten pathotype-specific resistance gene recently cloned (*Sr22*, *Sr33*, *Sr35*, *Sr45*, *Sr50*, *Yr10*, *Lr1*, *Lr10*, *Lr21*, *Lr22*) encodes for nucleotide binding sites and leucine rich repeat proteins. The resistance response of these genes is mediated by the direct or indirect recognition of Avr factors. So far, *AvrSr35* and *AvrSr50* have been characterised in wheat for stem rust (Salcedo *et al.*, 2017;Ortiz *et al.*, 2022).

2.2.7. Novel rust resistance genes used in study

Two newly cloned stem rust resistance genes have conferred near-immunity against *Ug99* and related pathotypes. The cloning of the genes opened a doorway to identifying perfect flanking markers for marker-assisted selection. Incorporating *Sr35* and *Sr45* into breeding populations can enhance protection against the devasting stem rust disease.

2.2.7.1. *Sr35*

A cloned stem rust resistance gene confers near-immunity against the virulent *Ug99 Pgt* pathotype discovered in Uganda during 1999. The gene was identified as *Sr35*, encoding coiled coil-nucleotide binding-leucine rich repeat (*CNL*) proteins. The gene was introgressed from a diploid *Triticum monococcum* into hexaploid bread wheat. The closest relative to *T. monococcum*, based on genomics, is the diploid *T. urartu*; the progenitor of the A sub-genomes to hexaploid *T. aestivum*. The *Sr35* gene is absent in *T. urartu* but is present when introgressed from *T. monococcum*. During comparative analysis, large segments of insertions and deletions were observed in the genomes of *T. urartu* and *T. monococcum* (Saintenac *et al.*, 2013; Salcedo *et al.*, 2017).

The cloning of the *Sr35* gene received priority since it confers near-immunity against the *Ug99* pathotype, related pathotypes and the TRTTF pathotype groups present in Iran, Yemen, and Africa (Singh *et al*., 2011). After the successful transfer of *Sr35* into hexaploid wheat (*T.*

aestivum), the gene remained effective against the virulent pathotypes (Saintenac *et al.*, 2013).

Sr35 present in *T*. *monococcum* was located on the long arm of chromosome 3A. Several molecular markers obtained from *Brachypodium distachyon* was used to map the *Sr35* gene between the *AK331487* and *AK332451* markers. The *Sr35* gene region was sequenced using three overlapping bacterial artificial chromosomes (BACs), these sequences consisted of *CNL* proteins. The sequence cluster consisted of five resistance genes encoding the same protein products namely, *CNL1*, *CNL2*, *CNL4*, *CNL6* and *CNL9* (Saintenac *et al.*, 2013).

Accession with mutations in *CNL9* were all susceptible to the virulent *Ug99* pathotype, this suggested that the *CNL9* gene confer resistance against the virulent *Ug99* pathotype. The mutations confirmed that the presence of *CNL9* is required to confer resistance and that the leucine-rich repeat region is essential for the functioning of the gene. Both *CNL9* and *Sr35* share the same pathotype specificity and based on various tests conducted regarding natural variation, mutations, and transgenic wheat lines, it was concluded that *CNL9* is designated as *Sr35* (Saintenac *et al.*, 2013).

Several SSR markers (*Xcfa2076*, *Xcfa2170*, *Xcfa2193*) linked to Sr35 was identified as useful for marker assisted selection. In 2014, the SSR markers were tested on wheat lines at the SU-PBL. The markers were undiagnostic in distinguishing between resistant and susceptible lines (Springfield, 2014). In 2014, a perfect dominant PCR marker was identified for *Sr35*. The marker was located spanning across the coding region of the *Sr35* locus. The marker specificities were communicated on https://maswheat.ucdavis.edu database.

2.2.7.2. *Sr45*

The *Sr45* resistance gene was derived from the diploid *Aegilops taushii*, the D-sub-genome progenitor of *Triticum aestivum* L. The gene was discovered in the Ae. *tauschii* accession number RL5289, the same accession the *Lr21* gene was sourced from (Steuernagel *et al.*, 2016). Singular deployment of the gene precluded its use in Canadian breeding programmes. Virulence surveys conducted in South Africa revealed low virulence to *Sr45*. The gene provide

effective resistance against *Ug99* and *Bgt* pathotypes from South Africa, Australia, and India (Periyannan *et al.*, 2014; Hatta *et al.*, 2021).

The linkage map of *Sr45* located the gene on the short arm of chromosome 1DS. Situated only 10 cM from the *Sr33* gene also derived from *Ae*. *tauschii*. Several studies have identified the presence of *Sr45* in breeding line “Thatcher” (+ *Lr21*) containing leaf rust resistance. Additional breeding lines carrying *Sr45* has been derived from cross pollination events. A PCR-based co-dominant marker *cssu45* was developed from the genomic sequence of *Ae*. *tauschii*. The PCR marker is closely associated with the *Sr45* gene at 0.35 cM and has flanked the gene in different genetic populations (Periyannan *et al.*, 2014; Steuernagel *et al.*, 2016) . The marker was tested on wheat lines at the SU-PBL and was diagnostic in distinguishing between resistant and susceptible lines (Springfield, 2014).

2.3. Powdery mildew disease

Powdery mildew of wheat is caused by *Blumeria graminis* (DC) E.O. Speer f. sp. *tritici* Em. Marchal (syn. *Erysiphe graminis* DC f. sp. *tritici* Marchal) is an ascomycete classified into the *Erysiphaceae* family. *B*. *graminis* is an obligate fungal parasite, highly specific in host species parasitism. Eight *B*. *graminis* formae speciales have been reported, certain forms parasitize wild grasses while others affect cereals. Based on classification, it is suggested that *Blumeria graminis* f.sp. *tritici* primarily colonise wheat cereal crops (Pietrusińska and Tratwal, 2020).

2.3.1. Life cycle of powdery mildew

The life cycle of *B*. *graminis* consists of two productive stages either sexual reproduction (ascosporal) or asexual reproduction (conidial). Optimal temperatures for disease progress can range from 5 – 30°C with a relative humidity of 50 – 100%, but for optimal performance, conditions should be 12 – 30°C with 100% humidity. Conidiation can occur every 7 to 10 days under these conditions. Symptoms of powdery mildew disease include white fluffy pustules

initially on lower leaf surfaces. Under favourable conditions, disease progresses to sheaths, stems and spikes; forming larger pustules (Pietrusińska and Tratwal, 2020).

During sexual production dark fruiting bodies called chasmothecia, formerly cleistothecia (135 – 224 µm in diameter) are produced as overwintering structures. Chasmothecia are spherical structures surrounded by filamentous appendages, containing 8 – 25 immature asci. Ascospores are formed within asci and when matured are forcefully released from ascocarps (Pietrusińska and Tratwal, 2020). Upon contact with moist leaf surfaces, ascospores germinate forming germ tubes, and infects host via penetration pegs and haustorium formation. Germinated ascospores produce septate hyphae that contribute to colony formation. Conidiophores initiates when undifferentiated conidia are formed directly from hyphae (Jankovics *et al.*, 2015). During asexual reproduction, growing mycelia multiples conidiophores and conidia to spread infection; forming dense pustules of new conidia Conidiospores are colourless ellipsoid structures arranged in chains on conidiophores. Conidiation can produce successive cycles during a growing season, continuously infecting host tissue (Zeng *et al.*, 2017).

2.3.2. Genetic resistance to powdery mildew

Modern wheat breeding programmes prioritize high yielding components and desired agronomic traits. Selection pressure for these traits results in loss of genetic diversity for disease resistance. To restore diversity, wheat wild relatives possess high diversity for powdery mildew resistance with more than 50 *Pm* genes derived from these wild types. The resistance mechanisms of these genes can either be classified as pathotype-specific resistance or broad-spectrum resistance (Kang *et al.*, 2020).

The resistance mechanism of pathotype-specific powdery mildew genes is mediated by the presence of a dominant resistant gene (R-gene) and the corresponding avirulence gene (*Avr*) of the pathogen. The presence of a recessive allele in either the R gene or *Avr* gene results in disease susceptibility. Only six R-genes (*Pm2*, *Pm3*, *Pm8*, *Pm17*, *Pm21* and *Pm60*) have been cloned, all encoding for nucleotide-binding site leucine-rich repeat proteins.

Singular deployed R genes are short-lived when pathogen populations evolve. Typical “boom-and-bust” cycles are observed in these cases as virulence profiles change. During each cycle, a new R-gene is comprised by changes in the population genotype. Gene pyramiding is a favourable breeding strategy to prolong the efficiency of pathotype-specific resistance. However, the quantity of R genes stacked is not directly proportional to durable powdery mildew resistance. It is important to select the correct genes for stacking to ensure durability (Kang *et al.*, 2020).

The mechanism of broad-spectrum resistance is highly diverse, mediated by a multigenic base, with some overlapping qualities of pathotype-specific resistance. It displays a slow-mildewing effect with partial resistance or adult plant resistance (APR) expressed after seedling stage. Broad-spectrum resistance can be refined as either one of the following: incomplete expression of a dominant R-gene, resistance mediated by APR genes or the presence of minor genes with additive effects. Quantitative resistance does not eradicate the disease, but instead minimises inoculum production and duration. Some APR cultivars display qualitative resistance patterns, usually conferred by a single dominant APR gene (Kang *et al.*, 2020).

Widely deployed APR gene *Pm38* is associated with leaf rust and stripe rust resistance. It is a major gene with mendelian inheritance. Compared to qualitative resistance, the resistance conferred by APR genes are more durable and robust than R-genes. Some APR genes may provide additional protection against multiple pathogens. Through co-existence in a wheat variety, the durability of R-genes can be enhanced when combined with APR genes conferring quantitative resistance (Kang *et al.*, 2020).

2.3.3. Powdery mildew resistance genes used in study

The development of cultivars conferring resistance towards powdery mildew requires the availability of viable *Pm* genes. The wheat chromosome 7AL has been identified as a reliable source for powdery mildew resistance genes. Virulence profiles of *Pm* genes to *Bgt* isolates collected across the Western Cape province of South Africa was used for gene selection.

Genes with low virulence to tested *Bgt* isolates were selected for further evaluation (Kloppe *et al.*, 2022).

2.3.3.1. *Pm37*

Pm37 is a dominant resistance gene that was transferred from *T*. *timopheevii* subsp. *armeniacum* (AAGG, 2n = 28) into hexaploid wheat. The wheat germplasm with accession "NC-AG11" is a F_7-derived line from a cross between a soft red winter wheat cultivar "Saluda" and a *T*. *timopheevii* subsp. *armeniacum* accession PI 427315. Marking the first *Pm* gene to be transferred from *T*. *timopheevii* to the A sub-genome of bread wheat. The parental line "Saluda" possesses the *Pm3a* resistance gene (Perugini *et al.*, 2008). *Pm3a* is no longer effective against *Bgt* populations in United States, Brazil, Egypt, and Turkey. However, *Pm3a* has relatively low virulence to *Bgt* isolates collected across South Africa (Kloppe *et al.*, 2022).

Pm1 alleles (*Pm1a-e*) were differentiated from each other and from the resistance gene in "NC-AG11". The *Bgt* gene in "NC-AG11" was different from the five *Pm1* alleles and displayed no allelism to the multi-allelic *Pm1* locus. However, based on the observed ratio of the segregating pattern, the novel resistance gene in "NC-AG11" expressed linkage to the *Pm1* locus and could therefore be jointly transferred (Perugini *et al.*, 2008).

The linkage map of *Pm37* located the gene on the long arm of chromosome 7A, situated proximal to the *Pm1* locus. Seven SSR markers (*Xwmc273*, *Xwmc346*, *Xwmc525*, *Xwmc790*, *Xgwm332*, *Xcfa2019*, *Xcfa2040*) was polymorphic between "NC-AG11", "Axminster" and "Saluda". Two co-dominant SSR markers (*Xgwm332*, *Xwmc790*) closely linked to *Pm37* was diagnostic in distinguishing between resistant and susceptible lines. The markers were mapped 0.5 cM proximal and distal to the *Pm37* locus (Perugini *et al.*, 2008).

2.3.3.2. *Pm4b*

French wheat cultivar "VPM1", [*Aegilops ventricose*/*T*. *turgidum* L. var. *carthlicum* (*T*. *persicum*)//3***T*. *aestivum* cv. Marne], confers effective resistance against powdery mildew. This cultivar was developed through the complex interspecific cross between *Aegilops*

ventricosa and *Triticum persicum*. The *Pm4b* gene present in the “VPM1” cultivar was located on a chromosomal segment present in *T*. *persicum*. *Pm4b* was successfully translocated from *Triticum persicum* to the long arm of chromosome 2A in hexaploid *T*. *aestivum* L. In addition, the gene was used to improve powdery mildew in triticale (x *Triticosecale Wittmack*). The inheritance of *Pm4b* is as a single dominant gene (Wu *et al.*, 2018).

Genetic mapping of closely linked molecular markers to the *Pm4b* gene region was significantly limited due to its origin. However, based on previous marker research conducted, an STS marker (STS470) was developed and located 3.0 cM from the *Pm4b* gene. Another microsatellite marker developed from a random amplified polymorphic DNA (RAPD) fragment was located 4.9 cM from the gene. Genetic linkage analysis revealed that the *Pm4b* gene was located between the 2AL122 marker and the distal end of chromosome 2AL. The genome sequence of this region was used to design SSR primers. Twelve SSR primers were found to be polymorphic between the resistant and susceptible parental lines. The *Pm4b* gene was flanked by diagnostic SSR markers *Xics13* and *Xics43*, linked to the gene at a genetic distance of 1.3 and 1.7 cM, respectively (Wu *et al.*, 2018).

2.3.3.3. *MLAG12*

The *MLAG12* gene is a dominant resistance gene introgressed from *Triticum timopheevii* subsp. *armeniacum* into a hexaploid bread wheat background. The wheat germplasm with accession “NC-AG12” is a BC_2F_7- derived line from a cross between *T*. *timopheevii* subsp. *armeniacum* accession “PI 538457” with a soft red wheat cultivar “Saluda” (Maxwell *et al.*, 2009).

F_2-populations derived from the NC-AG12/Saluda cross was used to assess the gene action of the resistance in “NC-AG12”. F_2-populations derived from the cross between “NC-AG12”, and “Axminster” (*Pm1a*) was used to assess possible linkage of the resistance gene and the multi-allelic *Pm1* locus. The resistance in “NC-AG12” is conferred by a single dominant gene, with possible linkage to the *Pm1* locus at a recombination value of 11.1 cM. The gene

was therefore, temporarily designated as *MLAG12* until further allelism tests are conducted (Maxwell *et al.*, 2009).

Linkage map of MLAG12 located the gene on the long arm of chromosome 7AL. Nine SSR markers (*Xgwm332*, *Xwmc790*, *Xwmc116*, *Xcfa2040*, *Xmag2185*, *Xwmc525*, *Xwmc346*, *Xwmc273*, *Xwmc809*) was found to be polymorphic between the resistant and susceptible parental lines. Linkage analysis revealed that *MLAG12* was flanked by SSR markers *Xwmc346* and *Xwmc273* at a genetic distance of 6.6 and 8.3 cM, respectively (Maxwell *et al.*, 2009).

2.3.3.4. *MLUM15*

The *MLUM15* is the first documented powdery mildew resistance gene introgressed from *Aegilops neglecta* into hexaploid wheat. The wheat germplasm with accession “NC-UM15” is a BC_2F_8-derived line from a cross between soft red winter wheat cultivar “Saluda” and an *Ae*. *neglecta* accession “TTCC 223”. The parental line “Saluda” possesses the *Pm3a* resistance gene. High levels of virulence were displayed to “Saluda” in the *Bgt* isolates tested. “NC-UM15” displayed significantly lower levels of virulence, with recorded disease scores of 0 – 1. The inheritance of the resistance in “NC-UM15” was conferred by a single dominant gene temporarily designated as *MLUM15* (Worthington *et al.*, 2014).

Linkage maps generated of *MLUM15* located the gene on the long arm of chromosome 7A, along with at least twelve other temporary designated genes. The gene was mapped in close linkage with the multi-allelic *Pm1* locus on chromosome 7AL. Nineteen markers previously mapped to chromosome 7AL were tested for polymorphisms. Six SSR markers (*Xwmc116*, *Xwmc332*, *Xwmc525*, *Xwmc790*, *Xcfa2240*, *Xcfa2257*) and one STS marker (*Xmag2185*) was found to be polymorphic between resistant and susceptible lines. The markers were used to generate a basic linkage map, designed to calculate recombination frequencies and genetic distances in centimorgan (cM) between the resistance gene and the molecular markers. SSR markers *Xcfa2257* and *Xcfa2240* was mapped at 1.2 cM on either side of *MLUM15.* Although SSR marker *Xcfa2257* was previously located more proximal on

chromosome 7AL, several other studies have located the marker in close genetic linkage to *Xcfa2240* (Worthington *et al.*, 2014).

Chromosome 7AL is a hotspot for powdery mildew resistance genes introgressed from wild wheat relatives. Specifically, the distal region of the chromosome, possessing multiple powdery mildew resistance genes. Several of these genes are in linkage or allelic to the multi-allelic *Pm1* locus because of shared linkage with molecular markers. Worthington *et al.* (2014) proposed that *MLUM15* and *Pm1a* were allelic until further allelism tests are conducted. According to a recent study by Kloppe *et al.* (2022), co-segregation of virulence and avirulence was observed between the two alleles. It was proposed that alleles *Pm1a* and *MLUM15* could have different, but overlapping recognition specificities for avirulence effector alleles *AvrPm1a* and *AvrMLUM15*. Resulting in both *Bgt* resistance genes being recognised by both avirulence effector genes (Kloppe *et al.*, 2022).

2.4. Fusarium Head Blight

Fusarium head blight (FHB) is a fungal disease that affects cereal crops such as bread wheat (*Triticum aestivum* L.). Occurrence of FHB causes substantial loss to wheat production on a global scale (Van Coller *et al.*, 2022). *Fusarium* spp. are hemi-biotrophic fungal pathogens that can survive on both living or necrotic plant tissue (Brown *et al.*, 2010). The *Fusarium* spp. predominantly associated with wheat in South Africa is *Fusarium graminearum* sensu lato (s.l.) *Schwabe* (teleomorph *Gibberella zeae* (Schwein.) Petch.) causing head blight symptoms (Van Coller *et al.*, 2022; Beukes *et al.*, 2017).

Fusarium head blight is ranked the fourth most important plant fungal pathogen worldwide. The pathogen is predominantly observed in temperate climates where cereal crops are cultivated. Crops are most susceptible to infection during anthesis when FHB can systemically infest the entire spike (Shude, Yobo and Mbili, 2020). The infestation of *F. graminearum* reduces both the quantity and quality of wheat grain when conditions are favourable, inoculum levels are high and host material are susceptible. During high disease

progression, the pathogen can produce substantial levels of secondary metabolites, called mycotoxins, in the form of estrogenic zearalenone (ZEA) and trichothecene mycotoxins, such as deoxynivalenol (DON) and nivalenol (NIV). The ingestion of mycotoxins can cause acute health conditions in both humans and animals (Schiro *et al.*, 2018).

2.4.1. Causal organisms

Fusarium head blight is caused by species within the *F. graminearum* species complex (FGSC), comprising of more than 17 identified species (Beukes *et al.*, 2017). The causal pathogens are highly diverse with variations in environmental adaptations and requirements among species that results in disease distribution and epidemics in a variety of climatic conditions (Shude, Yobo and Mbili, 2020). The *Fusarium* species associated with wheat includes *F. graminearum*, *F. cerealis* (Cooke) Sacc, *F. avenaceum* (Fries) Saccardo, *F. culmorum* (W.G. Smith) Sacc., and *F. poae* (Van Coller *et al.*, 2022; Beukes *et al.*, 2017). The most predominant *Fusarium* species associated with wheat produced in South Africa and worldwide is *F. graminearum*. This may differ among various locations and time periods, depending on the temperature and humidity within the region (Boutigny *et al.*, 2011). The occurrence of *F. avenaceum* (fr.) Sacc and *F. culmorum* (Fc) (W.G. Smith) are commonly recorded in cooler regions of the world, while *F. graminearum* is predominant in temperate regions with higher relative humidity (**Figure 2.8**).

Figure 2.8. Global illustration of recorded *Fusarium graminearum* outbreaks, displaying the general distribution of the species (Shude, Yobo and Mbili, 2020)

2.4.2. Disease cycle

Fusarium graminearum is known for having both a sexual and asexual life cycle. *Fusarium spp.* produces haploid mycelia in both stages of the cycle. The asexual phase can consist of 3 different types of mitotic spore formations within the mycelial structures, namely microconidia, macroconidia and chlamydospores (**Figure 2.9**). Microconidia are formed directly from conidiophores within the perithecium, while macroconidia are produced directly from the sporodochium. These spores serve as colonising agents meant to initiate host infection via flowers, stems, or seeds and are usually dispersed by wind (**Figure 2.10**). Chlamydospores are formed either on or within fungal hyphae or macroconidia, which can either infect the host directly or lay dormant as overwintering structures used to restart the cycle once optimal conditions return (Ma *et al.*, 2013).

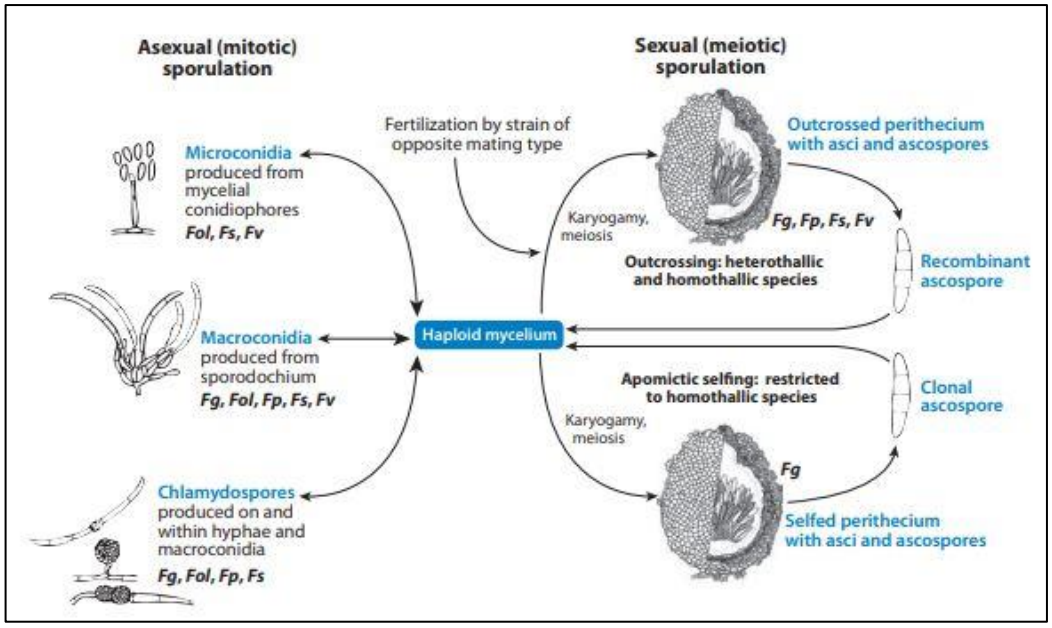

Figure 2.9. Schematic breakdown of the *Fusarium* spore formation among heterothallic and homothallic species (Ma *et al.*, 2013).

Although uncommon, *Fusarium spp.* can also produce ascospores as a source of inoculum that survives on plant residue left from the previous growing season (**Figure 2.10**). *Fusarium graminearum* is a homothallic species producing sexual ascospores without a compatible sexual partner during the binucleate phase. This is achieved by fusing two genetically identical binucleate cells (Trail, 2009). Homothallism in *F. graminearum* is mediated by the presence of both mating types (*Mat1-1* and *Mat1-2*) in the haploid phase. The formation of ascospores is mediated by meiosis within asci embedded in the perithecium (**Figure 2.10**). Asci abruption forcibly discharges matured ascospores into the environmental through air dispersal (Trail, 2009).

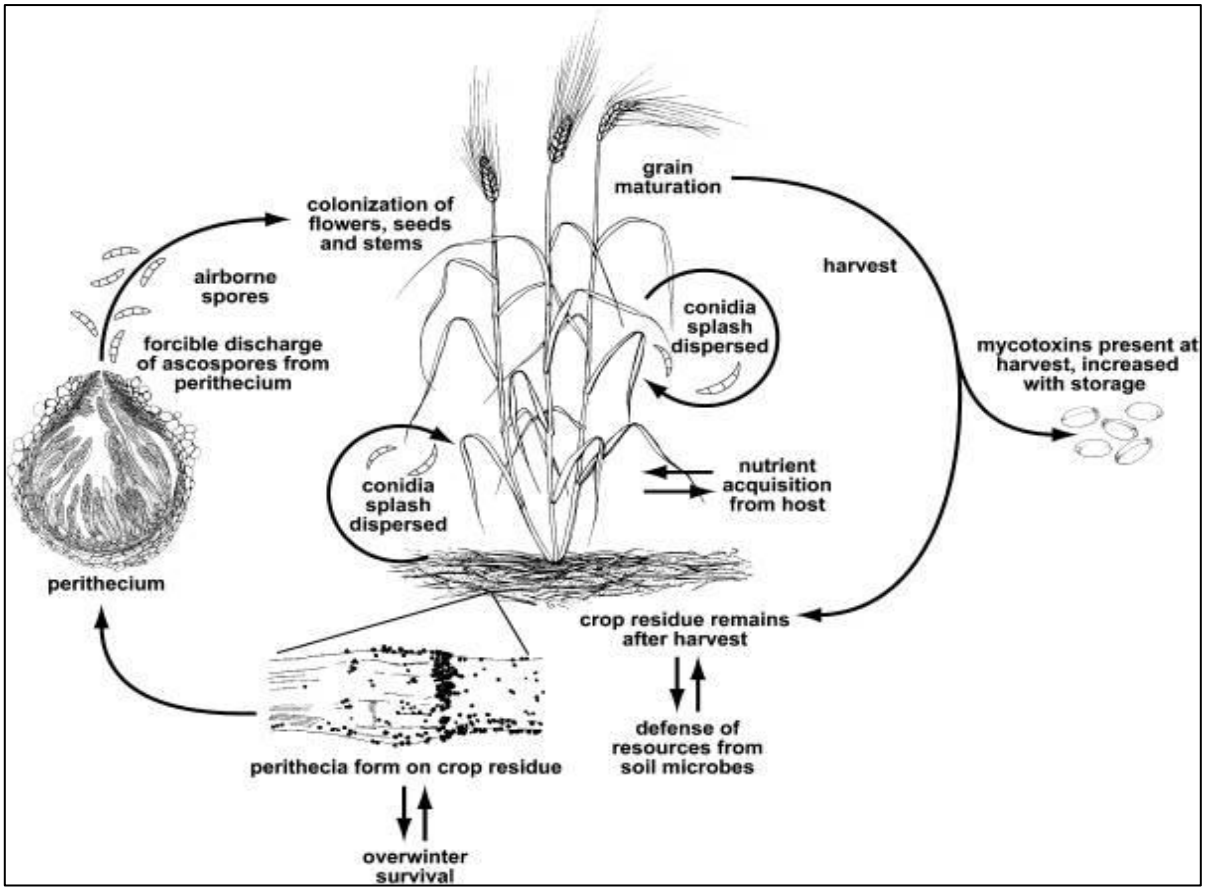

Figure 2.10. Life cycle of *Fusarium graminearum* on wheat host plant (Trail, 2009)

Fusarium graminearum infection is most damaging during the anthesis stage when anther extrusion (anther splitting) occurs to discharge matured pollen. Providing a natural opening for pathogen entry (Shude, Yobo and Mbili, 2020). A concurrent increase of temperature and relative humidity create favourable conditions for rapid disease development, with symptoms appearing between 3 – 6 days post infection (Osborne and Stein, 2007; Shude, Yobo and Mbili, 2020). During very specific conditions, symptom development of infected wheat-ears could occur within 2 days post inoculations, these conditions include; 36 h of constant moisture at 25°C. Initial infection of *F. graminearum* mimics the behaviour of a biotroph by spreading intercellularly and asymptomatically through the xylem and pith vessels (Trail, 2009).

The fungus then spreads intracellularly, rapidly infesting host tissue causing necrosis. Symptoms of water soaking are displayed shortly after colonisation, followed by final bleached appearance of infected florets. The appearance of pre-mature bleached spikes is a common symptom of FHB. Fungal colonisation of florets distinctly induces gene expression of

deoxynivalenol (DON) biosynthesis after infection. DON is the only mycotoxin with virulent properties in wheat, inducing fungal spread from florets into the wheat rachis. Further promoting necrosis of wheat heads and increasing DON accumulation in developing seed. Contaminated seed appear as shrivelled, undersized and discoloured (Shude, Yobo and Mbili, 2020).

2.4.3. Mycotoxin production

Mycotoxins are secondary metabolites produced by mycotoxigenic fungi. These naturally occurring toxins can be detrimental to the health and well-being of both humans and animals. Several mycotoxins have adverse health effects such as, carcinogenicity, genotoxicity, reproductive disorders, immunosuppression and gastrointestinal symptoms (Schaarschmidt and Fauhl-Hassek, 2018). Mycotoxins are formed by fungal species belonging to *Aspergillus* and *Penicillium* genera but in wheat it is primarily produced by *Fusarium* species. Mycotoxin content detected in wheat can include both zearalenone (ZEA) and type B trichothecenes (TCT-B), such as DON and nivalenol (NIV). These mycotoxins may also occur as their masked-forms, equally as detrimental (Malbrán *et al.*, 2014).

2.4.3.1. Zearalenone

Zearalenone is one of the most hazardous toxins of wheat grain. It is an estrogenic mycotoxin that disrupts endogenous estrogenic response in mammals. The detection of ZEA in grain can occur in the field prior to harvest. However, the accumulation of ZEA predominantly occur in silos when wheat grain is stored under improper conditions (Caglayan, Şahin and Üstündağ, 2022). Once ZEA has entered the digestive system of mammals the mycotoxin gets metabolized into two metabolites (α-ZEA and β-ZEA). If high quantities of ZEA is detected in mammals, it can cause reproductive incapability in animals and hyperestrogenism in humans (Rai, Das and Tripathi, 2020).

2.4.3.2. Trichothecenes

Trichothecenes are sesquiterpenoid mycotoxins that enhances the virulence of *F. graminearum.* These forms of mycotoxins have two central hexane cyclic rings and a tetrahydropyran (**Figure 2.11**). Four types of trichothecenes can be characterised namely, type A, B, C and D. Type A trichothecenes contains T-2 toxin and an acetylated derivative HT-2 toxin, primarily produced by *F. poae*, *F. sporotrichioides* and *F. langsethiae*. Type C and D trichothecenes are not mycotoxins produced by fungal pathogens of wheat and rarely occur in food products and animal feed (Pestka, 2007; Zingales, Fernández-Franzón and Ruiz, 2021). The most prominent form of mycotoxins on wheat is type B trichothecenes, producing DON and infrequently NIV along with their acetylated derivatives 3-acetyldeoxynivalenol (3-DON), 15-acetyldeoxynivalenol (15-ADON) and 4-acetylnivalenol (4-ANIV), respectively (Zingales, Fernández-Franzón and Ruiz, 2021). Type B trichothecenes are primarily produced by *F. graminearum* and *F. culmorum*, with *F. poae* known to induce the biosynthesis of NIV and type A mycotoxins (Zingales, Fernández-Franzón and Ruiz, 2021).

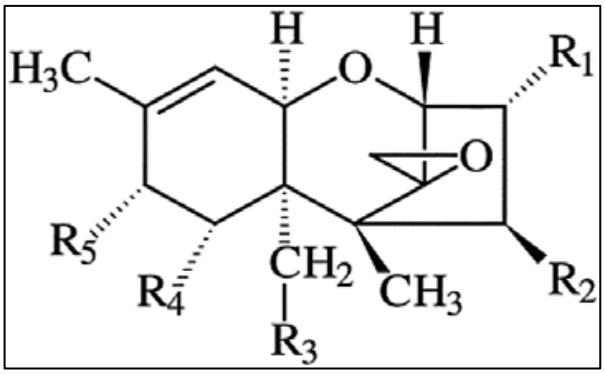

Figure 2.11. Chemical structure of a trichothecene mycotoxin (Khaneghah *et al.*, 2018)

2.4.3.2.1.Deoxynivalenol

DON is a type-B trichothecene biosynthesized by *Fusarium graminearum* and *F. culmorum*. DON is classified as a group 3 carcinogen by the International Agency for Research on Cancer (IARC). According to the FAO, the regulated maximum daily intake of DON and

DON derivatives (3-Ac-DON and 15-Ac-DON) is 1 ppb (parts per billion) body weight. The level of DON recorded to cause intoxication in humans is 50 ppb body weight. The Joint FAO/WHO Expert Committee on food Additives has set limits for DON content in various food categories, for wheat (1000 ppb), bread (500 ppb) and cereal-based products for toddlers (200 ppb) (Khaneghah *et al.*, 2018).

DON consumption can cause both chronic and acute effects. Chronic effects of DON exposure are frequently associated with weight loss, anorexia and change in nutritional efficiency. The most frequent acute effects are associated with vomiting, diarrhoea, anorexia, malaise, abdominal discomfort, and increased salivation. However, DON sensitivity of an organism is highly dependent on the metabolism, absorption, distribution, and detoxification once digested. The toxicity of DON is frequently mediated by the inhibition of protein synthesis in eukaryotic organisms. DON interacts with the 60s ribosome binding site, inhibiting the translation of the peptidyl transferase enzyme (Khaneghah *et al.*, 2018).

Modified derivatives of DON are naturally occurring masked forms of the mycotoxin, equally as toxic. The modified forms can be categorized into free-, modified forms- and matrix-associated-, mycotoxins with four hierarchal levels (Rychlik *et al.*, 2014). The analytical quantification of masked mycotoxins is a challenge as the composition of the toxin varies but the toxicity remains. Ingested food contaminated with deoxynivalenol-3-glucoside (DON-3-Glc) can enable resistance against acidic conditions of digestive enzymes. Once digested, it can convert DON-3-Glc to free DON during the interaction with the gut microbiome. Consequently, reactivating the mycotoxin and increasing the overall DON content ingested (Bryła *et al.*, 2018).

Masked forms of DON may originate from fungal metabolites. The most described are 15-acetyl deoxynivalenol (15-ADON) and 3-acetyl deoxynivalenol (3-ADON), which are descendants from 3,15-diacetyl deoxynivalenol. Detectable levels have been recorded in *Fusarium*-contaminated wheat-products. Mycotoxins may be altered via the plants defence systems by converting it into polar metabolites or via food processing systems (Khaneghah *et al.*, 2018).

2.4.3.2.2.Nivalenol

NIV is a type-B trichothecene biosynthesized by multiple *Fusarium* species. In comparison to DON, the only molecular difference is located at the C-4 position with an additional hydroxyl group (Zingales, Fernández-Franzón and Ruiz, 2021).

The toxic effects of NIV ingestion are considered more aggressive than DON ingestion based on animal studies. According to IARC, NIV is classified as a group 3 carcinogen (unclassifiable carcinogenicity to humans) deeming it non-cancerous to humans and animals. Although NIV exposure has been associated with oesophageal and gastric carcinomas, inadequate evidence exists to effectively evaluate carcinogenicity in exposed animals. NIV accumulation causes feed refusal, reduction in feed conversion efficiency, and affects liver weights in chicken. Like DON toxicity, NIV is also associated with gastrointestinal complications (Zingales, Fernández-Franzón and Ruiz, 2021).

The hazardous effects of NIV is frequently observed in countries such as China and South America (Zingales, Fernández-Franzón and Ruiz, 2021). The deposition of NIV in South African wheat grain is relatively low, with no major health concerns of NIV in wheat and wheat based products (Beukes *et al.*, 2017).

2.4.4. Management strategies

Agronomic strategies can reduce the incidence and severity of FHB infections. Effective methods that successfully reduced inoculum levels were crop rotations with known non-host crops, soil tillage and plant residue removal. Management practices that are less efficient can include cultivation of early maturing cultivars, monitoring disease outbreaks through disease forecasting, early planting of material, controlling weeds that may act as alternative hosts and optimise crop irrigation. Post-harvest management is highly effective in reducing both FHB and DON accumulation in grain during silos storage. These methods can include increasing the fan's wind speed used to dry and cool stored kernels. Indirectly, discarding and sorting through light weight damaged kernels by blowing them away (Shude, Yobo and Mbili, 2020).

Chemical control methods are evaluated to assess its efficacy on reducing FHB infections. Demethylation inhibitors (DMI) are the most generic form of fungicides used to control FHB infection and DON accumulation. A recent study conducted by Paul *et al* (2018) reported on the use of DMI fungicides applied during the Feekes 10.5.1 growth stage, presenting promising results for reducing FHB and DON. According to Cromey *et al* (2001), the timely application of tebuconazole fungicides were effective in reducing 90% of observed FHB incidence, resulting in an 14% increase in yield. Along with research reported by Palazzini, Torres and Chulze (2018), scheduled application of triazole-base fungicides has successfully reduced FHB severity, DON accumulation and directly improved yield outcomes and grain quality. The application of quinone inhibitor based fungicides has not been favourable in managing FHB, instead it has been reported to increase DON accumulation in infected wheat (Paul *et al.*, 2018). Although certain fungicides are effective in reducing FHB occurrence and DON accumulation, no fungicide has been identified to completely control the fungal disease. Therefore, the integration of chemical control along with other management strategies are recommended (Dweba *et al.*, 2017).

2.4.5. Genetic resistance to FHB

Disease resistance towards FHB is mediated by five different types of resistance. Type I resistance prevents initial infection of the fungal pathogen. Type II resistance prevents further spread of pathogen to neighbouring florets after initial infection has occurred. Type III resistance involves reduced fungal infection of developing seed. Type IV resistance is the ability to minimise loss of grain yield and quality even when the host is severely infected by FHB. Type V resistance is the ability to reduce mycotoxin accumulation in infected seed, responsible for pathogen virulence (Dweba *et al.*, 2017).

Easily identified sources of FHB resistance are predominantly mediated by type I resistance. This form of resistance can be evaluated under favourable field conditions by artificial spray inoculation methods. The most reliable form of resistance evaluated under a controlled environment is type II resistance. This form of resistance is commonly evaluated by

point inoculation of florets, restricting symptoms development to only inoculated spikes. Breeding lines evaluated for both type I and II resistance can reduce FHB incidence (initial infection) and severity (spread within spike). The integration of both resistance types into a single genotype will confer a stable and durable form of FHB resistance (Dweba *et al.*, 2017).

Germplasm are primarily evaluated for type I and II FHB resistance, with a gradual increased interest in type III and V resistance (Gilbert and Tekauz, 2000). FHB resistance is a complex quantitative trait mediated by multiple genes, strongly influenced by genotypic and phenotypic interactions. Resistance to the fungal disease is inherited quantitatively, resulting in slow breeding progress and genetic gain. The success of resistance breeding is influenced by the virulence profile of the pathogen in a given population, the availability of genetic resistance germplasm conferring desirable resistance type and the selected methodology to evaluate and select resistance (Dweba *et al.*, 2017).

Over 100 quantitative trait loci (QTLs) have already been identified. Some having larger effects (*Fhb1*, *Fhb2* and *Fhb5*) than others, with varying inheritance stability (Buerstmayr, Ban and Anderson, 2009). The major *Fhb1* QTL was derived from the “Chinese Spring” cultivar “Sumai3”, a frequently used source of FHB resistance. *Fhb1* was genetically mapped using the resistant parent “Sumai3” and the QTL was found to be located on the distal region of chromosome 3BS, accommodating seven genes (Dweba *et al.*, 2017).

2.5. Wheat breeding programmes

Wheat breeding has been practiced in South Africa since the late 1800s, reportedly initiated in the Western Cape province. During 1902 and 1904, the first initial series of artificial crosses were conducted to breed for resistance towards stem rust, better milling quality and reduced premature grain shedding. The breeding efforts during the early periods produced three wheat varieties of market value, releasing the very first wheat cultivars bred in South Africa, namely, “Union”, “Darlvan” and “Nobbs”. Breeding efforts were further advanced during 1913 by Prof

JH Neethling of Stellenbosch University, releasing 26 new wheat varieties that remained widely cultivated from 1914 to 1961 (Nhemachena and Kirsten, 2017).

Plant breeding has always been the art and science of altering the traits of crops to develop improved characteristics. The improvement of traits during conventional plant breeding can be achieved primarily through basic phenotypic selection. Successful crop improvements have been achieved through phenotypic selections of important agronomic traits, but the underlying genotypic and environmental interactions affecting these traits have made it challenging (Acquaah, 2012).

2.6. Wheat pre-breeding programmes

Pre-breeding is a technique used to identify novel traits or trait combinations to improve yield components, introduce resistance or tolerance to biotic and abiotic stressors and enhance the nutritional quality of grain. One of the most notable sources of novel traits or alleles can be obtained from the single largest wheat germplasm bank at CIMMYT. The germplasm collection contains over 150 000 samples of ‘exotic’ and non-exotic material such as, landraces, obsolete varieties, chromosome translocation lines, primary synthetic genotypes, breeding lines and related species from the primary (*Triticum*) and secondary (*Aegilops*) gene pools. Using genetic and phenotypic tools, novel traits from unadapted germplasm can successfully be deployed into suitable genetic backgrounds through strategic crossing events and selection methods (Sukumaran *et al.*, 2022).

Novel genes are discovered through mapping of traits to locate its genomic regions on a wheat chromosome. Genetic maps are obtained through genome-wide association mapping (GWAS) and quantitative trait loci (QTL) mapping. GWAS rapidly provides high resolution mapping by exploiting linkage disequilibrium. The criteria required to precisely locate the gene of interest is a large population size, high trait heritability and simple trait components. QTL mapping, also referred to as linkage mapping is a complementary mapping technique to

GWAS, where mapping populations are generated from characterised wheat lines vary in a trait of interest (Sukumaran *et al.*, 2022).

2.6.1. Recurrent mass selection

Mass selection is one of the oldest breeding strategies used for self-pollinating crops. It was common practice for farmers to store seed from best performing crops and sow them for the next cropping season. Although commonly used for self-pollinating crops, the breeding strategy can be applicable to cross-pollinating crops as well. Selections are primarily made from a genetically diverse population with high genetic variation among individuals. The main goal of mass selection is for genetic improvement of genotypes through increased frequencies of desired quantitative traits in the breeding population. Successive generation cycles can be required for adequate mass selection, referred to as recurrent mass selection (Acquaah, 2012).

The goal of breeding programmes is to enhance the genetic composition of base populations by facilitating cross pollination for recombination of genetic material. Successful recombination can be facilitated through successive cross pollination and the incremental genetic gain within the population will occur as favourable gene frequencies continuously increase. The recurrent mass selection is a cycle that comprises of four main principles; parental lines are cross pollinated to recombine genetic material, the F_1 progeny produced after recombination are non-inbred lines, breeding material generated are phenotypically and genotypically evaluated, and the best performing breeding material are selected as crossing parents for the next cycle (**Figure 2.12**). The final selection criteria can be imposed on a single desired quantitative trait or on a complex of traits (Rutkoski, Krause and Sorrells, 2022).

2.6.1.1. Male sterility

Generating artificial crosses in self-pollinating crops such as wheat can be very labour-intensive during emasculation of florets prior to anthesis and pollen introduction from donor material. The reproductive system of wheat can therefore function as a restricting factor to

accelerate crossing cycles for recurrent mass selection. Male sterility can facilitate successful cross pollination between breeding material, utilising either dominant or recessive sources of male sterility genes already identified in wheat (Rutkoski, Krause and Sorrells, 2022).

Chinese researchers have incorporated male sterility since the late 19th century, using the dominant male sterility gene *Ms2.* They developed a base population segregating for male sterile (female) and fertile (male) plants using recurrent selection breeding. Female tillers were selected and naturally cross pollinated with male tillers under field conditions. Several cultivars were released using recurrent selection facilitated by male sterility (Guttieri, 2020).

During 1999, a segregating base population was established at the SU-PBL using the dominant male-sterility gene *Ms3*. The gene was transferred from a male sterile line "KS87UP9" into recipient spring wheat "Inia66". F_1 progeny segregated in a 1:1 ratio for male sterility, producing 50% male sterile plants (Marais, Botes and Louw, 2000). The gene was initially isolated through chemical-induced mutagenesis (ethyl-methanesulfonate) from a hard red spring wheat "Chris" with *Aegilops tauschii* cytoplasm. The dominant gene was then transferred to wheat and was effective in conferring dominant male sterility (Guttieri, 2020).

The phenotypic expression of the gene is temperature sensitive; the gene remains stable under controlled greenhouse temperatures of 16 – 25°C, with incomplete expression during temperatures exceeding 25°C (Guttieri, 2020). The *Ms3* gene cannot be used effectively under field conditions, with failure to produce new cultivars. A different approach to using *Ms3* populations was through hydroponic tiller culture under controlled growth chamber conditions (Marais, Botes and Louw, 2000).

2.6.2. Marker-assisted selection

Marker-assisted selection (MAS) is a selection method focused on molecular data generated from DNA markers. Conventional MAS in breeding programmes is the identification of DNA markers closely associated with genes of interest, the validation of the diagnostic markers in the evaluated germplasm, and the selection of individual lines based on molecular data generated from the validated markers. The introduction of MAS to breeders initially

proposed that selections for desired alleles could be made solely on molecular data without phenotypic validation. However, in modern breeding systems MAS is used in conjunction with conventional selection strategies, and phenotyping methods to facilitate gene pyramiding, backcross introgression and the development of superior breeding lines in breeding programmes (Rutkoski, Krause and Sorrells, 2022).

Several agronomically significant traits are complex quantitative traits and requires QTL mapping techniques to identify marker-trait associations. Molecular markers are used in marker-assisted breeding to molecularly characterise breeding material. Selections for complex traits such as disease resistance are more precise using MAS compared to relying on phenotypic expression for selection. Subsequently, shortening the breeding cycle for crop improvement.

Many QTLs closely associated with resistance genes have already been successfully identified in wheat. QTL-MAS can identify novel genes and alleles of interest for introduction into pre-breeding programmes for introgression. The integration of MAS and a derivative of MAS namely, genomic selection can increase the efficiency of breeding programmes by also detecting minor effect QTLs along with large effect QTLs. Genomic selection can also detect breeding lines with high genomic estimated breeding values (GEBV) for the traits of interest. GEBV-based selection predicts that each breeding line selected will display a superior phenotype, reducing the generation time required for selecting crossing parents (Kang *et al.*, 2020).

Marker-assisted pyramiding is a technique facilitated by MAS, involving the simultaneous deployment of multiple genes or QTLs into a single genetic background. Gene pyramiding is important to strengthen durability for broad-spectrum and long-term disease resistance. The introgression of several resistance genes and QTLs have been the primary goal of pyramiding in pre-breeding programmes (Hasan *et al.*, 2021). The initial introduction of gene pyramiding was not favourable before MAS as certain genes expressed epistatic effects, making it difficult to phenotype masked genes (Joshi and Nayak, 2010). Several resistance genes can confer

resistance against different isolates or pathotypes. The introduction of multiple genes requires multiple mutational or recombination events to occur before new virulent pathotypes emerge.

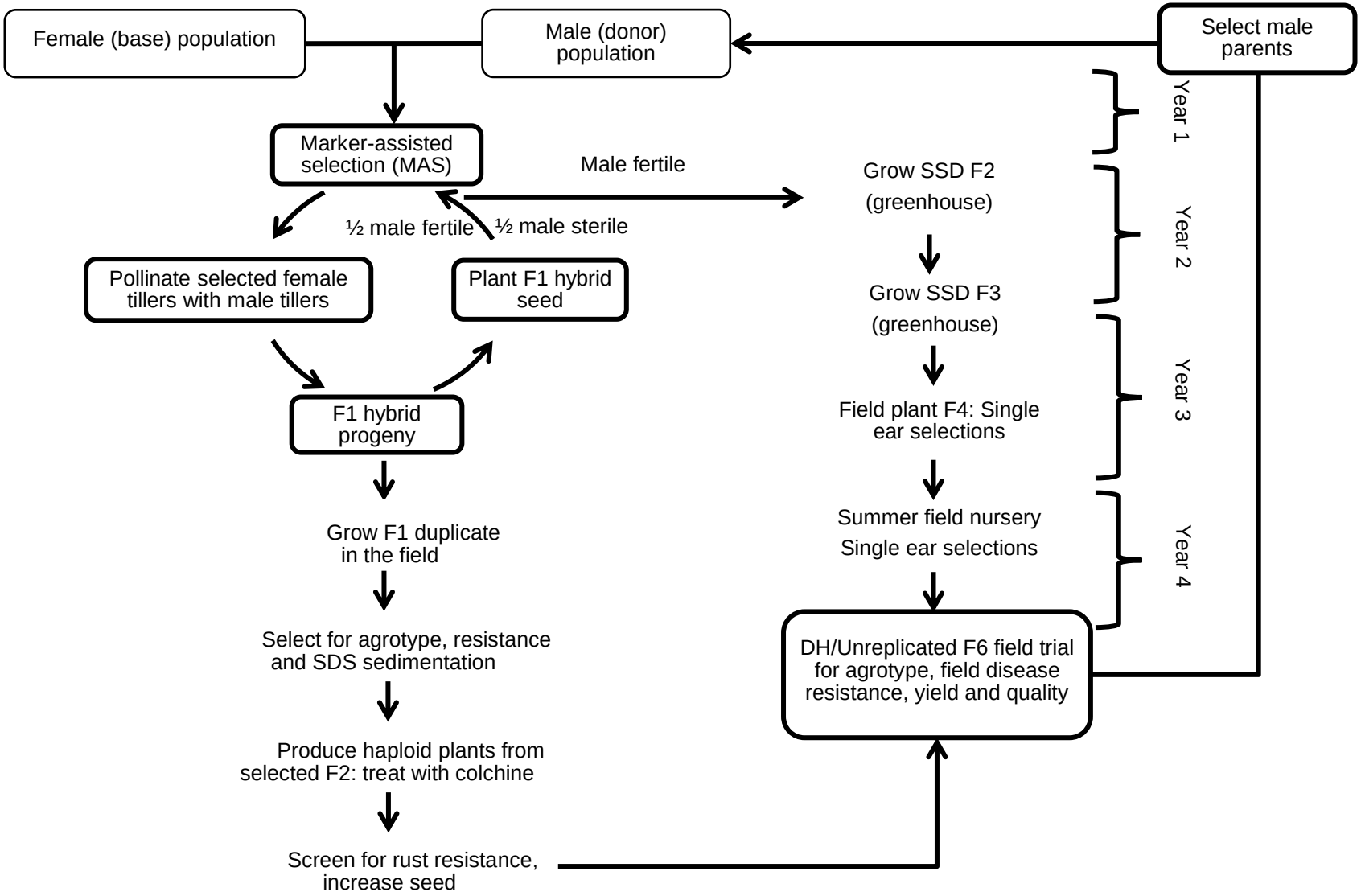

Figure 2.12. Schematic diagram of MS-MARS facilitated breeding programme at the SU-PBL (Springfield, 2014).

Chapter 3. Materials and Methods

3.1. Introduction

The aim of the study was to identify crossing parents with disease resistance to introduce into the male-sterility mediated marker-assisted recurrent selection (MS-MARS) pre-breeding programme (**Figure 2.12**). The donor populations characterised for disease resistance comprised of the SU-PBL's 2020 wheat nursery and an FHB CIMMYT nursery. The two nurseries were screened to identify rust, powdery mildew and FHB resistance for introduction into the recurrent population. The female population was a highly diverse recurrent population established at the SU-PBL in 1999. The recurrent population segregated for rust resistance and dominant male sterility (Marais, Botes and Louw, 2000).

Genomic DNA extractions was performed on both male and female populations. The extraction procedure was derived from a protocol designed by Doyle and Doyle (1987). All populations were molecularly characterised prior to the MS-MARS cycle using the standard panel of markers at the SU-PBL (Wessels and Botes, 2014). Additionally, 28 selected genotypes from the SU-PBL's 2020 wheat nursery were molecularly screened with markers for powdery mildew genes *Pm37*, *Pm4b*, *MLAG12* and *MLUM15*. Five genotypes from the FHB CIMMYT nursery were molecularly screened with targeted markers for FHB QTLs *Qfhs.ifa.5A*, *7AQTL* and *Qfhs.ndsu.3BS*.

Validation of the MS-MARS scheme was done by selecting male sterile tillers from the recurrent base population (segregating in a 1:1 ratio for male sterility/fertility) and cross pollinating it with selected donor lines from the male populations. The F_1 hybrid seed generated after cross pollination was planted for the next MS-MARS cycle as the new segregating base population. The male fertile seed were allowed to self-pollinate, and were field planted (**Figure 3.1**).

Powdery mildew resistance was phenotypically assessed at the seedling stage using a vacuum-operated settling tower. The infection type of each genotype was scored accordingly.

Type II FHB resistance was evaluated using an adjusted spray inoculation method. Inoculated material was phenotypically assessed for disease severity, mycotoxin accumulation, fusarium damaged kernels (FDK) and yield parameters.

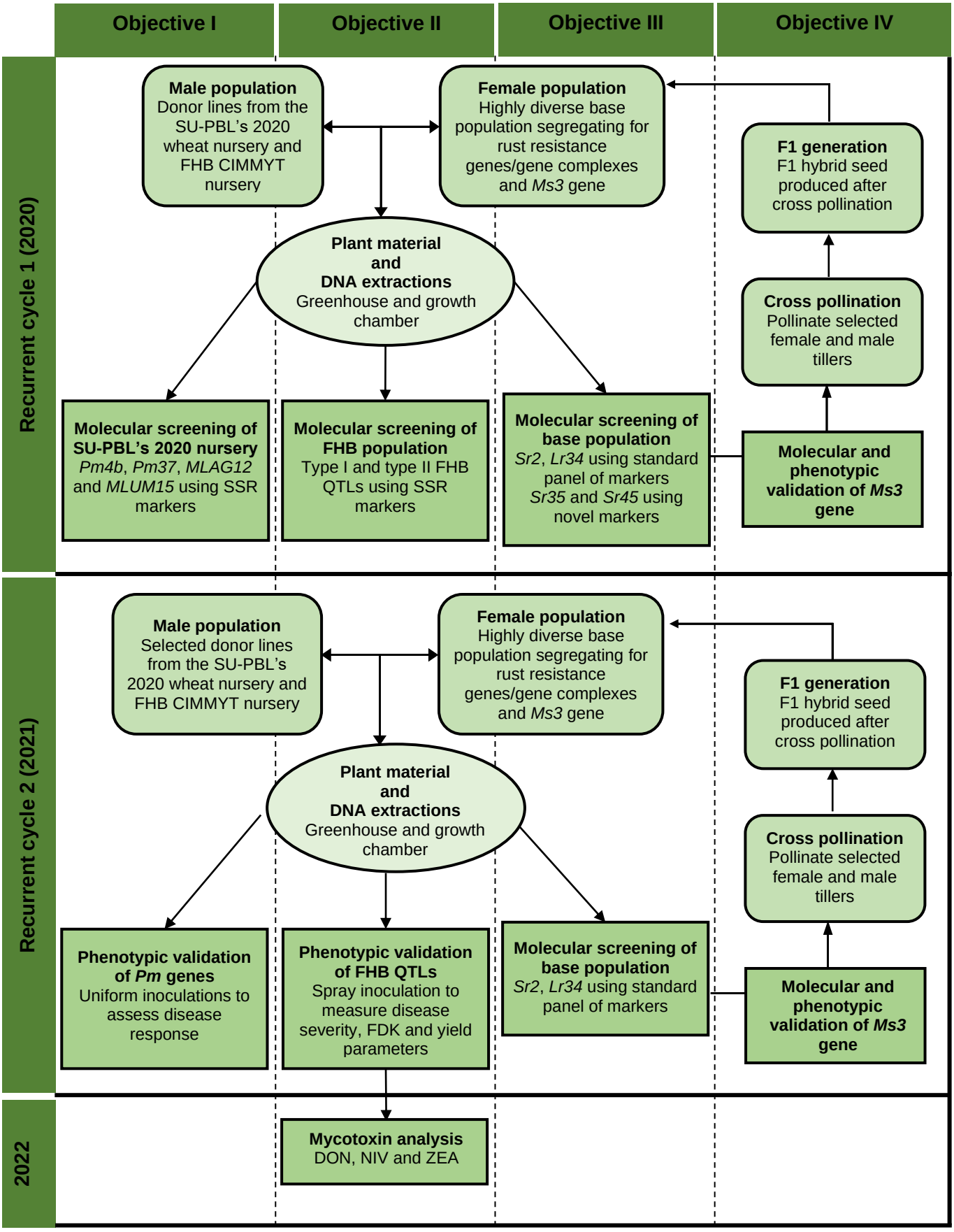

Figure 3.1. Schematic diagram of workflow towards completion of research project

3.2. Plant material

The plant material used for this study comprised of an F_6 segregating base population established at the SU-PBL in 1999. This population was used as the female recipients during the MS-MARS pre-breeding scheme. The recurrent population had high genetic diversity and segregated for rust resistant genes and gene complexes such as, *Lr34*/*Yr18*/*Pm38*, *Sr2*/*Yr30*, *Lr19*, *Lr21*, *Sr31*/*Lr26*/*Yr9*, *Lr24*/*r24* and *Lr37*/*Sr38*/*Yr17*. The base population also segregate for the *Ms3* gene, located on the centromeric region of chromosome 5AS. Gene segregation occurred in a 1:1 ratio for male sterility and fertility. Hybrid seed planted for the 2020 MS-MARS cycle conformed to the 1:1 segregating ratio.

During the 2020 MS-MARS cycle, a total of 480 pots were planted for the recurrent population, with five seeds sown per pot. The donor population was obtained from the SU-PBL's 2020 wheat nursery (20USP, 20US3M and 20US1M) of 320 wheat entries and an FHB CIMMYT wheat nursery of 28 wheat entries. The greenhouse layout included four benches on either side of the greenhouse, each with six rows containing 20 pots. The recurrent population was planted on the one side and the donor population was planted on the other. The material was planted in a greenhouse at the Welgevallen experimental farm, Stellenbosch University.

For the 2021 MS-MARS cycle, a total of 285 pots were allocated for the recurrent population, with five seeds sown per pot. The donor population was reduced to only 28 and 5 selected entries from the SU-PBL's 2020 wheat nursery and the FHB CIMMYT nursery, respectively. Plant material was grown in a cooled greenhouse with temperatures ranging between 10 – 35°C at the Welgevallen experimental farm, Stellenbosch University.

Plant material used in the FHB inoculation trial comprised of an FHB CIMMYT nursery initially containing a total of 56 wheat entries; 29 of the entries sourced from the SU-PBL's F_6 population and 27 entries from an FHB CIMMYT nursery. Five selected genotypes were carried through to the 2021 FHB inoculation trial, with two wheat lines belonging to SU-PBL's F_6-population and three to the FHB CIMMYT nursery. Three (3) replicates of each entry, including "Sumai3" (resistant control) and "PAN3471" (susceptible control) were planted. The

experimental design was a completely randomised block design with randomisation implemented through differential inoculation. The sowing date commenced in May 2022, with a total of six seeds sown into 9 litre planting bags filled with peat soil. The plant material was grown in a cooled glasshouse with night and day temperatures ranging between 10 – 19°C and 20 – 40°C, respectively. Induced humidity ranged between 30 – 70%.

Plant material used for powdery mildew assessment was sourced from the SU-PBL's 2020 wheat nursery. The selected 28 wheat entries were carries through for phenotypic evaluations. Nine seeds were sown into $9 \times 9 \times 9$ cm nursery plant pots. The material was planted in a growth chamber until the two-leaf stage and transferred to a growth cabinet after *Bgt* inoculations. Incubation conditions were set at 18°C under 12 hr light and dark photoperiod cycles.

Plant material was irrigated daily with nutrient solution consisting of 164 g Sol-u-fert T3T, 2 g Microplex, 0.05% Jik and 77 ml potassium nitrate in 100 L H_2O. During the 2021 MS-MARS cycle, EZ fertigation nutrient solution was used to drip irrigate crossing material in the greenhouse. The concentrated solution was diluted in a 1:4 ratio with municipal water.

3.2.1. Genomic DNA extraction of wheat material

The CTAB (Cetyl trimethylammonium bromide) DNA extraction method developed by Doyle and Doyle (1987) was used to extract the genomic material from wheat lines. The primary leaves from wheat lines were cut with sterile scissors at the two-leaf stage (14 days) and placed into 2 ml microcentrifuge tubes. Each microcentrifuge tube contained 3 steel ball bearings with 500 µl CTAB buffering solution [100 mM Tris-Cl (pH 8) 1.4 M NaCl, 20 mM EDTA (pH 8)], and was placed into a Qiagen® Tissue Lyzer (Qiagen, South Cross Biotech, Claremont, RSA) for 30 sec set at 30 Hz.

Once completely ground, the samples were placed into a preheated water bath for 15 min set at 55 – 60°C. The samples were removed from the water bath and allowed to cool. Once cooled, 500 µl of C:I (480 ml Chloroform: 20 ml Isoamylalcohol) was added to each microcentrifuge tube and centrifuged at 14000 rpm for 10 min. The supernatant formed was

transferred to a clean 1.5 ml labelled microcentrifuge tubes, followed by the addition of 400 µl of C:I. After the samples were mixed by inversion, they were centrifuged at 14000 rpm for 5 min. The supernatant formed after centrifuging the samples were transferred to a different set of 1.5 ml microcentrifuge tubes and received 50 µl of 3 M Sodium Acetate, followed by 500 µl of pure ethanol stored at -4°C.

The samples were slowly mixed by inversion until the genomic DNA of each wheat sample was precipitated within the microcentrifuge tubes. The precipitated DNA samples were centrifuged at 14000 rpm for 2 min to form a pellet at the bottom of the microcentrifuge tube. The DNA pellets were washed twice with 70% ethanol and allowed to air dry. Once dried, the DNA was resuspended with 25 µl of ddH_2O.

The quality and quantity of the extracted DNA samples were tested using a ThermoFisher Nanodrop® ND-1000 Spectrometer (ThermoFisher Scientific Inc., Kempton Park, South Africa). The quality of the samples was determined based on 260/230 and 260/230 absorbance ratios. The quantity (ng/µl) of the DNA samples was determined based on Beer-Lambert Law by measuring the absorption of light for each sample. The results obtained was used to calculate the dilutions of each DNA sample to a final concentration of 100 ng/µl.

3.3. Molecular characterisation of plant material

The stock solutions of all primer sets used in the study was sourced from Integrated DNA Technologies (Whitehead Scientific Inc, Stikland, RSA). The primer sets were diluted to a final concentration of 10 pmol/µL for PCR reaction mixtures. All PCR reactions were performed in a SimpliAmp™ Thermal Cycler (Applied Biosystems™, Fairland, RSA). PCR products amplified were visualised using 2% agarose gel stained with ethidium bromide and 6% polyacrylamide gel electrophoresis.

3.3.1. Marker identification for powdery mildew resistance genes

The SU-PBL's 2020 wheat nursery was molecularly characterised for powdery mildew resistance. Two microsatellite markers were identified for each powdery mildew resistance

gene. The *Pm* genes selected for molecular screening included *Pm4b*, *Pm37, MLAG12* and *MLUM15* (Table 3.3). Primer sets for *Pm4b* were obtained from supplementary material provided by Wu *et al* (2018). The primer sequences for *Pm37*, *MLAG12* and *MLUM15* were sourced from GrainGenes database (https://wheat.pw.usda.gov/), a genomic database for Triticeae and Avena. PCR amplification conditions for each microsatellite marker obtained from the database was used as a guideline for further optimisation.

The PCR protocol and reaction conditions for *Pm4b* were optimised using a total reaction volume of 16 µL, consisting of 10 µL Taq DNA Polymerase 2x Master Mix Red, 0.64 µL forward and reverse primer (10 pmol/ µL), 1 µL DNA sample (100 ng/µL) and 3,72 µL ddH_2O. The amplification conditions were 95°C for 4 min, 94°C for 30 sec, 58°C for 40 sec, 72°C for 30 sec, with 35 cycles and a final extension for 7 min at 72°C. The positive control for the flanking markers was “Chinese Spring”.

The PCR protocol for *Pm37* had a total reaction volume of 16.5 µL, consisting of 10 µL Taq DNA Polymerase 2x Master Mix Red, 0.5 µL forward and reverse primer (10 pmol/µL), 0.5 µL DNA sample (100 ng/µL) and 5 µL ddH_20. Amplification conditions for *Xgwm332* was 95°C for 3 min, 94°C for 30 sec, 60°C for 30 sec, 72°C for 30 sec, with 40 cycles and a final extension for 7 min at 72°C. PCR reaction conditions for Xwmc790 were 95°C for 3 min, 94°C for 30 sec, 61°C for 30 sec, 72°C for 7 min, with 35 cycles and a final extension for 7 min at 72°C. The positive control for the flanking markers was “Steenbras”.

The PCR protocol for *MLAG12* had a final reaction volume of 16 µL, consisting of 10 µL Taq DNA Polymerase 2x Master Mix Red, 0.5 µL forward and reverse primer (10 pmol/µL), 1 µL DNA sample (100 ng/µl) and 4 µL ddH_20 to bring reaction to volume. Amplification conditions for *Xwmc273* and *Xwmc346* was 95°C for 5 min, 94°C for 30 sec, with an annealing temperature of 51°C and 61°C for 30 sec, respectively, 72°C for 30 with 40 cycles and a final extension for 7 min at 72°C. The controls used for the flanking markers was “Chinese Spring” and “SST027”.

The PCR protocol for *MLUM15* had a final reaction volume of 16 µL, consisting of 10 µL Taq DNA Polymerase 2x Master Mix Red, 0.5 µL forward and reverse primer (10 pmol/µl), 1

µL DNA sample (100 ng/µL) and 4 µL ddH_20 to bring reaction to volume. Amplification conditions for *Xcfa2257* and *Xcfa2240* was 95°C for 5 min, 94°C for 30 sec, 60°C for 30 sec, 72°C for 30 sec, with 30 cycles and a final extension for 10 min at 72°C. No known positive controls were available for the gene of interest. The marker was tested on several breeding lines with no further molecular characterisation of nursery populations.

The banding patterns produced by the tested microsatellite markers was visualised using 6% polyacrylamide gel electrophoresis.

3.3.2. Marker validation of FHB resistance QTLs

Microsatellite markers used to identify FHB resistance QTLs (*Qfhs.ifa.5A*, *7AQTL*, *Qfhs.ndsu.3BS*) were obtained from a mapping population developed by (Röder *et al.*, 1998). The primer sets for each SSR marker used in this study are listed in (**Table 3.4**). The sequencing information for each primer set was obtained from GrainGenes (https://wheat.pw.usda.gov).

PCR reaction mixtures for each marker contained 5.75 µl dH_2O, 6.25 µl Taq DNA Polymerase 2X Master Mix RED, 0.5 µl forward and reserve primer (10 µM) and 1 µl DNA (100 ng/µl), with a reaction total of 14 µl. The PCR amplification conditions were 3 min at 94°C; 44 cycles with 30 sec at 94°C, 30 sec at 60°C and 30 sec at 72°C, with a final extension of 7 min at 72°C. The annealing temperature for SSR marker gwm233 was adjusted to 50°C. The positive control used for the targeted QTLs was “Sumai3” and the negative control was “PAN3471”.

PCR products generated from SSR markers *gwm304*, *gwm293*, *gwm130*, *gwm233* and *Barc133* was visualised using a 6% polyacrylamide gel electrophoresis. PCR products produced by *gwm493* and *gwm533* were visualised using 2% agarose gel electrophoresis.

3.3.3. Marker identification for novel rust resistance genes

The cloned stem rust resistance genes *Sr35* and *Sr45* were screened on the female population. In 2014 the genes were introduced into the recurrent population at the SU-PBL

(Springfield, 2014). Several crossing cycles were performed to accumulate the gene frequencies in the population. PCR based dominant marker *NL9* was identified for *Sr35* and co-dominant marker *cssu45* was identified for Sr45. The primer sequences used for gene amplification is listed in (**Table 3.5**)

. The primer sets for each molecular marker was supplied from Integrated DNA Technologies (Whitehead Scientific Inc, Stikland, RSA). All PCR reactions were performed in a SimpliAmp™ Thermal Cycler (Applied Biosystems™, Fairland, RSA).

The PCR reaction for *Sr35* had a total reaction volume of 16.7 µL consisting of 10 µL of Taq DNA Polymerase 2x Master Mix Red, 0.7 µL *NL9* forward and reverse primer (10 pmol/ µL), 1.3 µL DNA sample (100 ng/µL) and 4 µL ddH_2O. The PCR amplification conditions were optimised to 95°C for 5 min, 94°C for 30 sec, 51°C for 30 sec, 72°C for 40 sec with 32 cycles and a final extension at 72°C for 5 min.

The PCR reaction for *Sr45* has a final reaction volume of 12.5 µL consisting of 6.25 µL Red mix, 0.25 µL *cssu45* forward and reverse primer (10 pmol/ µL), 0.75 µL DNA sample (100 ng/µL) and 5 µL ddH_2O. The amplification conditions were 95°C for 3 min, 94°C for 30 sec, 60°C for 30 sec, 72°C for 30 sec with 35 cycles and a final extension at 72°C for 7 min.

3.3.4. Molecular characterisation of recurrent population for rust resistance

The segregating base population was molecularly screened for rust genes *Lr34* and *Sr2*. The PCR markers used to amplify these genes form part of a standard panel of markers at the SU-PBL. Molecular characterisation of rust resistance was performed prior to each MS-MARS cycle. A total of 360 and 120 entries, respectively, were used to represent the recurrent population for the first and second crossing cycle.

The PCR reaction mixture for *Lr34* had a total reaction volume of 17,4 µL, consisting of 10 µL Taq DNA Polymerase 2x Master Mix Red, 0.3 µL *Dint-9* forward primer and *Lr34* reverse primer, 0.25 µL *CSLV34* forward and reverse primer, 1.3 µL DNA sample (100 ng/µL) and 5 µL ddH_2O. Amplification conditions were 94°C for 5 min, with 35 cycles at 94°C for 40 sec, 57°C for 40 sec, 72°C for 40 sec and a final extension for 7 min at 72°C. The positive control

was “Chinese Spring”, amplifying PCR fragments with 517 bp and 150 bp and the negative control was ddH_2O.

The PCR reaction mixture for *Sr2* had a total volume of 12.9 µL, consisting of 7.5 µL Taq DNA Polymerase 2x Master Mix Red, 0.45 µL *CSSr2* forward and reverse primer, 1.5 µL DNA sample (100 ng/µL) and 3 µL ddH_2O. The amplification conditions were 95°C for 2 min, with 40 cycles of 95°C for 30 sec, 60°C for 40 sec, 72°C for 50 sec and a final extension of 72°C for 5 min. The positive control was “Steenbras”, amplifying a PCR fragment of 337 bp before enzyme digestion and 172 bp after. For enzyme digestion, each PCR product received a total volume of 2.5 µL enzyme digestion, containing 1 µL ddH_2O, 1.25 µL Buffer and 0.25 µL *BspHI* (*PagI*) enzyme. The negative control was “Chinese Spring”.

3.4. Polyacrylamide gel electrophoresis preparation

Silver-stained polyacrylamide gel electrophoresis was used to visualise the PCR products of microsatellite markers used in this study. The PAGE gel technique entailed a four-step process.

3.4.1. Plate preparation

The plate glue used in this study was prepared by creating a stock solution; 125 µl plate glue with 25 ml pure ethanol. A series of dilutions were made using 500 µl plate glue stock and 1500 µl pure ethanol. A 1:3 dilution of the stock was created and labelled as “PG1”. The plate glue was further diluted by adding 1740 µl of the 1:3 dilution to 140 µl of 10% acetic acid and was labelled “PG2”. Two glass plates were sterilised by spraying 70% ethanol and wiping it clean with sterile tissue paper. The two plates had the same width but differed in length. The longer plate was further cleansed using windscreen cleaner “Wynn’s C-thru” across the entire plate and left for 3 min to dry. Once dried, a clean piece of sterile tissue was used to remove residual product. The short plate was prepared by applying 2 ml of plate glue (PG2) and was left for 30 sec until dry. Once dried, a clean piece of sterile tissue paper was used to wipe the plate until all the glue was set. Plastic spacers were used to separate the two plates by 1 mm

once they were assembled, with each of the treated surfaces facing each other. Once the plates were joined, a rubber seal was used to secure the plates in position.

3.4.2. Gel mixture

The PAGE gel mix used in this study was prepared by creating a 40% Acrylamide stock solution. The solution consisted of 76 g of Acrylamide, 4 g of Bis-acrylamide and 200 ml ddH_2O, stored in a 250 ml bottle covered in aluminium foil. The stock solution was used to create a 6% sequencing gel mix by adding 37.5 ml of 40% acrylamide stock solution, 90.09 g urea and 50 ml 5x TBE to 200 ml of ddH_2O. The 6% sequencing gel mixture was stirred until urea particles was completely dissolved and filled to 250 ml. The bottle containing the mixture was covered with aluminium foil and stored at 4°C. The PAGE gel was prepared by adding 160 ml 6% sequencing gel mix to a 200 ml flask, followed by 160 µl N, N, N", N"-Tetramethylethylenediamine (TEMED) and 800 µl 10% APS (created by adding 0.1 g APS to 1 ml dH_2O). The contents were mixed well and carefully poured into the 1mm space between the two joined plates and allowed to set.

3.4.3. Sample loading

Approximately one hour after the gel was cast, loading buffer (98% formamide, 10mM EDTA pH 8.0, 0.05% w/v bromo phenol blue, 0.05% w/v/xylene cyanol FF) was added in volumes equivalent to the total volume of each PCR sample. The samples were then denatured at 95°C for 15 min and immediately placed on ice. Twelve microlitres of each sample and only 3 µl of Hyper ladder (100 bp) was loaded to the gel. The PAGE gel ran at 70 W for approximately 6 hours.

3.4.4. Silver staining

Fixing solution was prepared with 210 ml pure ethanol, 1879.5 ml roH_2O and 10.5 ml pure acetic acid added just before using the solution. Staining solution was prepared with 2.1 g

silver nitrate ($AgNO_3$) dissolved in 2100 ml roH_2O. Developing solution was prepared using 31.5 g sodium hydroxide (NaOH) dissolved in 2100 ml roH_2O, with 8.505 ml formaldehyde added to solution just before use. After electrophoresis, the plates were completely covered with ice for two minutes. The long plate was carefully removed from the short plate. The short plate was placed on a shaker ready for gel staining. Fixing solution was poured over the plate and distributed for 20 minutes. The gel was rinsed twice with roH_2O for 5 minutes. Silver staining solution was distributed across the gel for 20 minutes and rinsed once with roH_2O for 10 sec. Developing solution was poured onto the gel and allowed to distribute until banding patterns appeared. The duration for distribution ranged between 20 to 30 minutes. Once clear bands were visible, the gel was rinsed once with roH_2O.

3.5. Disease assessment for powdery mildew resistance

3.5.1. Inoculum production of *Bgt* isolates

Dry stems and leaves carrying *Blumeria graminis* f.sp. *tritici* (*Bgt*) chasmothecia (formerly cleistothecia) were sampled from wheat lines planted at Vergenoegd experimental farm, Stellenbosch University. The leaves were sampled in late November 2020 and stored in a brown paper bag until further use. “Morocco” seeds were planted in 25 cm^2 plastic pots containing potting soil, 9 seeds were sown in 10 pots every second week. The “Morocco” seedlings grew until the two-leaf stage (14 days) before they were inoculated with *Bgt* isolates. Once inoculated, the seedlings were incubated in a growth chamber set at 16 h light cycles at 20°C and 8 h dark cycles at 18°C. The humidity was maintained by spraying the plants with roH_2O twice a day, as well as placing a large beaker of water in the centre of the growth chamber. The light intensity exposure was at a constant 90 µmol. The maintenance of fresh spores was done once a week, by brushing one-week old conidia over healthy “Morocco” seedlings at the two-leaf stage (14 days). Once, conidiospore formation was optimal, induced humidity was no longer required.

3.5.2. Construction of vacuum operated settling tower

A vacuum operated settling tower was designed to perform uniform inoculations on wheat lines (**Figure 3.2**). The settling tower designs were modified from a model developed by Reifschneider, Boiteux and Brasilia, (1988). The dimensions of the settling tower was $500 \times 100 \times 100$ mm. The material composition of the tower was primarily plexiglass. The thickness of the plexiglass was 5 mm and was particularly important to ensure durability for high pressure testing. A vacuum was connected to the tower via an air valve that controlled the suction of air within the settling tower. The vacuum had a suction power of 680 torr, powerful enough to form a vacuum within the system. A protocol derived by Delventhal *et al.* (2016) was used as a baseline to perform the wheat seedling assays.

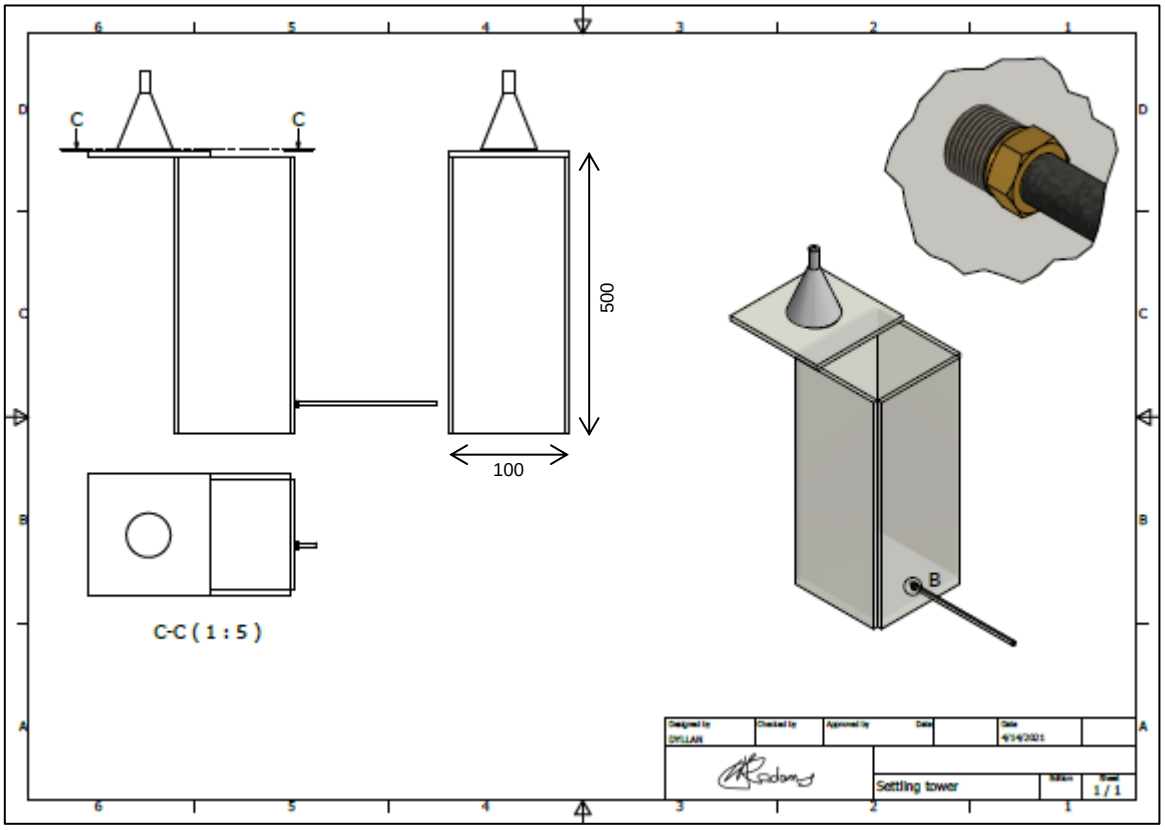

Figure 3.2. Diagram of vacuum operated settling tower used for uniform inoculation of *Bgt* isolates

3.5.3. Wheat seedling inoculations with *Bgt* isolates

Plant material was assessed for powdery mildew resistance during the seedling stage. (**Figure 3.3a**). For inoculation preparation, plant pots were positioned laterally on a rigid piece of paper.

Primary and secondary leaves of each seedling was taped to the surface of the paper, with the abaxial surface upwards (**Figure3.3b**). The tape was placed at the base and tip of each leaf to secure it to the surface. Pots were placed horizontally on the base of the settling tower (**Figure 3.3d**). Leaf segments of “Morocco” seedlings containing fresh *Bgt* spores were placed in the basket attached to the lid of the settling tower. The lid of the settling tower was secured in place and the top valve closed. The air valve connected to the vacuum pump was opened prior to switching on the vacuum pump. A period of 30 sec was given for the vacuum to form within the settling tower before closing the bottom air valve and switching off the pump (**Figure 3.3d**). The vacuum within the settling tower was broken by opening the air valve attached to the lid, allowing a rush of air to disperse the conidiospores. The density of the conidia was determined by placing a haemocytometer at the base of the settling tower during each inoculation procedure. The density of conidiospores was calculated under a 40x magnified light microscope. The desired spore density of 4×10^{3} conidia cm^{-2} was required for inoculations. The spores were allowed to settle for 5 min before removing the pots from the settling tower and incubated in a growth chamber under 12 hr light/dark cycles at 18°C (**Figure 3.3e**).

3.5.4. Disease evaluation

The infection type of each wheat lines was scored at 6-, 11- and 14-days post inoculation on a 0-9 scale adopted by Leath (1990) (**Figure3.3f**). The disease scoring was as follows: 0 – no sign of infection (immune), 1-3 – visible necrosis to mycelium growth, 4 – first sign of active mycelium growth, 5 – presence of one or two *Bgt* pustules, 6 - <20% leaf area infected with *Bgt* pustules, 7 – between 20-50% leaf area covered with pustules, 8 – presence of medium to large pustules across 50-90% of leaf area, 9 – presence of large pustules with 100% coverage (Xue *et al.*, 2021). The disease response for each wheat lines was determined based on the measured infection type (**Table 3.1**).

Table 3.1. Infection types and the corresponding disease response of inoculated material

Infection type	Disease response	Symptoms
0 – 1	Highly resistant (HR)	No symptoms to slight discolouration
2	Resistant (R)	Necrotic lesions
3 – 4	Moderately resistant (MR)	Detection of mycelium growth
5 – 6	Moderately susceptible (MS)	Presence of conidial pustules
7 – 9	Susceptible (S)	Between 50-100% coverage

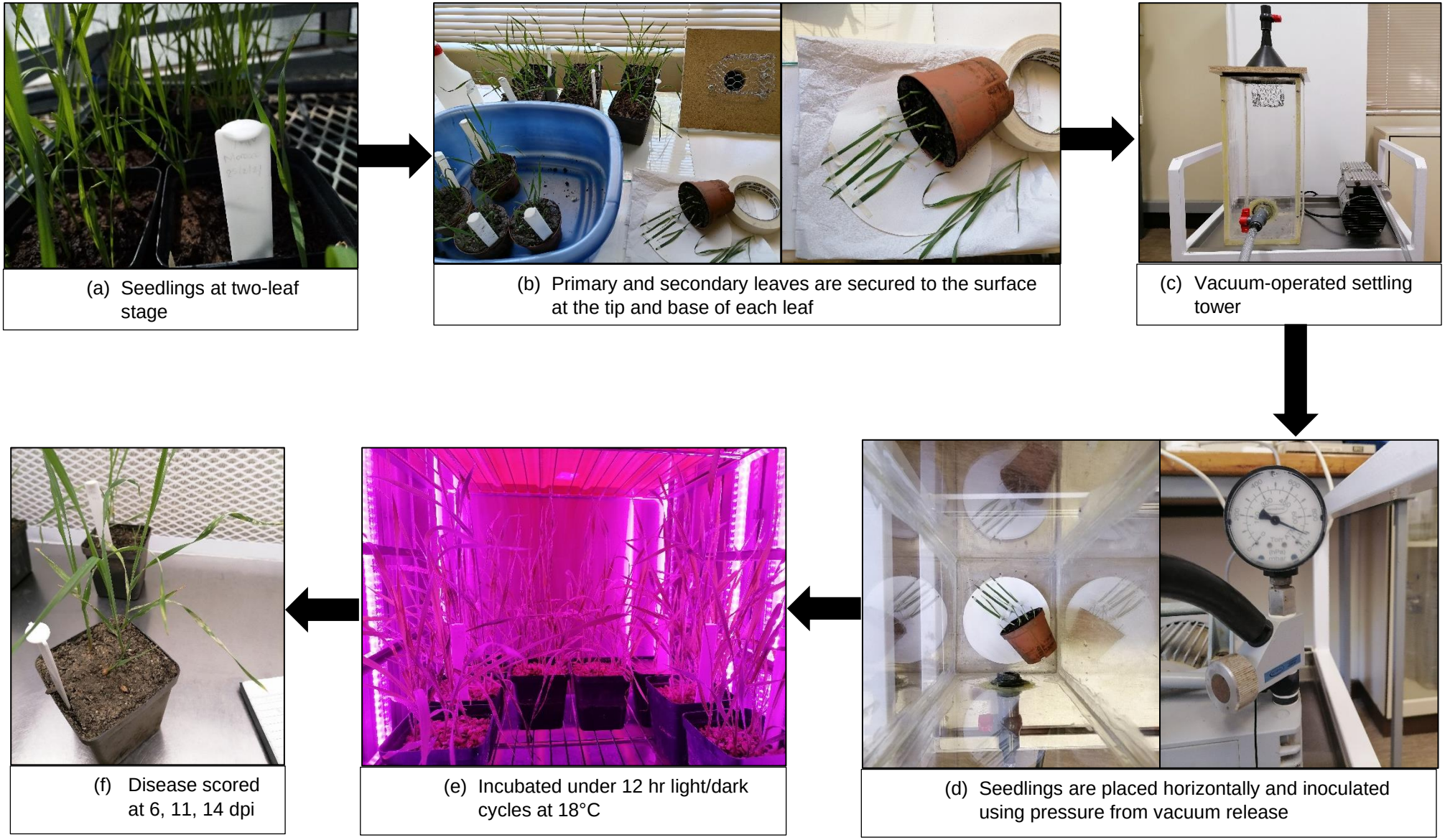

Figure 3.3. Diagram illustrating the powdery mildew inoculation procedure from (a) seedling selection to (f) disease scoring

3.6. Phenotypic assessment of FHB resistance

3.6.1. Inoculum preparation

Three DON producing *Fusarium graminearum* isolates were used in this study, namely "W-2-922", "W-2-952" and "W-2-962" (**Table 3.7**). The isolates were obtained from Plant pathology department, Stellenbosch University (Dr Gert van Coller). Fresh isolates were cultured onto Potato Dextrose Agar (PDA^+) media infused with streptomycin and incubated at 25°C. One week old cultures were used to induce sporulation of macroconidia in two ways; (a) plating agar plugs onto water agar (WA) media with incarnation leaves and (b) placing autoclaved filter paper infused with a CuZn solution onto fresh PDA^+ plates containing 1 mL scraped mycelia. The cultured plates of each method were left to produce spores for (a) 2-3 weeks and (b) 3 days.

The spore suspensions were made a day prior to inoculations by dislodging spores from media plates. Concentrated spore suspensions were filtered through sterile cheese cloth to separate dislodged mycelia from conidiospores. The spore concentration was determined using a haemocytometer placed under a 40x magnified light microscope. The macroconidia were counted on both the upper and lower five blocks of the haemocytometer only on the large outer blocks (**Figure 3.4**). The spore concentration was calculated using the following equation: $(upper + lower\ block) \div 2) \times 2000 = spores/ml$. The desired final concentration of the spore suspension was 50 000 spores/mL for each isolate. The spore suspension was diluted accordingly using tween.

Plants were inoculated during anthesis when only yellow anthers were visible outside the floret. For a plant to be inoculated, more than 50% of the tillers should be in anthesis. The number of plants ready for inoculation was counted prior to inoculum production. The volume of spore suspension required was calculated using 20 µl inoculum/plant.

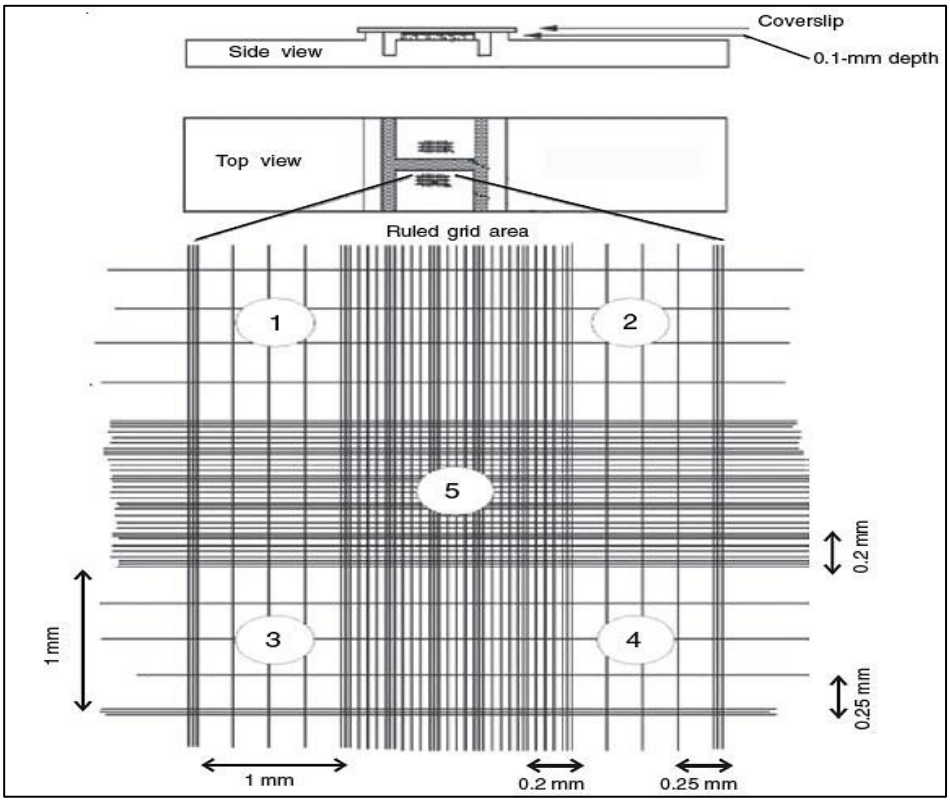

Figure 3.4. Diagram of haemocytometer used to calculate spore concentration; macroconidia from Fusarium spore suspension was counted in grids 1-5.

3.6.2. Inoculation and disease evaluation

The spore suspension was kept on ice for the duration of inoculations. An adjusted spray inoculation method was used to evaluate wheat lines by inoculating the 3rd floret from the top of the spike with a pipette. The inoculated wheat lines were clearly labelled and covered with a paper bag before being incubated at 25°C for 72 hours with 100% relative humidity. Once 72 hours had passed, the pots were returned to the greenhouse where disease severity was measured at 14-, 21- and 28-days post inoculation. The disease severity was rated as follows: Total number of infected florets ÷Total number of florets×100=% Disease severity.

3.6.3. Assessment of yield parameters affected by FHB

The FHB CIMMYT population evaluated under greenhouse conditions was phenotypically assessed for yield parameters (**Table 3.2**). The experimental design had three replicates consisting of five genotypes and two controls. A total of six seeds were sown for each genotype and control. Measurements were taken on all the plant material excluding regrowth of undeveloped tillers.

The yield-related traits were measured by hand (ruler, scale) and mobile application (SeedCounter) (Rhoda, 2018). The traits measured by hand included tiller number, plant height, spike length, spikelet number, floret number, grain number per spike and grain weight. The traits measured by mobile application included grain length, grain width and grain area. Additional yield parameters calculated included harvest index, thousand kernel weight (TKW), heading date and flower fertility.

Table 3.2. Summary of yield parameters assessed at the SU-PBL (Rhoda, 2018)

Yield-related trait	**Measurement of trait**	**Unit**
Tiller number	Number of tillers counted per plant	Numeric
Plant height	Length measured from the base of the tiller to the base of the spike	mm
Spike length	Length measured from the base of the spike to the top of the spike, excluding awns	mm
Spikelet number	Number of spikelets per spike	Numeric
Floret number	Number of florets per spike	Numeric
Grain number	Number of grains harvested per spike after hand-threshing	Numeric
Grain weight	Weight of grain threshed per spike measured on a scale	g
Harvest index	Grain weight per plant divided by weight of aboveground biomass	%
Thousand Kernel Weight	Grain weight per plant divided by grain number per plant multiplied by 1000	g
Heading date	Number of days from planting to more than 50% of spikes emerged from flag leaf sheath	days
Flower fertility	Grain number per spike divided by floret number per spike	%
Grain length, width, and area	Measured using SeedCounter mobile application	mm, mm^2

3.6.4. Mycotoxin extraction of inoculated wheat grain

The quality of inoculated material was assessed through liquid chromatography tandem mass spectrometry (LCMS/MS) to quantify the level of mycotoxin contamination. The mycotoxins ZEA and type B-trichothecenes, namely DON and NIV were analysed. For mycotoxin extraction, wheat grain was finely milled to flour with a Perten Labmill 3100 and filtered through a 0.35 mm sieve to refine flour samples. A preferred weight of 5 g was weighed into 50 mL Falcon tubes, samples with less than 5 g were weighed to the nearest integer. Extraction buffer (70% Methanol and 30% HPLC water) was added in a 4 ml:1 g ratio to the weighed flour samples. The samples were mixed vigorously using a vortex to suspend all the flour in the extraction buffer. The tubes were placed at an angle in an incubator/shaker set at 200rpm for 30 minutes at 25°C. Once incubation was complete, samples were transferred to a centrifuge set at 4°C and 500rcf for 10 minutes. Approximately 2 ml of supernatant was removed using a sterile syringe and filtered through a 0.20 µm filter into a sterile 2 ml microcentrifuge tube. The samples were incubated overnight in a refrigerator set at 4°C and transferred to a centrifuge set at 4°C and 14 000 rpm for 10 minutes. Approximately 1.8 ml of clear supernatant was transferred into glass vials with fitted caps. Extracted samples and standards were sent to the Central Analytical Facility (CAF) at Stellenbosch University, for LCMS/MS analyses (**Table 3.3**).

Table 3.3. List of standards ($mg.kg^{-1}$) used to detect mycotoxin content

Standard name	Deoxynivalenol and Nivalenol	Zearalenone
Standard 1	0.032	0.064
Standard 2	0.160	0.320
Standard 3	0.800	1.600
Standard 4	4.000	8.000
Standard 5	20.000	40.000
Standard 6	100.000	200.000

3.7. Validation of MS-MARS pre-breeding scheme

3.7.1. Molecular and phenotypic screening of dominant male sterility (*Ms3*) gene

A PCR based marker was recently developed for *Ms3* and was used to validate male sterility in the recurrent population (Guttieri, 2020). In 1999, the gene was transferred into the recurrent population at the SU-PBL. The primer sets used to amplify the gene was obtained from Integrated DNA Technologies (Whitehead Scientific Inc, Stikland, RSA).

The PCR reaction mixture for *Ms3* had a final volume of 12.475 µL, consisting of 0,3125 µL forward primer, 0.5 µL reverse primer, 0.5 µL DNA sample (100 ng/µL) and 4.9125 µL roH_2O to bring mixture to volume. The amplification conditions were 95°C for 5 min, 95°C for 30 sec, 58°C for 30 sec, 72°C for 30 sec, with 35 cycles and a final extension of 7 min at 72°C. The PCR product was visualised using 2% agarose gel electrophoresis.

The reliability of the molecular marker was validated through phenotypic screening. Molecularly characterised recurrent lines were phenotypically assessed based on flower morphology. Recurrent lines with spawning awns and multiple aborted seeds from lack of pollination was identified as sterile. While lines with multiple seed was identified as fertile.

3.7.2. Phenotypic selection and preparation of crossing material

The MS-MARS pre-breeding scheme at the SU-PBL was designed to facilitate cross pollination through a hydroponic tiller culture. The hydroponic system was designed to maintain 320 male sterile (female) tillers in nutrient rich solution while being cross pollinated with selected male donor tillers. Prior to cross pollination, male sterile and donor tillers were selected based on morphological characteristics (**Figure 3.5a**). Selections for male sterile and donor tillers were conducted during the flowering stage. Selection criteria for male sterile tillers were opened spike awns, florets with smaller anthers shrivelled in composition and the presence of non-viable pollen (**Figure 3.5b**). Male sterile tillers were ready for cross pollination when flag leaves were just below the spike and the stigma was receptive. The incision was made just below the second last internode with all the leaves removed beside the flag leaf and stored in nutrient solution. Florets of male sterile tillers were cut to expose receptive stigma prior to cross pollination. Male donor

tillers were cut when anthers were actively shedding pollen. Tillers with only yellow anthers visible outside the spike or within the florets were cut. Selected tillers were stored in nutrient solution with all the leaves removed from the stem (**Figure 3.5c**). Ripe pollen from anthers were shed during the preparation, allowing for synchronised pollen shed during cross pollination.

3.7.3. Cross pollination of parental lines

The hydroponic system consisted of 600×450×160 mm galvanised steel trays coated with black anti-fungal paint used to arrange male sterile tillers. Trays were filled with pH neutral nutrient solution to capacity with an electrical conductivity of 2 dSm^{-1}. The male tillers were arranged in narrow galvanised steel trays that can accommodate 70 tillers. The narrow trays contained floral foam drenched in nutrient solution. The male tillers were stacked in a canopy-like formation approximately 600 mm above the male sterile tillers (**Figure 3.5d**). The trays were incubated in a growth chamber under 14h light and 10h dark cycles set at 16°C and12°C, respectively. (**Figure 3.5e**). A period of 5-6 days was allowed for cross pollination before the male tillers were discarded. The male sterile tillers were maintained in clean nutrient solution replaced every second week until seed ripening. Seed ripening usually occurred after 5 – 7 weeks, followed by oven drying at 37°C for 3-5 days (**Figure 3.5f**).

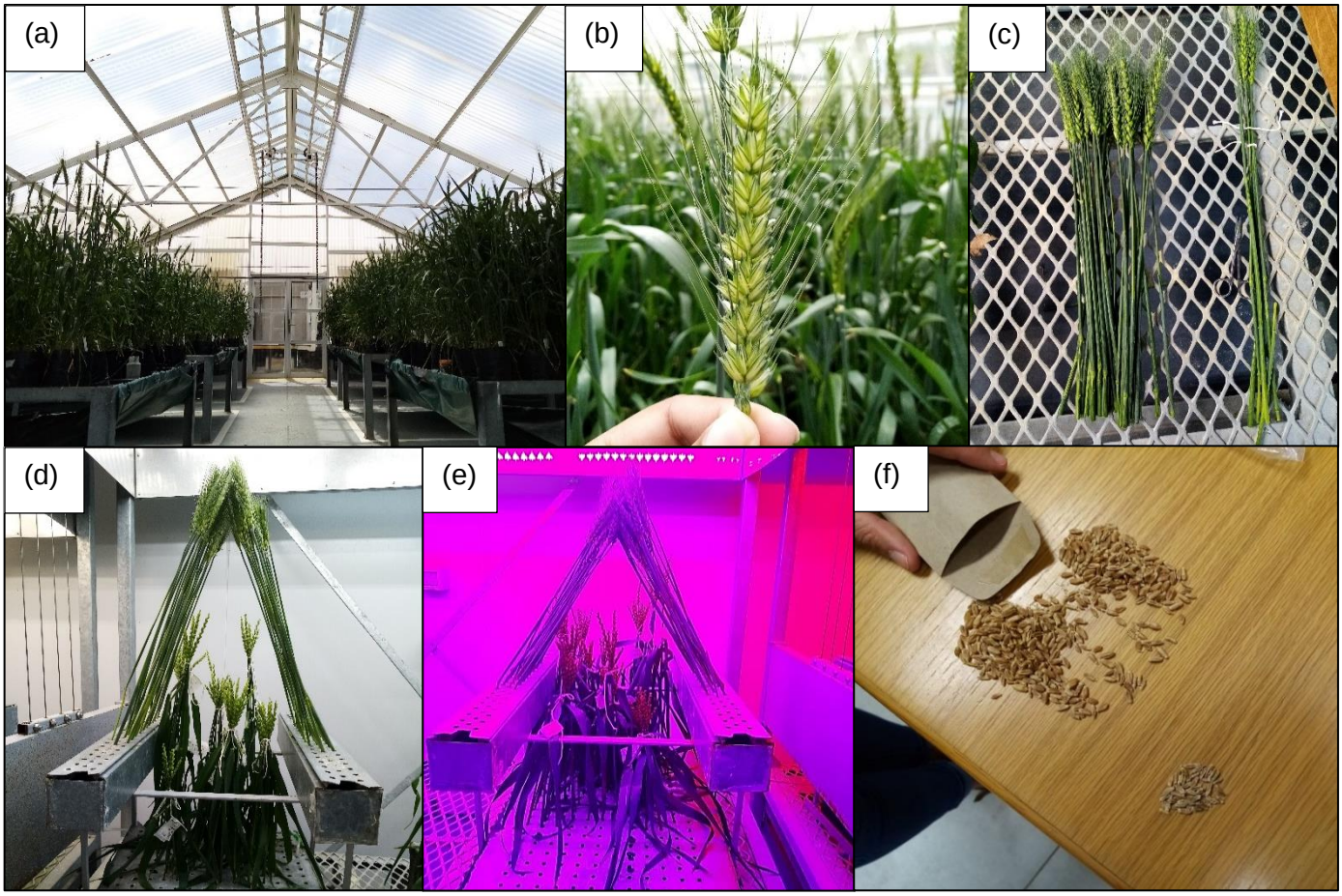

Figure 3.5. MS-MARS pre-breeding scheme at the SU-PBL facilitated by hydroponic tiller culturing. (a) male and female populations planted on either side of the greenhouse. (b) female (male sterile) tiller with open glumes. (c) male (donor) tillers with all leaves stripped. (d) stacking of female tillers at the base and male tiller in canopy formation. (e) LED photoperiod optimised for accelerated growth. (f) Hybrid seed produced after cross pollination

Table 3.4. Primer sequences of each microsatellite marker used to identify the powdery mildew resistance genes

Gene	SSR marker	Primer sequence (5'->3')	T_A (°C)	Fragment size (bp)	References
Pm4b	*Xics13*	F: AGGGAAATACTGACGTAGCTT	58	252, 264	Wu *et al.*, 2018
		R: GTCAAGAGGAAGAAGGAAAAG			
	Xics43	F: CCCACCTGTCATACTCTGTT	58	201, 217	
		R: CTCTGGCCCAATGATAGC			
Pm37	*Xgwm332*	F: AGCCAGCAAGTCACCAAAAC	60	193	Perugini *et al.*, 2008
		R: AGTGCTGGAAAGAGTGAAGC			
	Xwmc790	F: AATTAAGATAGACCGTCCATATCATCCA	61	76	
		R: CGACAACGTACGCGCC			
MLAG12	*Xwmc273*	F: AGTTATGTATTCTCTCGAGCCTG	51	179	Maxwell *et al.*, 2009
		R: GGTAACCACTAGAGTATGTCCTT			
	Xwmc346	F: CTGAAGTTCCAGCCAACACA	61	203	
		R: ATTCCCTCATCCCGTTGC			
MLUM15	*Xcfa2257*	F: GATACAATAGGTGCCTCCGC	60	167	Worthington *et al.*, 2014
		R: CCATTATGTAAATGCTTCTGTTTGA			
	Xcfa2240	F: TGCAGCATGCATTTTAGCTT	60	280	
		R: TGCCGCACTTATTTGTTCAC			

Table 3.5. Primer sequences of microsatellite markers used in this study to identify closely linked FHB QTLs.

FHB QTL	SSR marker	Primer sequence (5'->3')	T_A (°C)	Fragment size (bp)	Visualisation	Reference
Qfhs.ifa-5A	*Xgwm304*	F: AGGAAACAGAAATATCGCGG	60	208	6% PAA	Röder *et al.*, 1998
		R: AGGACTGTGGGGAATGAATG				
	Xgwm293	F: TACTGGTTCACATTGGTGCG	60	305	6% PAA	Röder *et al.*, 1998
		R: TCGCCATCACTCGTTCAAG				
7AQTL	*Xgwm130*	F: AGCTCTGCTTCACGAGGAAG	60	121	6% PAA	Röder *et al.*, 1998
		R: CTCCTCTTTATATCGCGTCCC				
	Xgwm233	F: TCAAAACATAAATGTTCATTGGA	50	248	6% PAA	Röder *et al.*, 1998
		R: TCAACCGTGTGTAATTTTGTCC				
Qfhs.ndsu-3BS	*Xgwm493*	F: TTCCCATAACTAAAACCGCG	60	211	2% Agarose	Röder *et al.*, 1998
		R: GGAACATCATTTCTGGACTTTG				
	Xgwm533	F: AAGGCGAATCAAACGGAATA	60	159	2% Agarose	Röder *et al.*, 1998
		R: GTTGCTTTAGGGGAAAAGCC				
	Barc133	F: AGCGCTCGAAAAGTCAG	60	125	6% PAA	Röder *et al.*, 1998
		R: GGCAGGTCCAACTCCAG				

Table 3.6. PCR markers used to amplify recently cloned rust genes *Sr35* and *Sr45*.

Gene	PCR marker	Primer sequence (5'->3')	T_A (°C)	Fragment size (bp)	References
Sr35	*Nl9*	F: CTCATCAACTGCTTGAGCGAAC	51	719	Saintenac *et al.*, 2013
		R: GTATCTAGCGAACCTCAATCG			
Sr45	*Cssu45*	F: CGAGTTTCAATACTTCGCCC	60	220	Periyannan *et al.*, 2014
		R: GATTACTATGCAATAGGGCCC			

Table 3.7. *Fusarium graminearum* isolates used in this study obtained from the Northern Cape wheat producing regions of South Africa.

Isolate ID	Host	Cultivar	Province	Locality	Year	Species	Chemotype
"W-2-922"	Wheat	"Kariega"	Northern Cape	Bull Hill	2009	*F. graminearum*	15-ADON
"W-2-952"	Wheat	"Baviaans"	Northern Cape	Hopetown	2009	*F. graminearum*	15-ADON
"W-2-962"	Wheat	"Kariega"	Northern Cape	Barkley-Wes	2009	*F. graminearum*	15-ADON

Chapter 4. Results and Discussion

4.1. Molecular characterisation of plant material

4.1.1. Marker identification and validation for powdery mildew

The microsatellite marker information for *Pm4b*, *Pm37*, *MLAG12* and *MLUM15* was obtained from literature and GrainGenes database. Two microsatellite markers were identified for each of the four powdery mildew resistance genes. The PCR conditions were optimised for each individual marker and was validated by screening the respective positive controls and SU-PBL's 2020 wheat nursery.

4.1.1.1. Microsatellite markers for *Pm37*

The co-dominant SSR markers *Xgwm332* and *Xwmc790* was used to flank the *Pm37* gene. The SU-PBL's 2020 wheat nursery was molecularly characterised using the above-mentioned markers. The SSR marker *Xgwm332* was located 0.5 cM proximal from the *Pm37* gene on chromosome 7AL. A PCR fragment size of 193 bp was observed in homozygous resistant lines and 195 bp was observed in homozygous susceptible lines. The co-dominant SSR marker *Xwmc790* was located 0.5 cM distal from the gene. A PCR fragment size of 76 bp was observed in homozygous resistant lines and 100 bp was observed in homozygous susceptible lines.

4.1.1.1.1.*Xgwm332*

The PCR product generated from co-dominant marker *Xgwm322* was visualised using 2% agarose gel electrophoresis and 6% polyacrylamide gel electrophoresis to visualise PCR products. The banding patterns visualised using the 6% PAGE gel was more distinct in visualising banding patterns than the 2% agarose gel. The desired fragment size of approximately 193 bp could be identified with both methods. However, using 2% agarose gel

to visualise the fragment sizes could not differentiate between 193 bp and 195 bp. The 6% PAA gel was annotated to score the marker profiles. PCR fragment sizes of 193 bp and 195 bp was observed in both positive control “Steenbras” and two negative controls “Morocco” and “Avocet” (**Figure 4.1**). The SU-PBL’s wheat lines amplified PCR fragment sizes of 193 bp and 195 bp, similar to the controls. No variation in PCR products were observed between positive and negative controls. “Morocco” was a known negative control for powdery mildew, with no viable powdery mildew resistance genes present in the cultivar. The expected fragment size for “Morocco” was 195 bp. However, the desired fragment of 193 bp was also amplified in “Morocco”. The co-dominant SSR marker *Xgwm322* was not effective in discriminating between resistant and susceptible wheat lines.

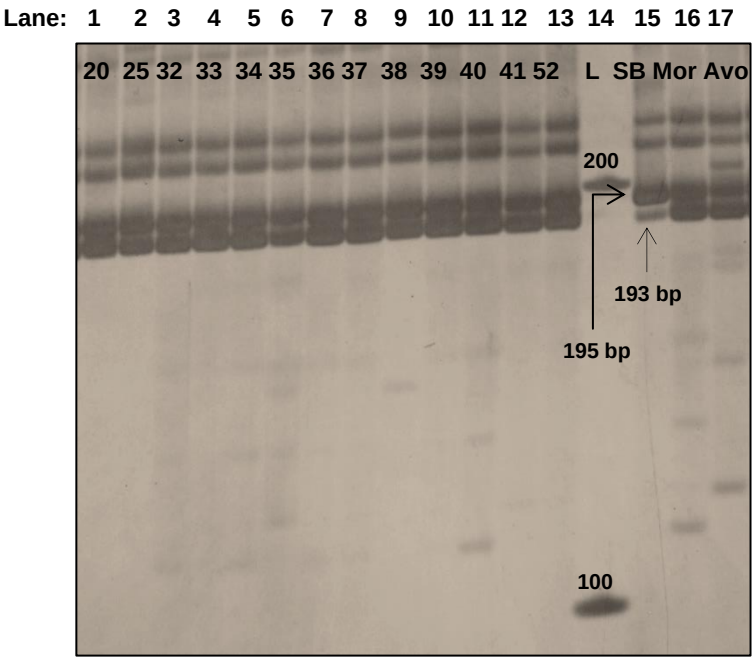

Figure 4.1. The optimization of co-dominant SSR marker *Xgwm332* for *Pm37*. Lane 1-13: samples of the selected SU-PBL’s 2020 wheat nursery. Lane 14: 100 bp Ladder. Lane 15: Steenbras (Positive control). Lane 16: Morocco (Negative control). Lane 17: Avocet (Negative control).

According to Emara *et al.* (2016), the co-dominant SSR marker *Xgwm332* was diagnostic in detecting homozygous resistant and susceptible lines. The susceptible wheat lines amplified fragment sizes above 200 bp and not 195 bp as reported by Perugini *et al.* (2008). The resistant lines amplified a PCR fragment size of 193 bp as expected from literature. The

genetic mapping of the gene located co-dominant marker *Xgwm332* at a genetic distance of 0.5 cM. The close association between the marker and gene was expected to increase the reliability in differentiating between resistant and susceptible lines. However, the marker was not reliable in detecting homozygous resistant and susceptible lines.

4.1.1.1.2.*Xwmc790*

The co-dominant SSR marker *Xwmc790* amplified a PCR fragment size of 76 bp. Three distinct banding patterns were observed for the SSR marker *Xwmc790* (**Figure 4.2**). The positive control “Steenbras” amplified a PCR fragment size of 76 bp. The negative control “Morocco” amplified a PCR fragment size of 100 bp and “Avocet” amplified a product of 210 bp. Wheat lines in lane 2-9 amplified PCR fragment sizes of 100 bp, similar to the negative control “Morocco”. Wheat line “P6” amplified a PCR fragment size of 76 bp, similar to the positive control “Steenbras”. The PCR product generated from the co-dominant SSR marker *Xwmc790* was effective in discriminating between resistant and susceptible wheat lines.

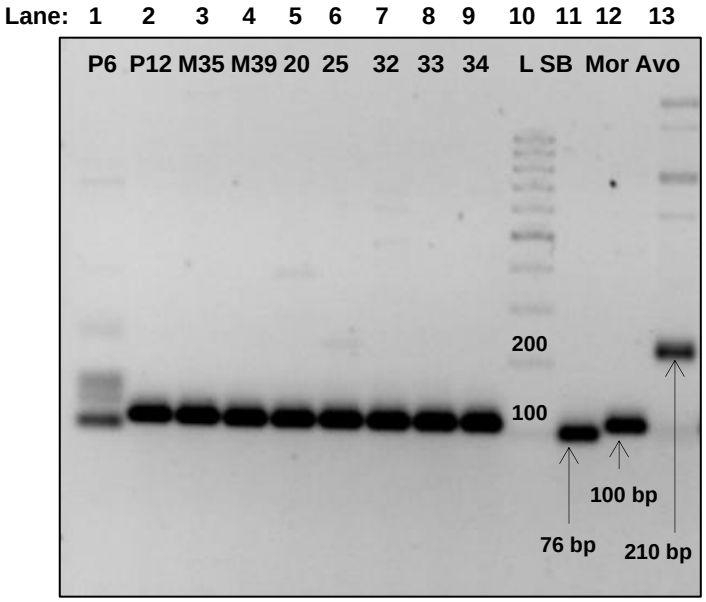

Figure 4.2. The optimization of co-dominant SSR marker *Xwmc790* for *Pm37*. Lane 1-9: selected samples of the SU-PBL nursery 2020. Lane 10: 100bp Ladder. Lane 11: “Steenbras” (Potential positive control). Lane 12: “Morocco” (Negative control). Lane 13: “Avocet” (Negative control).

GrainGenes marker report for *Xwmc790,* indicated a desired PCR fragment size of 149 bp was expected for the gene (https://wheat.pw.usda.gov). No additional literature validated the reported fragment size as indication of gene presence. Instead, a PCR fragment size of 76 bp was reported for the marker (Perugini *et al.*, 2008; Emara *et al.*, 2016). A gel electrophoresis image supplied by Emara *et al.* (2016) correlated with the images provided in this study. The known positive control used in their study amplified a fragment size of 76 bp and negative lines amplified fragments ranging between 100 – 200 bp as observed in this study. The co-dominant SSR marker *Xwmc790* was diagnostic in detecting between resistant and susceptible lines.

4.1.1.2. Microsatellite markers for *Pm4b*

The co-dominant SSR markers *Xics13* and *Xics43* was used to flank the *Pm4b* gene. These markers were used to molecularly characterise selected lines from the SU-PBL's 2020 wheat nursery. The co-dominant SSR marker *Xics13* was located 1.3 cM from the gene of interest on chromosome 2AL. A PCR fragment size of 264 bp was expected to amplify in homozygous resistant individuals and 252 bp in homozygous susceptible individuals. The co-dominant SSR marker *Xics43* was located 1.7 cM from the gene of interest. A PCR fragment of 201 bp was expected in homozygous resistant individuals and 217 bp in homozygous susceptible individuals. The PCR products were visualised using 6% silver-stained polyacrylamide gel electrophoresis.

4.1.1.2.1.*Xics13*

The PCR fragments generated by *Xics13* was visualised using 6% polyacrylamide gel electrophoresis. The expected fragment size of 264 bp was expected for the co-dominant marker *Xics13* in wheat lines with the *Pm4b* gene. The positive control "Chinese Spring" amplified a PCR fragment size of 262 bp (**Figure 4.3**). The PCR fragment size of 262 bp observed in "Chinese Spring" fell within an acceptable range of the resistant product size of 264 bp, with only two base pair differentiation. The test samples in lanes 5, 6 and 8 amplified

the same banding pattern as “Chinese Spring”. The susceptible control “Morocco” amplified fragment sizes of 253 bp and 262 bp. Wheat line “79” displayed the same banding pattern as “Morocco” even though the bands may not seem contiguous. Wheat lines “54” and “129” displayed a unique band size of 270 bp, not observed in either control. However, the banding pattern of these samples strongly resembles the PCR product amplified in “Morocco”. The PCR fragment size of 253 bp observed in “Morocco” fell within the acceptable range of the susceptible product size of 252 bp. The positive control “Chinese Spring” amplified the desired PCR fragment size in the homozygous state. However, the negative control “Morocco” also amplified the desired PCR fragment size in the heterozygous state. Therefore, the co-dominant SSR marker *Xics13* was unsuccessful in distinguishing between resistant and susceptible lines.

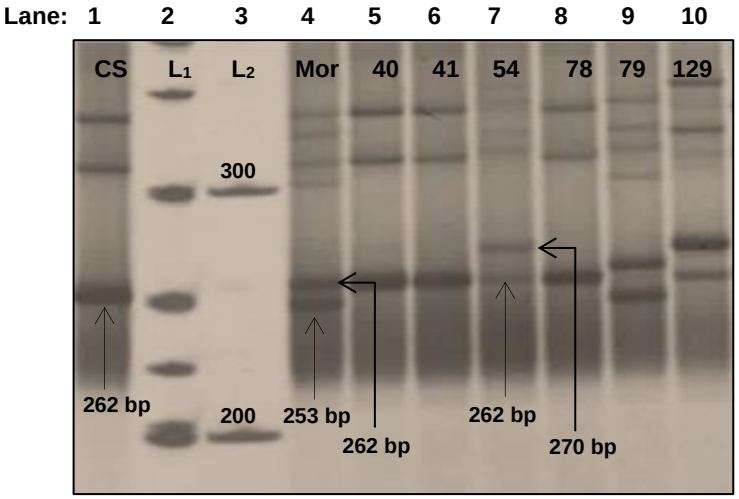

Figure 4.3. The optimisation of co-dominant SSR marker *Xics13* for *Pm4b*. Lane 1: “Chinese Spring” (positive control). Lane 2: 50 bp Ladder. Lane 3: 100 bp Ladder. Lane 4: “Morocco” (negative control). Lane 5-10: selected lines from SU-PBL’s 2020 wheat nursery.

According to Wu *et al.* (2018), homologous resistant and susceptible lines amplified band sizes of 264 bp and 252 bp, respectively. “Chinese Spring” and wheat lines “40”, “41” and “78” produced banding patterns similar to the homozygous resistant lines. Heterozygous lines amplified both fragments of 264 bp and 252 bp. “Morocco” and wheat line “79” produced banding patterns similar to the heterozygous resistant lines. The unique PCR fragment size of 270 bp observed in wheat lines “54” and “129” that was not reported by Wu *et al.* (2018).

4.1.1.2.2.*Xics43*

A PCR fragment size of 201 bp was expected for the co-dominant marker *Xics43* in homozygous resistant lines and 217 bp in homozygous resistant lines. The heterozygous state was expected to amplify both PCR fragments of 201 bp and 217 bp. The positive control "Chinese Spring" and the negative control "Morocco" amplified clear fragment sizes of 201 bp and 214 bp (**Figure 4.4**). The PCR fragment size 214 bp amplified in both controls fell within the acceptable range of susceptible product size 217 bp. The same banding pattern was observed in wheat lines "2" and "6". Multiple PCR fragments were observed in test samples "1", "4" and "5". Clear band sizes could not be determined for these PCR products.

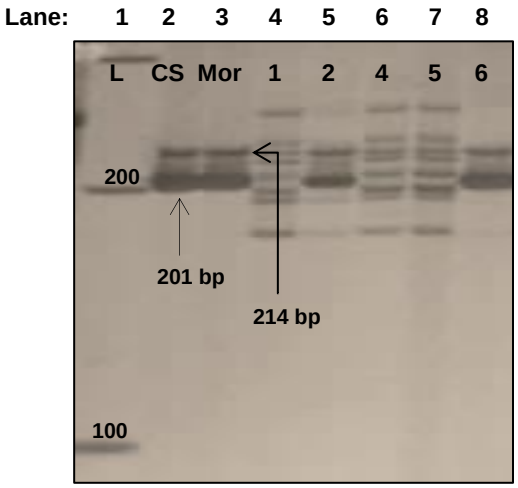

Figure 4.4. The optimisation of co-dominant SSR marker *Xics43* for *Pm4b*. Lane 1: 100bp Ladder. Lane 2: Chinese Spring (positive control). Lane 3: Morocco (positive control). Lane 4-8: samples of the selected SU-PBL's 2020 wheat nursery.

According to Wu *et al.* (2018) homozygous susceptible lines amplified a fragment size of 217 bp and heterozygous lines amplified both 201 bp and 217 bp. However, multiple banding patterns were also observed for homozygous susceptible lines, with no clear distinction which fragment was 217 bp. Two distinct banding patterns were observed for co-dominant SSR marker *Xics43*. The banding pattern observed in "Chinese Spring" amplified the desired fragment of 201 bp. However, the desired banding pattern was also observed in negative

control “Morocco”. The co-dominant SSR marker *Xics43* was unsuccessful in distinguishing between the positive and negative controls. Therefore, it could not be considered as a good diagnostic marker for detecting *Pm4b*. The linkage between SSR marker *Xics43* and the gene is fairly close with a genetic distance of 1.7 cM. However, the co-dominant SSR marker *Xics13* is closer to the targeted gene at 1.3 cM.

4.1.1.3. Microsatellite markers for *MLAG12*

Co-dominant SSR marker *Xwmc346* and dominant SSR marker *Xwmc273* was used to flank the temporarily designated *MLAG12* gene. The markers were linked to the resistant allele located on chromosome 7AL. The co-dominant SSR marker *Xwmc346* was located 6.6 cM from the gene of interest and generated a PCR fragment of 203 bp resistant individuals. The dominant marker *Xwmc273* was located 8.3 cM from the gene of interest and generated a PCR fragment size of 179 bp in resistant lines. These markers were used to molecularly characterise selected lines from the SU-PBL’s 2020 wheat nursery.

4.1.1.3.1.*Xwmc346*

The expected PCR fragment size for co-dominant marker *Xwmc346* was 203 bp. However, multiple fragments were observed for this marker around the desired amplicon region. Wheat cultivars available at the SU-PBL was screened in search of potential controls for the SSR marker. The controls used were “Chinese Spring” and “Steenbras”, which both flanked fragment sizes of 202 bp, 217 bp and 221 bp (**Figure 4.5**). While the “SST027” control amplified fragments sizes of 198 bp and 215 bp. The test samples in lane 3, 9, 13, and 14 showed the same banding pattern as the positive controls “Chinese Spring” and “Steenbras”. While the test samples in lane 7 and 16 amplified the same fragment sizes as the negative control “SST027”. Unique banding patterns were observed in lanes 2, 7, 10, 11, 12 and 15. These test samples shared fragment sizes observed in “Chinese Spring” and “Steenbras” (202 bp, 217 bp and 221 bp) but amplified an additional fragment size of 198 bp similar to “SST027”. No contamination was observed in the water control.

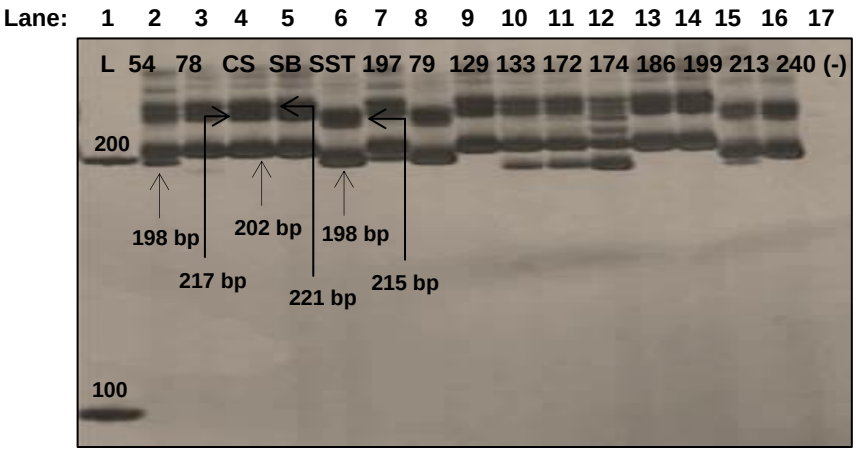

Figure 4.5. The optimization of dominant SSR marker *Xwmc346* for *MLAG12* visualised with silver-stained 6% PAA gel. Lane 1: 100bp Ladder. Lane 2-3: selected lines from SU-PBLs 2020 wheat nursery. Lane 4: Chinese Spring (positive control). Lane 5: Steenbras (positive control). Lane 6: SST027 (negative control). Lane 7-16: selected lines from SU-PBLs 2020 wheat nursery. Lane 17: dH_2O control.

Three distinct banding patterns were observed for co-dominant marker *Xwmc346*. The PCR fragment size of 202 bp amplified in “Chinese Spring” and “Steenbras” fell within an acceptable range as the desired product size of 203 bp. Test samples with the same PCR products as “Chinese Spring” were scored as homozygous resistant lines. The PCR fragment size for homozygous susceptible lines were not reported in literature, even though the segregation ratios for the SSR marker *Xwmc346* included heterozygous lines and homozygous susceptible lines (Maxwell *et al.*, 2009). However, the negative control “SST027” and the test samples in lanes 7 and 16 were scored as homozygous susceptible lines. Test samples in lanes 2, 7, 10, 11, 12 and 15 amplified PCR fragment sizes of 202 bp and 198 bp was scored as heterozygous lines. The co-dominant marker *Xwmc346* was diagnostic in detecting resistant and susceptible lines.

4.1.1.3.2. *Xwmc273*

The expected PCR fragment size for dominant marker *Xwmc273* was a single band of 179 bp. However, multiple fragments were observed for this marker around the desired amplicon region. “Chinese Spring” and “Steenbras” was used as positive controls, and “SST027” was used as the negative control. ‘Chinese Spring” amplified PCR fragment sizes of 186 bp, 195

bp and 201 bp (**Figure 4.6**). Test samples in lanes 5 – 13 amplified band patterns similar to "Chinese Spring". PCR fragment sizes of 186 bp, 195 bp and 209 bp was amplified in "Steenbras" and negative control "SST027", sharing the same banding pattern. Test samples in lanes 2 – 4 amplified the same banding patterm as "Steenbras and "SST027". A unique banding pattern was observed for test sample in lane 1, compared to the PCR products displayed in the controls. The PCR fragment sizes of 179 bp, 189 bp, 195 bp and 209 bp was amplified test sample "P6" displayed in lane 1. Test sample "P6" was the only test sample to generate a fragment size of 179 bp. The results for dominant SSR marker *Xwmc273* was inconclusive, with no distinction between resistant and suscepitible lines. The PCR products displayed by test sample "P6" could be a false positive. The SSR marker *Xwmc273* is therefore, not a good diagnostic marker in detectting resistant and susceptible lines.

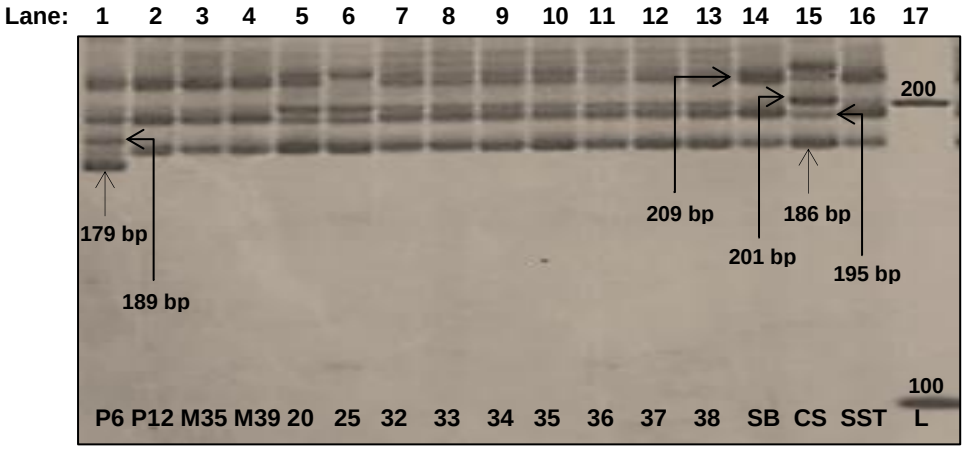

Figure 4.6. The optimisation of co-dominant SSR marker *Xwmc273* for *MLAG12*. Lane 1-13: samples of the selected SU-PBL nursery 2020. Lane 14: Steenbras (potential control). Lane 15: Chinese spring (potential control). Lane 16: SST027 (potential control). Lane 17: 100 bp Ladder.

4.1.1.4. Microsatellite markers for *MLUM15*

The *MLUM15* gene was the first powdery resistance gene to be introgressed from *Aegilops neglecta* (2n=4x=28; genomes UUMM) into hexaploid wheat (2n=6x=42; genomes AABBDD). The physical location of the gene was mapped to the distal 1% of chromosome 7AL, along with *MLAG12* and *Pm37*. The dominant SSR markers *Xcfa2257* and co-dominant SSR marker *Xcfa2240* located 1.2 cM distal and proximal to *MLUM15* was used to flank the gene. The

expected PCR fragment sizes for *Xcfa2257* and *Xcfa2240* was 167 bp and 280 bp, respectively (https://wheat.pw.usda.gov).

4.1.1.4.1.*Xcfa2257*

A PCR fragment size of 167 bp was expected for dominant SSR marker *Xcfa2257* in homozygous resistant lines. “Chinese Spring” and “Steenbras” was used as positive controls and “Morocco” as a negative control. Two distinct banding patterns were observed for dominant SSR marker *Xcfa2257* (**Figure 4.7**). “Chinese Spring” and “Steenbras” amplified the same banding patterns, producing fragment sizes of 152 bp and 181 bp. The negative control “Morocco” displayed no amplified PCR products. Wheat lines in lane 5 – 7 amplified banding patterns unique to the controls, with fragment sizes of 148 bp and 175 bp. The desired PCR fragment size of 167 bp was not observed in the controls. However, the controls used for the dominant marker *Xcfa2257* were not known positive controls for the gene of interest. Although the controls have been recorded to have viable powdery mildew resistance genes. No additional gel electrophoresis images were available in literature to validate the results obtained. The dominant SSR marker *Xcfa2257* was not a good diagnostic marker for distinguishing between resistant and susceptible lines.

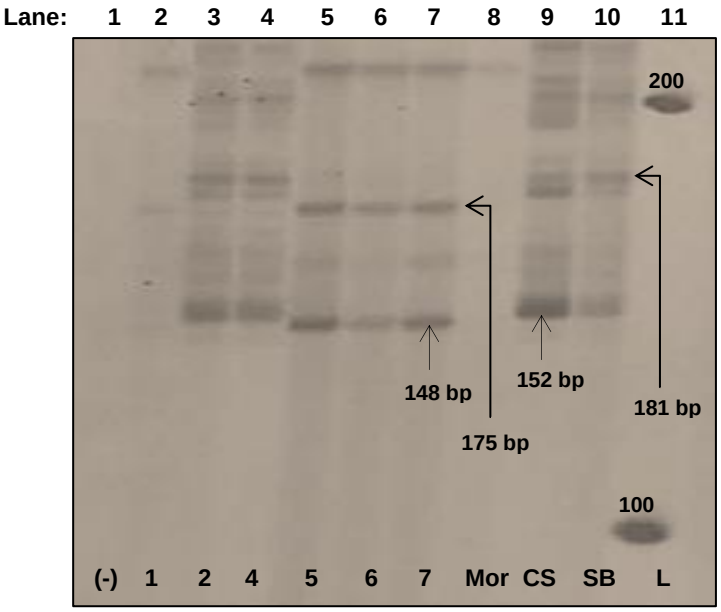

Figure 4.7. The optimisation of co-dominant SSR marker *Xcfa2257* for *MLUM15* visualised with silver-stained 6% PAA gel. Lane 1: water control. Lane 2-7: selected lines from the SU-PBL's 2020 wheat nursery. Lane 8: "Morocco" (potential control). Lane 9: "Chinese Spring" (potential control). Lane 10: "Steenbras" (potential control). Lane 11: 100 bp Ladder.

4.1.1.4.2.*Xcfa2240*

A PCR fragment size of 280 bp was expected for co-dominant SSR marker *Xcfa2240* in homozygous resistant lines. "Chinese Spring" and "Steenbras" was used as positive controls and "Morocco" as a negative control. Three distinct banding patterns were observed for the co-dominant marker (**Figure 4.8**). The positive controls "Chinese Spring" and "Steenbras" amplified PCR fragment sizes of 256 bp and 290 bp. The negative control "Morocco" also amplified PCR fragment sizes of 256 bp and 290 bp, similar to the positive controls. Test samples in lanes 5, 6, 7 and 9 amplified the same banding patterns as the controls. Test sample in lane 7 amplified a single PCR fragment size of 290 bp. Test sample in lane 10 amplified PCR fragment sizes of 256 bp, 290 bp and 294 bp. The co-dominant SSR marker *Xcfa2240* could not distinguish between the positive and negative controls. *Xcfa2240* was therefore, not a good diagnostic marker in distinguishing between resistant and susceptible lines.

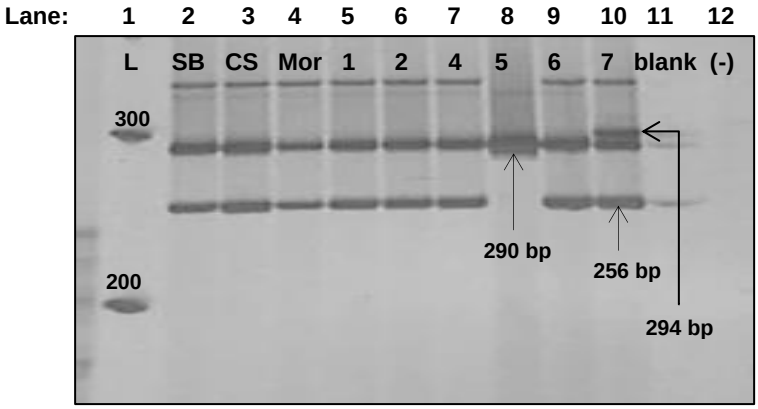

Figure 4.8. The optimisation of co-dominant SSR marker *Xcfa22240* for *MLUM15* visualised with silver-stained 6% PAA gel. Lane 1: 100 bp Ladder. Lane 2: "Steenbras" (potential control). Lane 3: "Chinese Spring" (potential control). Lane 4: "Morocco" (control). Lane 5-10: selected lines from the SU-PBL's 2020 wheat nursery. Lane 11: residue from previous sample. Lane 12: water control.

4.1.2. Marker identification for novel rust resistance genes

The cloning of the *Sr35* gene led to the development of a perfect dominant marker to flank the gene during MAS (Saintenac *et al.*, 2013). The *Sr35* gene confers near-immunity towards the virulent *Ug99* rust strain and related lineages, deeming the gene highly important in breeding programmes. The primer sequence information of the marker was obtained from MAS Wheat database (https://maswheat.ucdavis.edu/protocols/Sr35). The database contained marker reports and protocols for rust resistance genes. The PCR protocol obtained for *Sr35* was used as a guideline for further optimisation at the SU-PBL.

4.1.2.1. Molecular marker for *Sr35*

Sr35 was a resistant gene introgressed from *Triticum monoccocum* and was located on chromosome 3AL in *T. aestivum*. Saintenac *et al.* (2013) cloned the resistant gene and located a dominant marker spanning across the *Sr35* locus. The perfect dominant marker was used to molecularly characterise the segregating base population after the deployment of the *Sr35* gene in 2014 (Springfield, 2014). A PCR fragment size of 719 bp was expected for homozygous resistant lines (**Figure 4.9**). No PCR products was expected for homozygous

susceptible and heterozygous lines. The positive control used for the marker was a *Sr35* carrying wheat line labelled “C35”.

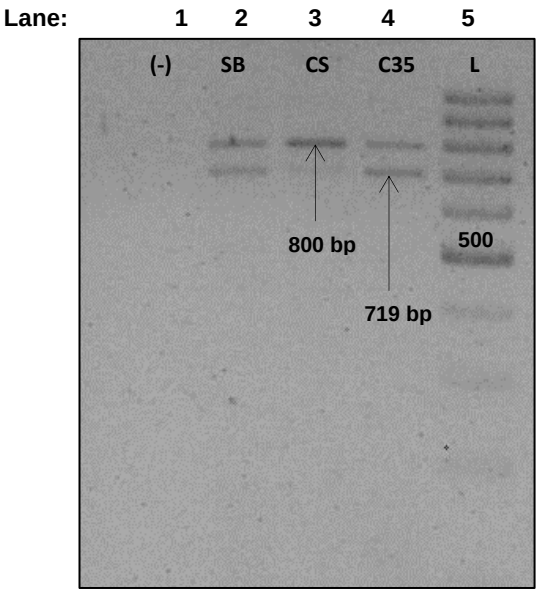

Figure 4.9. The optimisation of perfect dominant marker *NL9* for *Sr35* gene visualised with ethidium bromide stained 2% agarose gel. Lane 1: water control. Lane 2: “Steenbras” (positive control), Lane 3: “Chinese Spring” (negative control). Lane 4: “C35” (positive control). Lane 5: 100 bp Ladder.

Sr35 carrying line “C35” was used as a known positive control for the marker and was expected to amplify a single PCR fragment of 719 bp. PCR fragment sizes of 719 bp and 800 bp was observed in the positive control “C35” (**Figure 4.9**). The control “Steenbras” also amplified PCR fragment sizes of 719 bp and 800 bp, similar to “C35”. “Chinese Spring” amplified a single PCR fragment size of 800 bp. No contamination was observed for the PCR reaction, with no visible PCR products amplified in the water control. The PCR fragment size of 800 bp observed in *Sr35* carrying line “C35” was not reported in literature. Given that the water control was free of contaminants, the additional PCR fragment of 800 bp was not a result of contamination. After several attempts to completely optimise the molecular marker at the SU-PBL, a single dominant band was not obtained in the “C35” control. The molecular marker

for *Sr35* was therefore not reproducible and could not provide accurate diagnosis between resistant and susceptible lines.

4.1.2.2. Molecular marker for *Sr45*

The *Sr45* gene was a resistant gene introgressed from *Aegilops tauschii* and was located on chromosome arm 1DS in *T. aestivum*. A high-resolution mapping population was designed for the gene which resulted in the development of a co-dominant PCR marker *cssu45*. The marker was located only 0.39 cM from the gene of interest. A PCR fragment size of 220 bp was expected in homozygous resistant lines and 238 bp in homozygous susceptible lines (**Figure 4.10**). The co-dominant PCR marker was visualised using ethidium bromide-stained 2% agarose gel electrophoresis.

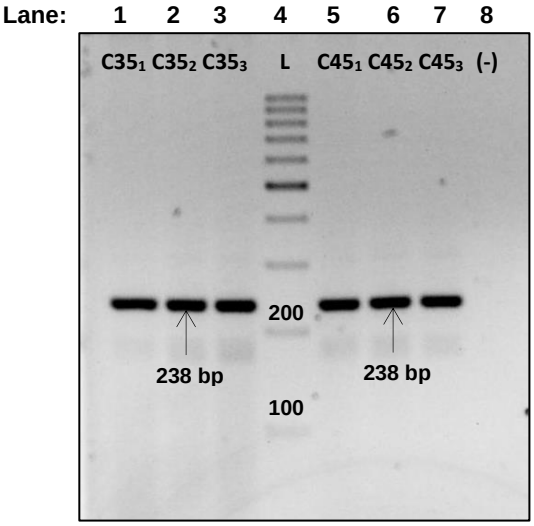

Figure 4.10. The optimisation of co-dominant marker *cssu45* for *Sr45* gene visualised with ethidium bromide stained 2% agarose gel. Lane 1-3: "$C35_{1,2,3}$" (negative control). Lane 4: 100 bp Ladder. Lane 5-7: "$C45_{1,2,3}$" (positive control). Lane 8: ddH_2O control

Sr45 carrying lines "$C45_1$", "$C45_2$" and "$C45_3$" were used as the positive control for the marker and was expected to amplify a PCR fragment size of 220 bp. *Sr35* carrying lines "$C35_1$", "$C35_2$" and "$C35_3$" were used as the negative control for the marker and were expected to amplify a PCR fragment size of 238 bp. The *Sr35* carrying lines amplified a PCR product of

238 bp. The *Sr45* carrying line amplified the same PCR fragment size of 238 bp as displayed in the negative control (**Figure 4.10**). No contamination was observed in the PCR reaction, with no products amplified in the water control. The co-dominant marker *Cssu45* could not distinguish between the positive and negative controls. In a study conducted by Springfield (2014), the marker was diagnostic and could distinguish between resistant and susceptible lines. The marker was used under the same conditions at the SU-PBL and was expected to be diagnostic.

4.1.3. Screening MS-MARS crossing parents for rust resistance genes

The female (male sterile) population was molecularly characterised for rust resistance genes *Sr35*, *Sr45*, *Lr34* and *Sr2*. The plant material was screened before each MS-MARS cycle to assess variation in gene frequencies. For the first MS-MARS cycle, a sample of 360 entries from a total of 2400 wheat lines was molecularly screened to represent the female population. The gene frequencies observed within the female population for *Sr2* gene was 27%. The gene frequency for *Lr34* within the female population was 35%. For the second MS-MARS cycle, a sample of 240 entries from a total of 2250 wheat lines was molecularly screened to represent the female population. The observed gene frequencies for the *Sr2* gene after the crossing event was 25%. The observed gene frequency for *Lr34* after the crossing event was 23%.

The gene frequencies of *Sr2* and *Lr34* was considerably lower during the MS-MARS cycles. The results obtained after the crossing events displayed a decrease in gene frequencies of 2% for *Sr2* and 12% for *Lr34* (**Figure 4.11**). The decrease in observed gene frequencies of *Lr34* between crossing cycles was unexpected, given that the allele frequency for *Lr34* in the male population was 89% after selections. The decrease in observed gene frequencies could be a consequence of the reduced sample size used to represent the female population during the second MS-MARS cycle. Only 11% of the entire population was molecularly characterised for the rust genes to represent the female population of the second MS-MARS cycle. The remaining 89% of the population was unaccounted for and could potentially contain the *Lr34* gene. A larger sample size of the female population would increase

the accuracy of observed gene frequencies. The negative selection of *Sr2* in the male population could explain the decrease in observed gene frequency between the first and second MS-MARS cycles. The allele frequency for *Sr2* in the male population was 32% after selections. The singular deployment of *Sr2* no longer provides effective protection and has been associated with pseudo-black chaff. However, only in combination with *Lr34* has the gene provided increased broad-spectrum resistance in the MS-MARS breeding scheme.

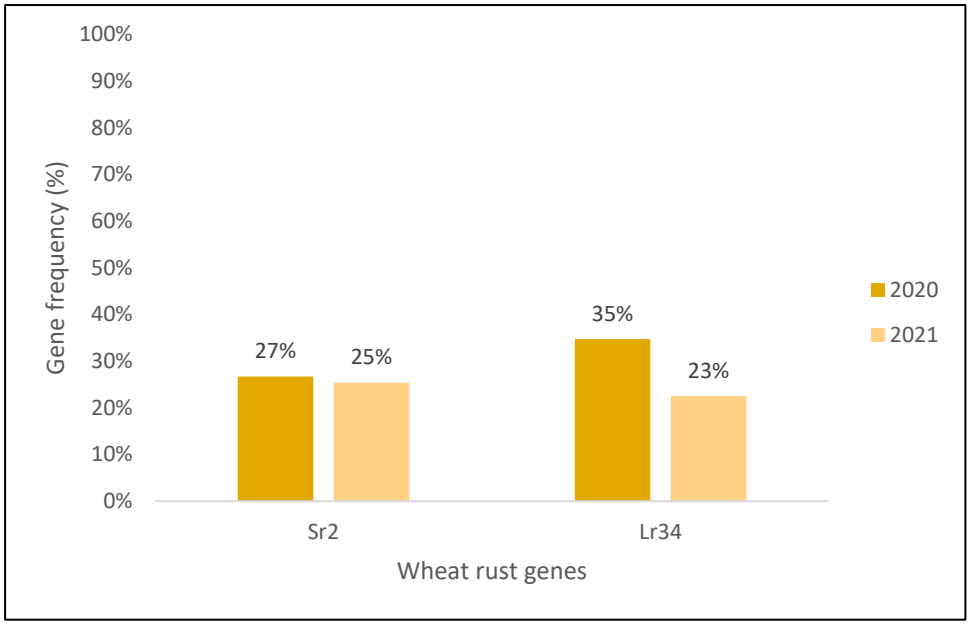

Figure 4.11. Observed gene frequencies of rust resistance genes *Sr2* and *Lr34* in the segregating base population recording during 2020-21 MS-MARS cycles

4.2. Disease assessment for powdery mildew resistance

Twenty-eight selected genotypes were molecularly and phenotypically characterised for powdery mildew resistance. The powdery mildew resistance genes previously introduced into the MS-MARS pre-breeding scheme was *Pm38* linked to leaf and stripe rust resistance (*Lr34*/*Yr18*/*Pm38*) and *Pm8* linked to three different rust genes (*Sr31*/*Lr26*/*Yr9*/*Pm8*). *Pm38* and *Pm8* deployed singularly no longer provides effective protection against powdery mildew outbreaks. *Blumeria graminis* f.sp. *tritici* isolates were obtained from Vergenoegd experimental farm, Stellenbosch. The isolates collected was used as a general representation of the *Bgt*

population in the cropping region. Disease assessment was performed on selected genotypes obtained from the SU-PBL's 2020 wheat nursery.

4.2.1. Phenotypic validation of Blumeria *graminis* f. sp. *tritici* isolates

Twenty-eight genotypes were phenotypically assessed for disease response to *Bgt* isolates. The measurements were recorded at 6-, 11- and 14-days post inoculation. The measured disease response of the twenty-eight genotypes was subjected to analysis of variance and correlation tests. The ANOVA was performed to identify variations between the measured trait recorded at different days post inoculation and genotypes. The coefficient of variation (CV) values generated for the traits ranged between 5% and 7%. Low variation was observed among the tested genotypes for *Pm* disease response. The conditions were constant for all tested genotypes with minimum environmental variation observed. The only variation observed was therefore attributed to the genotypic variations among genotypes. The p-value obtained was less than the critical value of 0.05, indicating that the measurements taken at 6-, 11- and 14-days post inoculation (dpi) was significantly different.

Disease response was scored according to the 0 – 9 scale developed by Leath (1990) (**Figure 3.1**). The positive control "Steenbras" performed significantly better than the negative control "Morocco". The negative control "Morocco" displayed nearly 100% disease coverage within the first six days post inoculation. The positive control "Steenbras" displayed no visible signs of infection at 6 dpi but displayed one-two visible pustules at 11 and 14 dpi. "Chinese Spring" displayed a disease response similar to "Morocco", with 50 – 100 % coverage at 6 dpi. Wheat lines "10US1M186", "20US1M037", "20US1M129", "20US1M186" and "20US1M199" displayed a disease response similar to "Steenbras" ranging from resistant to moderately resistant. The resistant lines maintained a low disease response from 6 dpi to 14 dpi. An overall increase in disease progression was observed at 11 dpi. In highly susceptible lines, multiple sporulation and mycelia colonies had formed at 11 dpi. In resistant lines, disease establishment had only occurred at 11 dpi, with no visible symptoms displayed at 6 dpi.

Overall disease progression at 6 dpi was relatively low, more than 50% of the genotypes displayed an infection type of 3. Several outliers were observed for disease progression measured at 6 dpi. Certain genotypes were highly susceptible with 100% coverage, and some were highly resistant with no visible symptoms at 6 dpi (**Figure 4.12**). Measurements taken at 11 dpi displayed increased disease progression across several genotypes. Disease progression at 11 dpi was therefore more dispersed than the progression recorded at 6 dpi (**Figure 4.13**). The disease progression observed at 14 dpi displayed a distribution pattern similar to the disease progression observed for measurements recorded 11 dpi (**Figure 4.14**). No significant difference was observed between disease progression recorded at 11 dpi and 14 dpi.

4.2.2. Phenotypic and genotypic interactions for powdery mildew assessment

The control “Steenbras” displayed a resistant disease response to the *Bgt* isolates collected. The pedigree of “Steenbras” supported the presence of viable powdery mildew resistance. Wheat variety “Siete-Cerros-66” was a crossing parent for “Steenbras”, with inherited resistance to powdery mildew. Extensive research was conducted on “Steenbras” regarding rust resistance over several years but very little in relation to powdery mildew resistance. According to Lutz *et al.* (1992), “Siete-Cerros-66” had the *Pm5* gene, specifically the *Pm5b* allele. The lack of molecular markers for the *Pm5* locus constrained previous studies from confirming the presence of the *Pm5b* gene in “Steenbras”. Nonetheless, viable powdery mildew resistance had been confirmed in “Steenbras” (Lutz *et al.*, 1992).

Pearson’s correlation analysis was conducted to evaluate the relationship between presence of *Pm* genes and disease response of selected wheat genotypes. The genotypes were molecularly characterised for four *Pm* genes. Resistant disease response at 6-, 11- and 14- dpi and molecular markers *Xwmc346* used to flank *MLAG12* was positively associated. Gene frequencies of the powdery mildew resistance gene *MLAG12* was the most prominent among the genotypes. *Bgt* isolates collected across the Western Cape region of South Africa had the lowest mean complexity of virulence to *MLAG12*, with a virulence frequency of zero

(Kloppe *et al.*, 2022). The *MLAG12* gene was effective in conferring resistance against the *Bgt* population collected at Vergenoegd, Stellenbosch.

Table 4.1. Disease response based on recorded infection types and the molecular marker profile of the selected genotypes.

Wheat line	Disease response			*Pm37*	*MLAG12*
	6 dpi	11 dpi	14 dpi	*Xwmc790*	*Xwmc346*
20US1M186	HR	MR	MR	0	1
20US1M037	R	MR	MR	0	1
20US1M129	MR	MR	MR	0	1
20US1M199	MR	MR	S	0	1
20US1M040	R	MR	MR	0	0
Chinese Spring	HS	HS	HS	n/a	1
Morocco	HS	HS	HS	0	n/a
Steenbras	HR	MR	MR	1	1

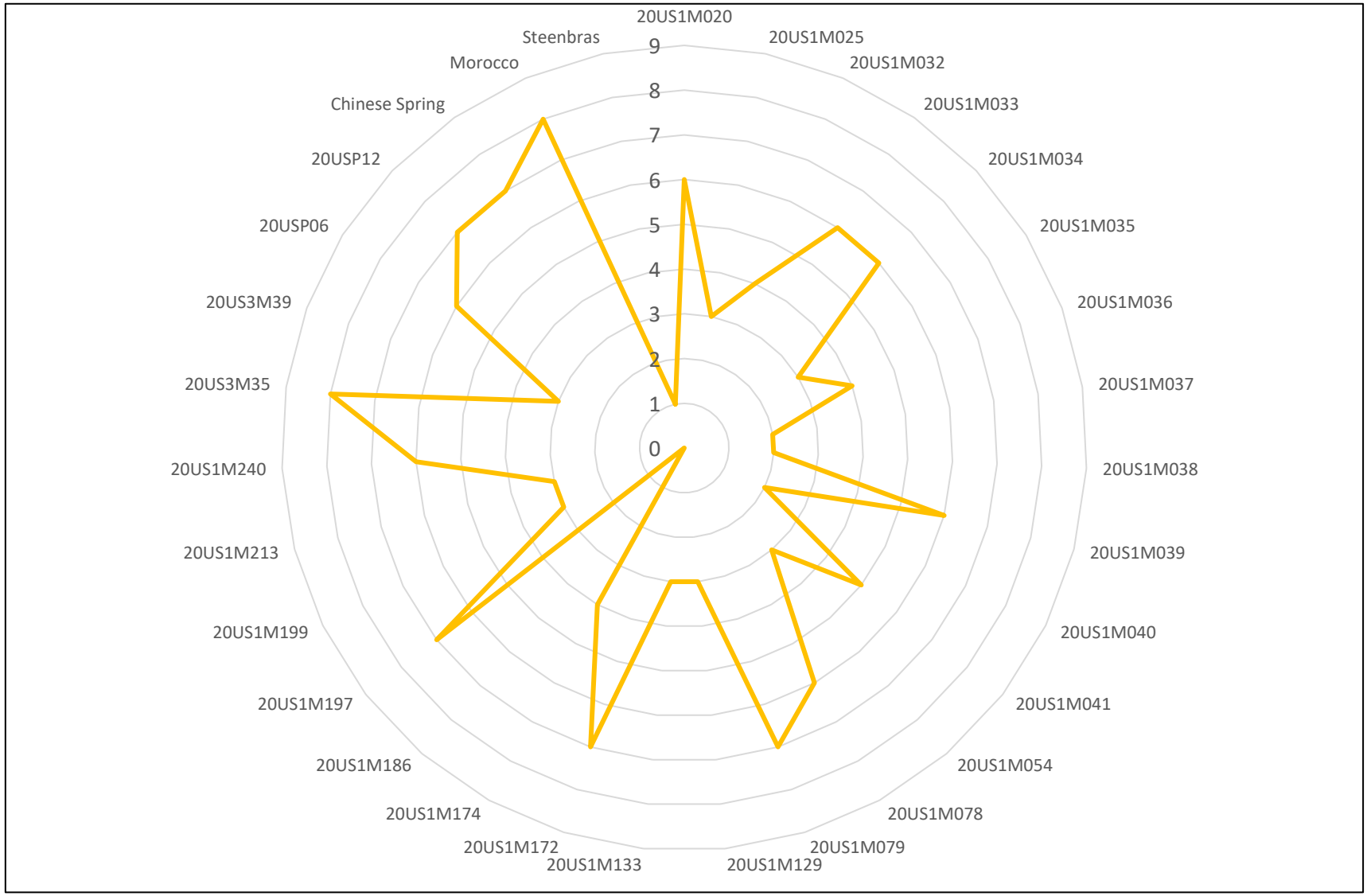

Figure 4.12. Powdery mildew disease progression measured in tested genotypes from the SU-PBL's 2020 wheat nursery at 6 days post inoculation. The infection types were plotted on the vertical axis with zero (0) being immune and nine (9) being highly susceptible.

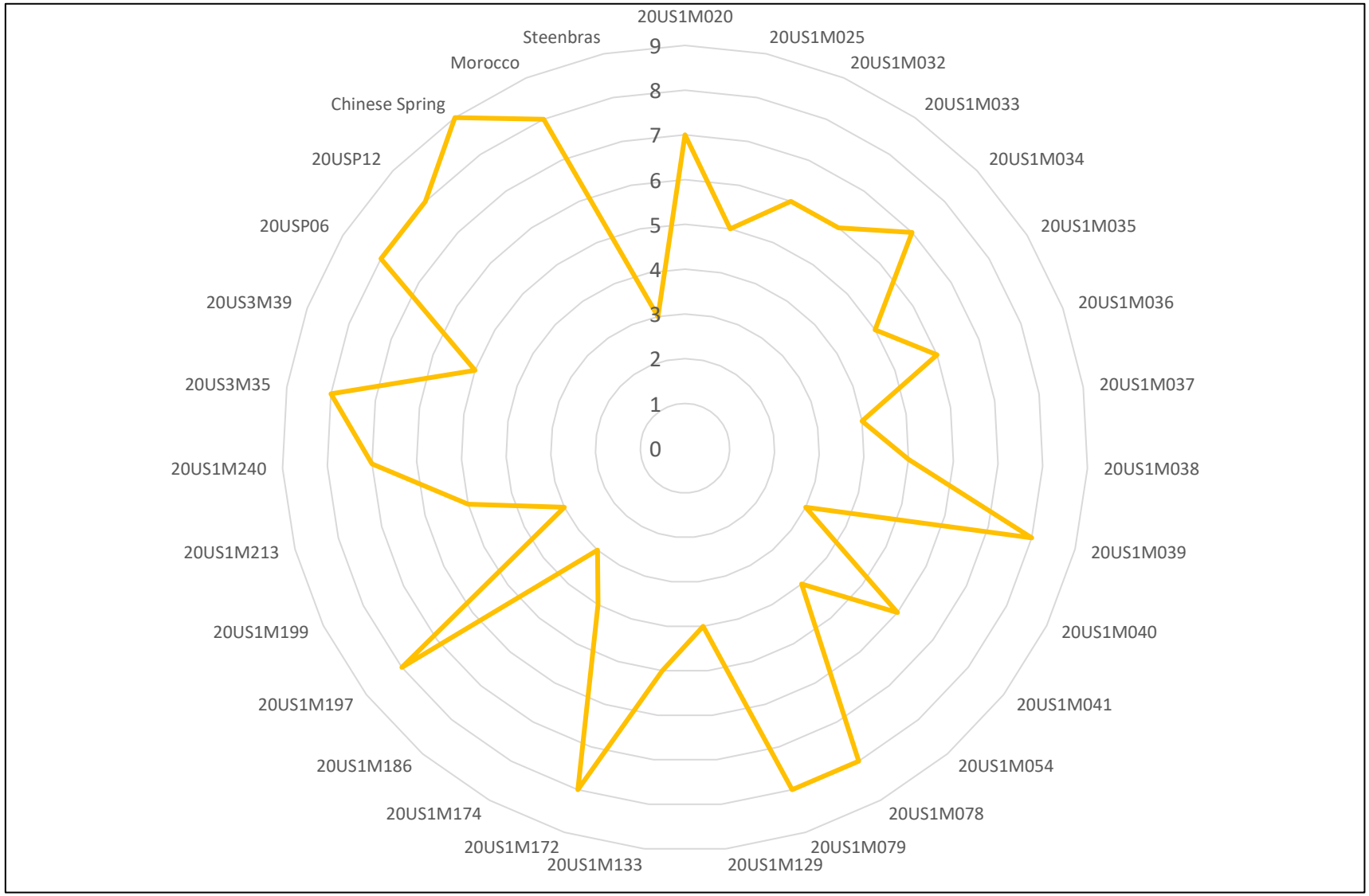

Figure 4.13. Powdery mildew disease progression measured in tested genotypes from the SU-PBL's 2020 wheat nursery at 11 days post inoculation. The infection types were plotted on the vertical axis with zero (0) being immune and nine (9) being highly susceptible.

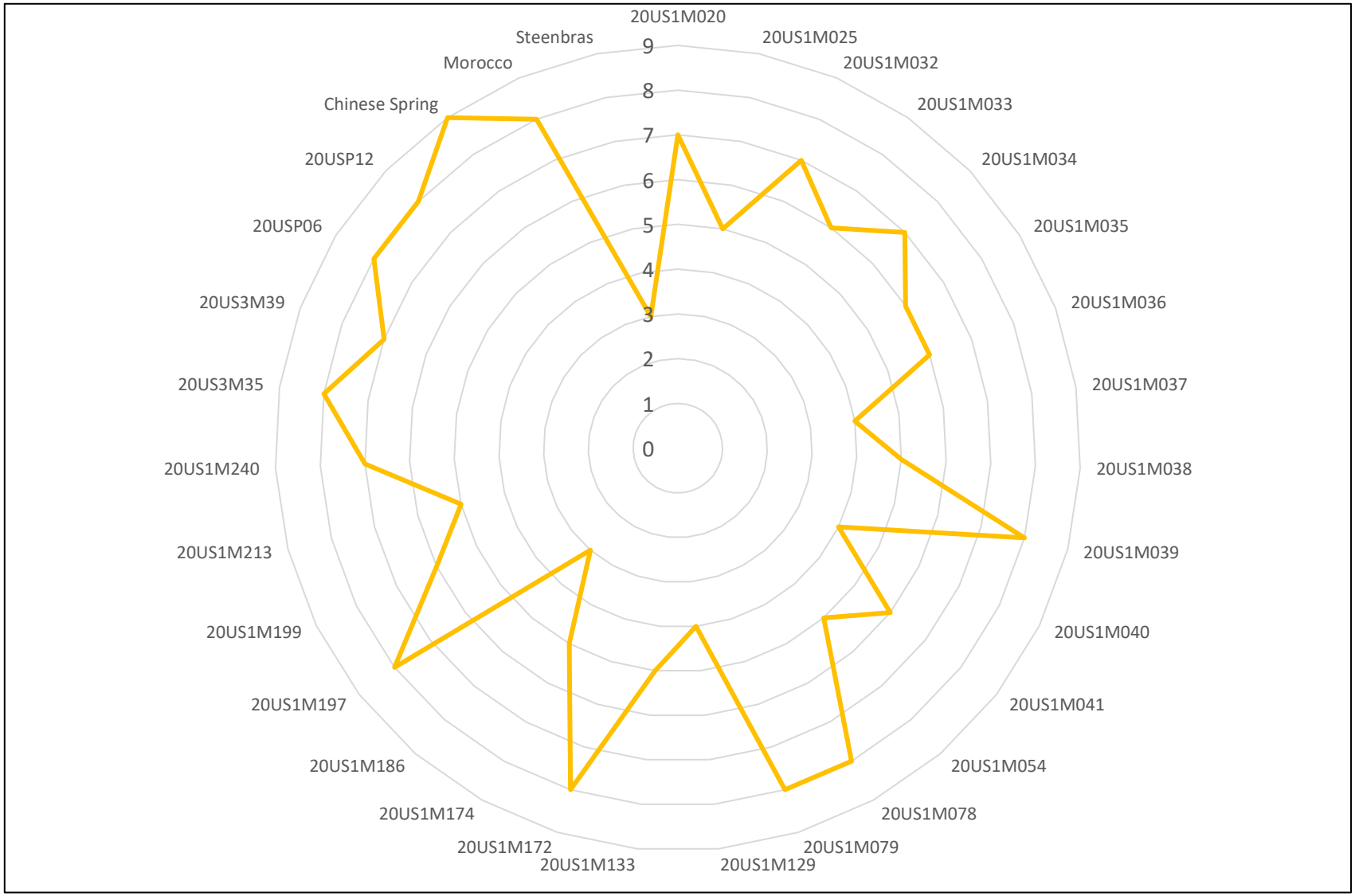

Figure 4.14. Powdery mildew disease progression measured in tested genotypes from the SU-PBL's 2020 wheat nursery at 14 days post inoculation. The infection types were plotted on the vertical axis with zero (0) being immune and nine (9) being highly susceptible.

4.3. Disease assessment for Fusarium head blight

The resistant control used in this study was “Sumai3” and the susceptible control was “PAN4371”. Three (3) experimental replicates were used to assess the phenotypic response of wheat lines exposed to *F. graminearum* isolates. A spray inoculation method was used to assess type II FHB resistance by measuring the percentage disease severity at 14-, 21-, and 28-days post inoculation (dpi). Water soaking and bleaching symptoms were observed at the infection site of all inoculated material, indicating successful inoculation. No natural infection was observed in control lines inoculated with roH_2O.

4.3.1. Phenotypic validation of *Fusarium graminearum* isolates

The resistant control “Sumai3” performed significantly better than the susceptible control “PAN3471”. Increased disease progression was observed across the measurements taken at 14-, 21- and 28-days post inoculations (**Figure 4.15**). Measurements for disease severity taken at 14 dpi was relatively low across all genotypes. An increase in disease severity for all genotypes were observed at 21 dpi and 28 dpi, excluding “Sumai3”. Disease progression observed in “Sumai3” remained low with only two florets affected at 14 dpi and 28 dpi. Initiation of infection at the infected site was observed in “Sumai3”, but no further spread of fungi to neighbouring florets occurred. The results validated that both type I and type II resistance (*Qfhs.ifa-5A*, *Fhb1*) was present in “Sumai3”.

Disease severity in wheat lines “6402”, “6411” and “6426” was low at 14 dpi with a disease severity less than 10%, but peaked at 21 dpi and continued to increase at 28 dpi. Wheat lines “5297” and “5450” displayed low disease severity of less than 10% at 14, 21 and 28 dpi (**Figure 4.15**). It was observed from the disease progression that no wheat line performed significantly better than “Sumai3” (Figure 4.16). Two wheat lines “5297” and “5450” displayed a resistant disease response of less than 10% disease severity. Disease progression remained relatively

low for “5297” and “5450” following initial infection at the inoculated site. Initial infection with no further spread of disease along the rachis was an indication of type II FHB resistance.

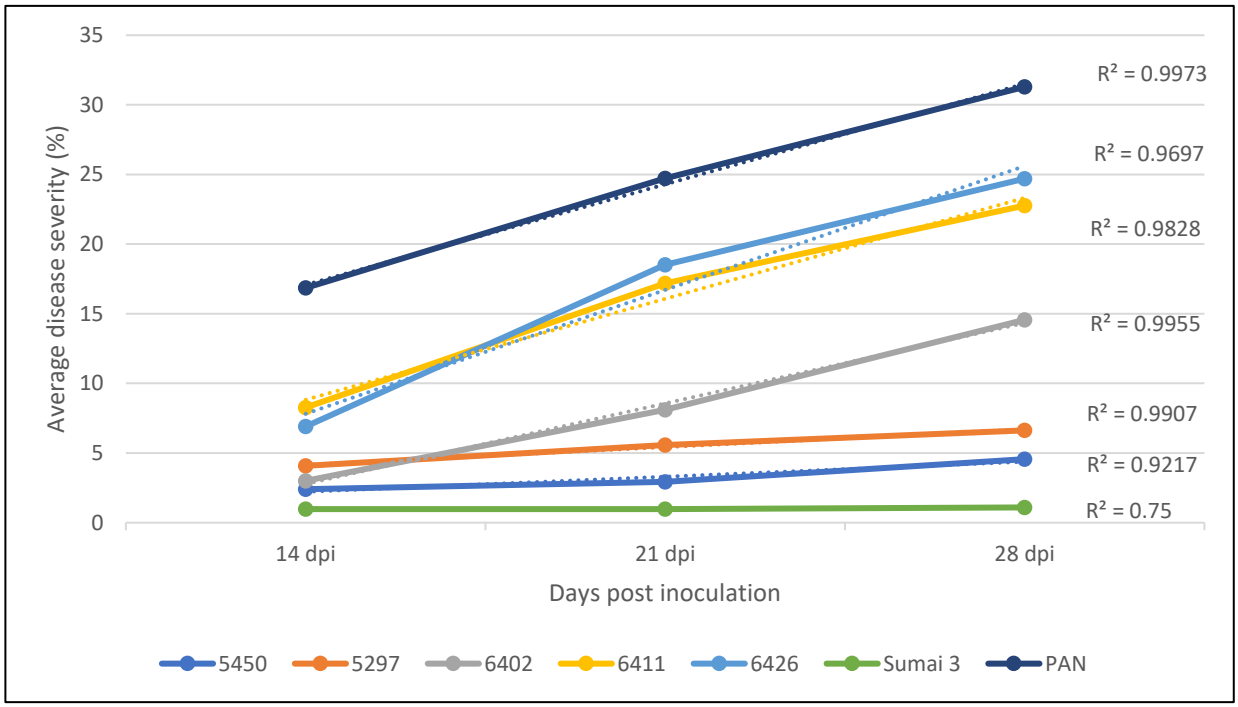

Figure 4.15. Average Fusarium head blight disease severity recorded across tested wheat lines at 14-, 21- and 28-days post inoculation. The coefficient of determination (R^2) was used to indicate the variation between variables.

Further evaluation was conducted to assess disease progression and the presence of closely linked FHB QTLs. Wheat line “5297” amplified both SSR markers (*gwm304*, *gwm293*) that flank *Qfhs.ifa-5A*. According to Buerstmayr *et al.* (2003), *Qfhs.ifa-5A* was primarily associated with type I resistance but also with type II resistance, although very rare. The low disease progression observed for “Sumai3” coupled with both *Qfhs.ifa-5A* and *Fhb1* being present in the cultivar depicted that both type I and II resistance was in effect.

4.3.2. Phenotypic variation in FHB resistance genotypes

Phenotypic assessment was conducted on five genotypes following FHB inoculations during anthesis. The phenotypic data included disease assessment as above-mentioned and yield parameters. The phenotypic data generated from evaluated yield parameters was fit to a general linear model for data description. The material was, subjected to a randomised

complete block design ANOVA analysis using Agrobase Generation II version 34.4.18. In addition to the ANOVA output, the coefficient of variation (CV) value and R^2 value for each yield parameter was generated. Traits with significant differences between entries were used to identify the best performing genotypes.

Grain number displayed significant differences between genotypes with a p-value of 0.0132. The trait had an acceptable CV value of 15.31% and a high R^2 value of 0.7709. Among the evaluated genotypes, wheat line “5297” produced the least number of grains with a grand mean of 23 grains per plant (**Figure 4.16**). Wheat line “5250” produced the largest number of grains with a grand mean of 33 grains per plant. Tukey’s honest significance (HSD) test was conducted to evaluate which genotypes significantly differed from the rest. Wheat line “5450” differed significantly from the positive control “Sumai3” but not from the rest of the tested wheat lines.

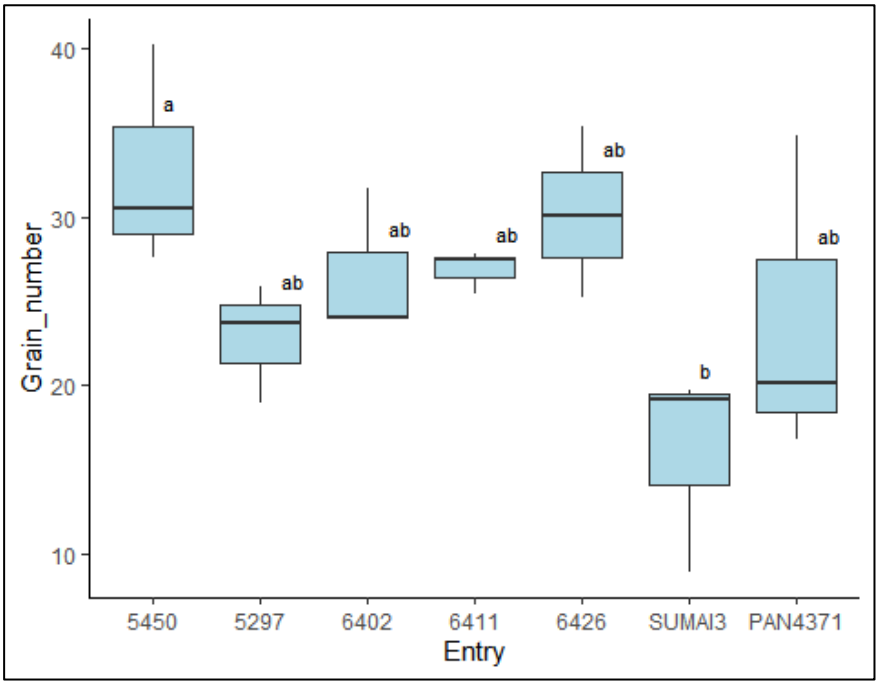

Figure 4.16. Boxplot of grain number distribution using Tukey HSD to differentiate between the five genotypes.

Tiller number displayed significant differences between genotypes with a p-value of 0.0006. The trait had a CV value of 19.35%, with a high R^2 value of 0.8506. Among the evaluated genotypes, wheat line “6411” produced the least number of tillers, with an average

of 3 tillers per plant. Wheat line “6402” produced the largest number of tillers, with an average of 8 tillers per plant (**Figure 4.17**). Tukey’s HSD test was conducted to evaluate which genotypes were significantly different from the rest. Wheat line “6402” differed significantly from wheat lines “5450”, “6411”, “6426”, “Sumai3” and “PAN4371” but not from wheat lines “5297”. However, the overall yield of wheat line “6402” was significantly lower. Tiller number was not a good yield parameter for identifying superior genotypes in relation to disease response.

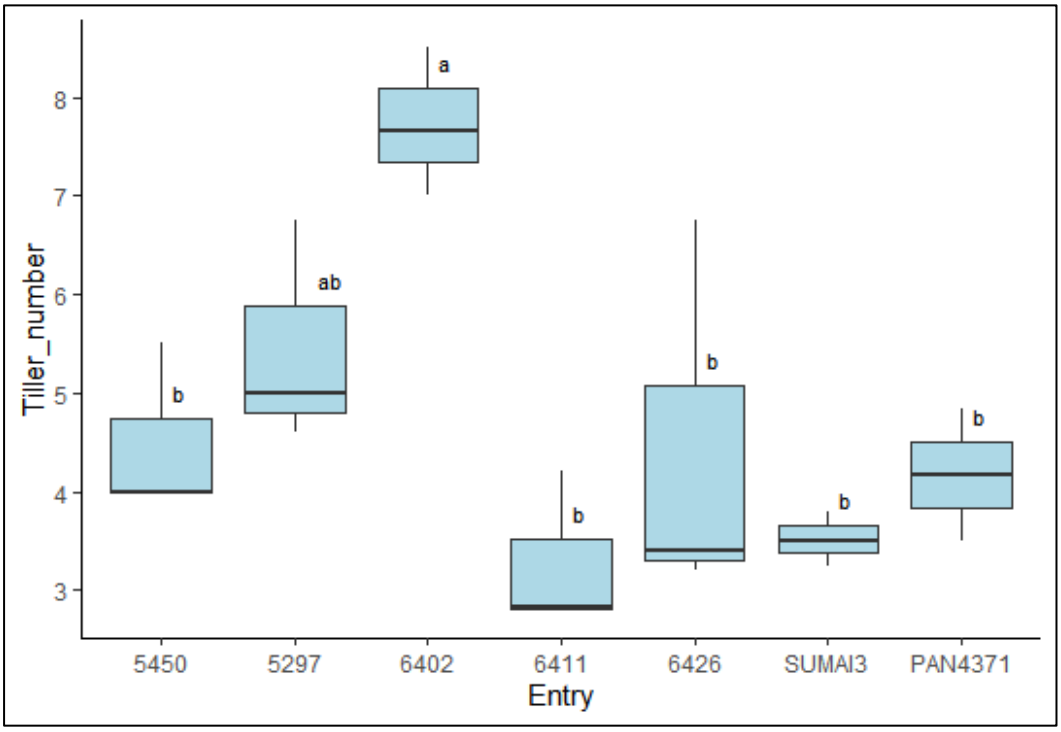

Figure 4.17. Boxplot of tiller number distribution using Tukey HSD to differentiate between the five genotypes.

Assessing the relationship between grain number and tiller number. Pearson’s correlation analysis displayed no association between the two traits. In addition, no association was observed between disease severity recorded at 14-, 21- and 28 dpi and the yield parameters (grain number, tiller number).

4.3.3. Evaluation of mycotoxin contamination by *F. graminearum* isolates

Fusarium graminearum isolates occurring in South Africa primarily produced ZEA, DON and less frequently NIV. The occurrence and magnitude of these mycotoxins highly depend on environmental conditions and chemotypes present in a region. The quantitative data generated from quantifying mycotoxin content in tested genotypes were subjected to analysis of variance (ANOVA). The most relevant results generated was the coefficient of variation (CV) and Fisher's least significant difference (LSD). Deoxynivalenol (DON) was the most prominent mycotoxin detected in tested genotypes. No detectable levels of NIV and ZEA were quantified in any of the tested samples. The CV value obtained for DON content in the wheat lines was 13.75%. The low CV value observed was a good indication of minimal environmental variation among tested samples.

"Sumai3" had the lowest mean level of DON accumulation at 0 043 mg/kg, compared to "PAN3471 accumulating the highest at 6.771 mg/kg across all three replicates (**Figure 4.18**). Wheat lines "5450" and "5297" accumulated low DON levels at 0.065 mg/kg and 0 225 mg/kg, respectively. Wheat lines "6402" "6411" and "6426" displayed high levels of DON with recordings above the threshold value of 1 mg/kg implemented by FAO regulations.

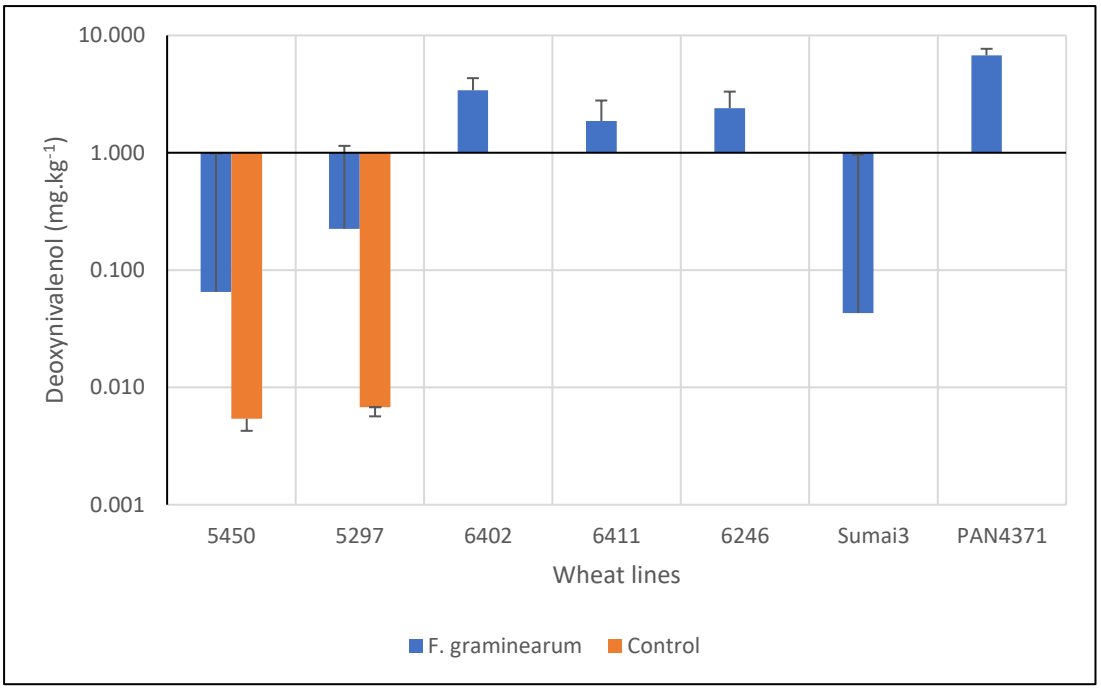

Figure 4.18. Detectable levels of deoxynivalenol content in wheat lines following inoculation with *Fusarium graminearum* isolates. The detectable levels of DON content was log transformed and displayed on the y axis with a vertical cross at 1.

DON content was detected in the controlled wheat lines inoculated with roH_2O. No detected disease severity was recorded for the controlled wheat lines. The grain harvested from the controlled wheat lines displayed no visible signs of FDK. However, the quantification of mycotoxin content in the controlled wheat lines displayed low levels of DON content. No significant differences were observed between DON content detected in the controlled wheat lines and the *F. graminearum* inoculated wheat lines. It was possible that latent natural infection occurred in the controlled wheat lines, with no sign of visible symptoms.

4.3.4. Interaction between disease severity, DON and FDK

Disease severity, DON content, Fusarium damaged kernels (FDK) and TKW was subjected to Pearson's correlation analysis. Significant positive linear relationships were observed between DON content, disease severity measurements taken at 14, 21 and 28 dpi as well as FDK under greenhouse conditions. The correlation coefficients ranged between -0.092 and 0.92 (**Figure 4.19**). The relationship between disease severity and DON content was positive and linear with a mean correlation coefficient of 0.856. High DON deposition was therefore a

contributing factor in disease severity. Moreover, supporting that DON mycotoxin acted as a contributing virulence factor to fungal colonisation and disease severity. The contributing factors influencing FHB colonisation also aided DON accumulation in infected grain. The relationship between DON content and FDK was positive and linear with a mean correlation coefficient of 0.60.

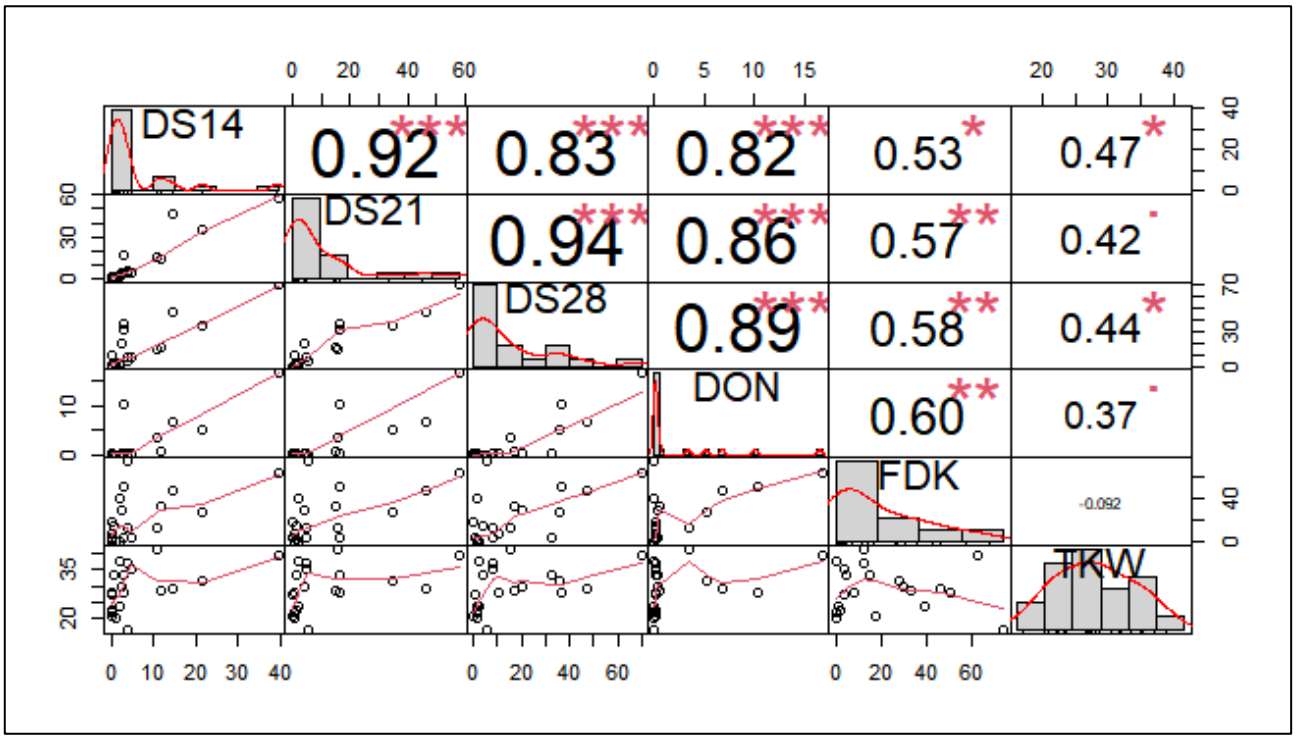

Figure 4.19. Correlogram of disease severity measured at 14, 21 and 28 dpi, DON content, percentage FDK and TKW. The relationship between these variables was determined using the correlation coefficients generated.

DON and FDK are considered primary traits as they both directly affect yield and economic value of grain. Low percentage FDK indicated better quantity grain regarding morphology and thousand kernel weight (TKW). Fusarium damaged kernels displayed a lower TKW than seed that were presumably healthy. However, no significant relationship was observed between FDK and TKW but only a low negative association.

Table 4.2. Statistical summary of Agrobase generated ANOVA output for yield parameters

Yield parameter	CV	R^2	H^2	Grand mean	LSD	S.E.D	p-value	t (2 sided)	MSE	Significance
Dry weight	20.72%	0.7817	0.504	6.374	2.3494	1.0783	0.0189	2.1788	1.74408	Significant
Floret number	8.18%	0.8277	0.664	56.714	8.258	3.7901	0.0023	2.1788	21.54762	Significant
Flower fertility	22.95%	0.5404	0.221	0.439	0.1793	0.0823	0.1716	2.1788	0.01015	Not significant
Grain number	19.87%	0.6875	0.448	25.619	9.0559	4.1563	0.0328	2.1788	25.9127	Significant
Grain weight	25.63%	0.7247	0.479	0.76	0.3467	0.1591	0.0243	2.1788	0.03798	Significant
Harvest index	33.78%	0.6725	0.474	0.139	0.0835	0.0383	0.0255	2.1788	0.0022	Significant
Seed width	8.43%	0.4414	0.131	2.614	0.3918	0.1798	0.2743	2.1788	0.0485	Not significant
Spike length	5.29%	0.8192	0.685	90.429	8.5155	3.9083	0.0016	2.1788	22.9127	Significant
Spike number	7.10%	0.6671	0.313	19.524	2.4655	1.1316	0.0965	2.1788	1.92063	Not significant
Tiller length	5.69%	0.6361	0.311	508.81	51.4626	23.6196	0.0974	2.1788	836.8254	Not significant
Tiller number	25.81%	0.708	0.554	4.857	2.2301	1.0235	0.0108	2.1788	1.57143	Significant
TKW	21.05%	0.551	0.277	28.952	10.8432	4.9767	0.1219	2.1788	37.15079	Not significant
Seed length	6.95%	0.6495	0.056	7.476	0.9241	0.4241	0.3802	2.1788	0.26984	Not significant
Seed area	11.40%	0.4723	0.091	15.048	3.0526	1.4011	0.3285	2.1788	2.94444	Not significant
Days to heading	0.00%	1	1	84.429	0	0	0	2.1788	0	Significant

Table 4.3. Statistical summary of ANOVA output for significant yield parameters after removing outliers. The yield parameters displayed significant differences between replicates.

Trait	CV	R2	H2	Grand mean	LSD	S.E.D	P value	t (2 sided)	MSE	Significance
Grain number	15.31%	0.7709	0.569	25.193	7.019	3.1502	0.0132	2.2281	14.8853	Significant
Harvest index	28.23%	0.803	0.586	0.142	0.076	0.0328	0.0179	2.306	0.00162	Significant
Tiller number	19.35%	0.8506	0.757	4.659	1.62	0.7359	0.0006	2.201	0.81241	Significant

4.4. Validation of the MS-MARS pre-breeding scheme

4.4.1. MS-MARS cycle 1 (2020)

The first MS-MARS cycle for this study was conducted from September to October 2020. The female population was represented by 360 entries generated from the previous MS-MARS cycle. The male population comprised of 320 wheat lines obtained from the SU-PBL's 2020 wheat nursery. Hybrid seed was sown across a total of 420 pots, with four seeds sown per pot. Donor material was planted across 320 pots, with four seeds sown per pot. Plant material was drip irrigated using nutrient solution. The female population was molecularly characterised for rust resistance genes. The male population was molecularly characterised for powdery mildew resistance genes, along with rust resistance genes and agronomic traits routinely screened at the SU-PBL. Selected tillers from both male and female populations were cut twice a week (Monday and Thursday) for eight consecutive weeks. Sixteen successful cross pollination sessions were completed, with each cutting session containing a range of 75-124 and 49-152 male and female tillers, respectively. A total of 790 male tillers was used to cross pollinate 842 female tillers, generating 1742 hybrid seed after successful cross pollination. The overall average cross pollination rate for the first MS-MARS cycle was 6.98%. The combined weight of the hybrid seed was 13.292 g, with a thousand kernel mass of 8.0605 g (**Table 4.6**).

4.4.2. MS-MARS cycle 2 (2021)

The second MS-MARS cycle in this study was conducted from June to August 2021. The female population was represented by 120 entries sourced from the F_1 segregating population generated after MS-MARS cycle 1 (2020). The male population comprised of 28 selected breeding lines from SU-PBL's 2020 wheat nursery and 5 selected breeding lines from the FHB CIMMYT nursery. The female population was molecularly characterised for rust resistance genes. The male population comprising of the FHB CIMMYT nursery was validated for

targeted FHB QTLs. Wheat tillers sourced from both male and female populations were cut twice a week (Monday and Thursday) for ten consecutive weeks. A total of 720 male donor tillers and 783 male sterile tillers were selected for cross pollination. The number of male fertile and male sterile tillers used during each crossing session ranged between 29 – 92 and 29 – 129 tillers, respectively. An average of 12.14% cross pollination was obtained. A total of 2059 hybrid seeds were harvested from 92.1% male sterile tillers used during cross pollination. The combined weight of the hybrid seed generated was 34.712 g, with an average thousand kernel mass of 21.239 g (**Table 4.7**).

4.4.3. Overall cross pollination for MS-MARS cycle 1 and 2

The overall average cross pollination percentage for MS-MARS cycle 1 and cycle 2 was 6.98% and 12.14%, respectively. Successful cross pollination increased by two-fold from the first cycle, yielding more hybrid seed. Although an increase was observed, the overall cross pollination percentage was still low. The purpose of the MS-MARS cycle was to facilitate successful cross pollination to maximise hybrid seed formation. Successful cross pollination is dependent on the receptivity of male sterile stigma and the shedding of viable pollen from the male donor. Wheat pollen only remains viable between 30 minutes to 3 hours after shedding. Depending on temperature and humidity, stigma was receptive between 6 – 13 days. Stigma receptivity needed to coincide with pollen shed for maximum seed development (Selva *et al.*, 2020). The low cross pollination observed could be a result of selecting tillers at the incorrect reproductive stage.

Floret structure is considerably important for successful cross pollination. A common morphological characteristic of male sterility were wide glumes, but this was not the case for all sterile tillers. Several sterile tillers with non-viable pollen had narrow glumes. During seed set it was observed that sterile tillers with wider glumes had a higher percentage cross pollination than sterile tillers with narrow glumes. Tillers with wider glumes and longer stigmatic hairs had better pollen reception than tillers with narrow glumes (Selva *et al.*, 2020). The distance between the donor lines and the male sterile tillers also determined the success of

cross pollination. Cross pollination was considerably higher when donor lines were stacked in closer proximity above the sterile tillers. Male tillers should therefore not be stacked too high above the male sterile tillers.

4.4.4. Heritability of dominant *Ms3* gene for MS-MARS cycle 1 and 2

The female population was harvested after tiller formation was complete and material was naturally dried. Male sterile and fertile tiller ratios were quantified for each pot across the planting benches. Chi-squared analysis was used to validate the heritability of the dominant male sterility (*Ms3*) gene. The data generated was analysed using chi-squared test to determine whether the dominant male-sterility gene segregated in the 1:1 ratio for male sterility and fertility. The goodness of fit to the 1:1 ratio was performed on the segregating populations used for MS-MARS cycle 1 and cycle 2. For MS-MARS cycle 1, the segregating population was planted across four benches. For MS-MARS cycle 2, the segregating population was planted across five benches. The chi-squared analysis was performed across each planting bench and the overall chi-squared analysis for the entire female population.

Chi-squared analysis for MS-MARS cycle 1 was calculated across four benches. The p-values obtained for each bench was greater than the critical value of 0.05 (**Table 4.4**). Bench 4 had a p-value of 1, displaying a perfect fit to the 1:1 segregating ratio. Based on the probability values obtained, all four benches displayed a good fit to the 1:1 ratio. The overall p value obtained for the female population was greater than the critical value of 0.05 (X^2 = 1.676; df = 1; p = 0.195), conforming to the 1:1 segregating ratio.

Chi-squared analysis for the MS-MARS cycle 2 was determined across five benches. The p values obtained for bench 2, 3 and 5 was greater than the critical value of 0.05 (**Table 4.5**). However, the p values for bench 1 and 4 was less than the critical value. The overall p value obtained for the female population was less than the critical value of 0.05 (X^2 = 20.164; df = 1; p < 0.001), deviating from the 1:1 segregating ratio.

Table 4.4. Inheritance of the dominant male sterility (*Ms3*) gene in the segregating population for MS-MARS cycle 1.

Bench number	Fertile	Sterile	X^2	Probability of fit to a 1:1 ratio
1	160	129	3.325	0.068
2	98	79	2.040	0.153
3	102	117	1.027	0.311
4	23	23	0.000	1.000
Overall	**383**	**348**	**1.676**	**0.195**

Table 4.5. Inheritance of the dominant male sterility (*Ms3*) gene in the segregating population for MS-MARS cycle 2.

Bench number	Fertile	Sterile	X^2	Probability of fit to 1:1 ratio
1	100	65	7.424	0.006
2	108	91	1.452	0.228
3	132	116	1.032	0.310
4	148	89	14.688	<0.001
5	137	115	1.921	0.166
Overall	**625**	**476**	**20.164**	**<0.001**

Deviation from goodness of fit to the 1:1 ratio observed for MS-MARS cycle 2, could be a result of incorrect phenotypic scoring of male sterile and male fertile tillers. The dominant male-sterility gene was highly thermo-sensitive and produced false negatives under high temperatures ranging between 31°C to 35°C. Extreme temperature conditions during anthesis may reduce the development of viable pollen in male fertile tillers leading to sterility (Santiago and Sharkey, 2019). The expression of sterility in the material was also affected by high temperatures leading to fertile anther development. This phenomenon is referred to as partial sterility observed when a plant has both sterile and fertile secondary tillers.

4.4.5. Molecular screening for dominant male sterility (*Ms3*) gene

The *Ms3* gene was located on the centromeric region of chromosome 5AS. A total of 360 entries were sampled to represent the female populations for the first MS-MARS cycle and 240 entries for the second cycle. The observed gene frequencies for *Ms3* during the first MS-MARS cycle was 44% (**Figure 4.20**). The observed gene frequency in the second cycle was 39%. The expected gene frequencies for *Ms3* in the segregating population was 50%. The

gene frequencies observed in the first MS-MARS cycle was relatively close to the expected gene frequency. However, the observed gene frequencies in the second MS-MARS cycle were significantly different than the expected gene frequency of 50%.

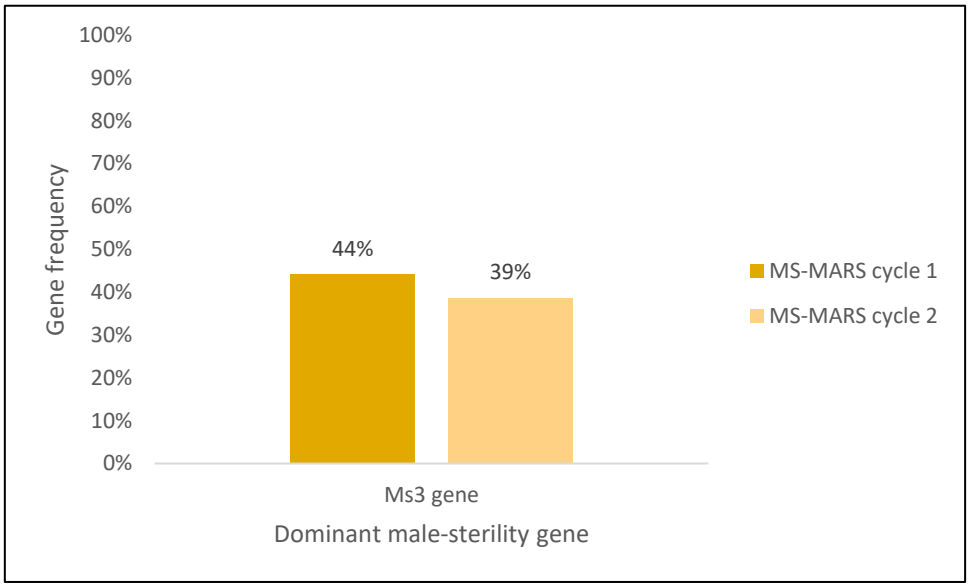

Figure 4.20. Gene frequencies of the dominant male-sterility (*Ms3*) gene in the segregating base population for MS-MARS cycle 1 and 2

Table 4.6. Cross pollination and hybrid seed production for MS-MARS cycle 1 (2020)

Crossing week	Male sterile	Male fertile	Possible combinations	Sterile seed harvested	Weight of seed per cross	Average % cross pollination	T.k.m (g)
1	49	90	4410	85	0.86	6.396	10.073
2	98	124	12152	310	2.493	10.465	8.041
3	138	110	15180	482	3.701	11.303	7.702
4	152	120	18240	383	2.61	8.084	7.351
5	142	101	14342	171	1.418	4.159	8.305
6	90	89	8010	123	0.932	5.196	7.354
7	93	81	7533	137	0.763	6.761	5.576
8	80	75	6000	51	0.515	3.456	10.082
Overall	**842**	**790**	**85867**	**1742**	**13.292**	**6.977**	**8.060**

Table 4.7. Cross pollination and hybrid seed production for MS-MARS cycle 2 (2021)

Crossing week	Male sterile	Male fertile	Possible combinations	Sterile plants sourced from	Sterile seed harvested	Weight of seed per cross	Average % cross pollination	T.k.m (g)
1	50	55	2750	49	5	0.196	0.496	37.083
2	71	71	5041	55	358	5.524	18.081	14.358
3	85	82	6970	83	76	1.746	3.195	15.587
4	129	84	10836	127	130	3.692	4.071	28.751
5	117	92	10764	116	97	1.808	3.465	27.911
6	106	85	9010	100	282	5.236	8.386	18.457
7	84	88	7392	61	122	1.901	5.956	21.991
8	58	69	4002	57	392	5.262	27.745	13.429
9	54	65	3510	52	497	7.411	35.786	15.461
10	29	29	841	29	100	1.936	14.266	19.360
Overall	**783**	**720**	**61116**	**729**	**2059**	**34.712**	**12.145**	**21.239**

Chapter 5. Conclusion

The aim of the study was to identify crossing parents to introduce into the male-sterility mediated marker-assisted recurrent selection (MS-MARS) pre-breeding programme. The SU-PBL's 2020 wheat nursery and FHB CIMMYT nursery used as male crossing parents were genotypically and phenotypically assessed for powdery mildew and fusarium head blight (FHB) resistance, respectively.

Microsatellite markers associated with powdery mildew resistance genes (*Pm37*, *Pm4b*, *MLAG12*, *MLUM15*) were identified from literature. The SSR marker *Xwmc790* associated with *Pm37* and *Xwmc346* associated with *MLAG12* was validated in this study. Co-dominant markers *Xwmc790* and *Xwmx346* could distinguish between resistant and susceptible lines. Moreover, the SSR marker *Xgwm332* associated with *Pm37*, the two flanking markers for *Pm4b*, *Xwmc273* associated with *MLAG12* and both flanking markers for *MLUM15* could not be validated in this study. The markers were unable to discriminate between resistant and susceptible lines.

Closely associated molecular markers were identified for novel stem rust resistance gene *Sr35*. The primer sequences for *Sr35* and *Sr45* were obtained from MASWheat database. The perfect dominant marker for *Sr35*, spanning across the genomic region of the gene, could not be validated through genotypic screening. Following several optimisation steps, the molecular marker failed to produce a single dominant band in the *Sr35* resistance donor line. The dominant marker was therefore not reproducible for utilisation in the laboratory. The female population could not be molecularly characterised for *Sr45*. Discrepancies occurred in PCR products amplified by *cssu45* used to flank *Sr45*. The desired fragment size of 220 bp failed to amplify in the *Sr45* resistant line. Instead, a fragment of 238bp was amplified in both resistant and susceptible lines.

The segregating base population was molecularly characterised for *Sr2* and *Lr34* prior to each MS-MARS cycle. The gene frequencies of both *Sr2* and *Lr34* decreased after the first crossing cycle. The male population used as crossing parents was the SU-PBL's 2020 rust nursery. This nursery was dominant for rust resistance. The decrease in gene frequency for *Sr2* was a response to its association with pseudo-black chaff. A trait undesired by plant breeders when expressed in fields. However, the decrease in gene frequency of *Lr34* by 12% was

unexpected, considering the gene was positively selected. The observed decrease in *Lr34* in the base population was a consequence of underrepresenting the base population. Only 11% of the base population was molecularly characterised for the rust genes. The remaining 89% of the population remained unaccounted for, potentially possessing the *Lr34* gene.

Twenty-eight selected genotypes from the SU-PBL's 2020 wheat nursery were phenotypically assessed for powdery mildew resistance. The genotypes were inoculated with isolates representing the general *Bgt* population obtained in Vergenoegd, Stellenbosch. The positive control "Steenbras" performed significantly better than the negative control "Morocco". "Steenbras" displayed no visible infection at 6 days post inoculation (dpi) with one-two pustules at 11, 14 dpi. "Morocco" displayed 100 % coverage at 6 dpi. The positive control "Steenbras" had inherent powdery mildew resistance, obtained from a crossing parent "Siete-Cerros-66". According to literature, "Siete-Cerros-66" had the *Pm5* gene pattern, specifically the *Pm5b* gene. Five genotypes displayed a disease response similar to "Steenbras" ranging from resistant to moderately resistant. Given the nature of the *Bgt* isolates used to evaluate disease response, the resistant phenotypes could be conferred by the *Pm5* gene pattern and additional unknown *Pm* genes. Genotypes with a resistant disease response displayed a positive association with SSR marker *Xwmc346* used to flank the temporary designated gene *MLAG12*.

Five genotypes from an FHB CIMMYT nursery were phenotypically assessed for type II FHB resistance, yield parameters and mycotoxin content. Disease severity recorded at 14 dpi was relatively low across all genotypes but rapidly increased at 21 dpi and 28 dpi in highly susceptible wheat lines. Two genotypes "5450" and "5297" displayed a resistant disease response similar to the positive control "Sumai3", with a disease severity less than 10%. Further evaluation was conducted to assess disease progression and the presence of closely linked FHB QTLs. Wheat line "5297" amplified *Qhfs.ifa-5A* primarily associated with type I resistance but also with type II resistance. Deoxynivalenol was the only detected mycotoxin in evaluated genotypes. Wheat lines "5450" and "5297" produced the lowest levels of DON content and minimal FDK. Wheat line "5450" also produced the largest quantity of grain per spike, following FHB infection.

Male sterile tillers were selected from the base population and cross-pollinated by donor tillers from the male population. The overall cross pollination percentage for MS-MARS cycle 1 and 2

was 6.98% and 12.14%, respectively. Although an increase was observed, the overall cross pollination percentage was considerably low. The low cross pollination observed was a result of selecting sterile tillers at the incorrect reproductive stage. Stigma receptivity of sterile tillers needed to coincide of viable pollen shed for maximum cross pollination. This was not satisfied, as increased temperatures in the greenhouse influenced the expression of male sterility and pollen shed. An additional contributing factor was the glume morphology of the selected sterile tillers. Cross pollination was higher for sterile tillers with wider glumes than with narrow glumes. Majority of the sterile tillers used expressed narrow glume morphology. The height of which the donor tillers were placed above the sterile tillers also played a role in the success of cross pollination. Cross pollination was considerably higher when donor tillers were stacked closer to the sterile tillers.

The inheritance of male sterility in the base population was validated using chi-squared analysis. The base population for the first crossing cycle segregated in a 1:1 ratio for male sterility and fertility. The *Ms3* gene therefore, expressed dominant inheritance in MS-MARS cycle 1. The base population for the second cycle deviated from the 1:1 ratio for male sterility and fertility. The dominant inheritance of the *Ms3* gene was therefore, not validated for MS-MARS cycle 2. Male sterile tillers were underrepresented for the second MS-MARS cycle. Deviation from goodness of fit to the 1:1 ratio observed for MS-MARS cycle 2, was a result of mistaking male sterile tillers for male fertile tillers. The *Ms3* gene was highly thermos-sensitive and was unstable under extreme temperature conditions, leading to partial sterility. Male sterile tillers with partial sterility were scored as male fertile tillers.

The aim of the study and subsequent objectives were satisfied. Five genotypes with resistance to powdery mildew were identified and molecularly characterised using diagnostic markers. Two superior genotypes with FHB resistance were identified. The two FHB genotypes were selected based on low recorded disease severity, low levels of DON content and minimal FDK.

Future studies should include additional molecular and phenotypic characterisation of the FHB CIMMYT nursery. Sample size and number of replicates should be increased to enhance the accuracy of the data generated. It should also include active powdery mildew resistance

breeding. Due to the expected change in climatic conditions worldwide, an increased risk of powdery mildew outbreaks is expected for South Africa. Extensive breeding for powdery mildew disease resistance through the deployment of several viable genes would reduce this threat.

References

Acquaah, G. (2012) 'Breeding Selected Crops', in *Principles of Plant Genetics and Breeding*, pp. 575–575. doi: 10.1002/9781118313718.part9.

Agenbag, G. M. *et al.* (2012) 'Identification of adult plant resistance to stripe rust in the wheat cultivar Cappelle-Desprez', *Theoretical and Applied Genetics*, 125(1), pp. 109–120. doi: 10.1007/s00122-012-1819-5.

Asseng, S. *et al.* (2017) 'Hot spots of wheat yield decline with rising temperatures', *Global Change Biology*, 23(6), pp. 2464–2472. doi: 10.1111/gcb.13530.

Beukes, I. *et al.* (2017) 'Mycotoxigenic Fusarium species associated with grain crops in South Africa-A review', *South African Journal of Science*. doi: 10.17159/sajs.2017/20160121.

Bhavani, S. *et al.* (2019) 'Progress in breeding for resistance to Ug99 and other races of the stem rust fungus in CIMMYT wheat germplasm', *Frontiers of Agricultural Science and Engineering*, 6(3), pp. 210–224. doi: 10.15302/J-FASE-2019268.

Boutigny, A. L. *et al.* (2011) 'Analysis of the Fusarium graminearum species complex from wheat, barley and maize in South Africa provides evidence of species-specific differences in host preference', *Fungal Genetics and Biology*, 48(9), pp. 914–920. doi: 10.1016/j.fgb.2011.05.005.

Brown, N. A. *et al.* (2010) 'The infection biology of Fusarium graminearum: Defining the pathways of spikelet to spikelet colonisation in wheat ears', *Fungal Biology*, 114(7), pp. 555–571. doi: 10.1016/j.funbio.2010.04.006.

Bryła, M. *et al.* (2018) 'Modified fusarium mycotoxins in cereals and their products—Metabolism, occurrence, and toxicity: An updated review', *Molecules*, 23(4), pp. 1–34. doi: 10.3390/molecules23040963.

Buerstmayr, H. *et al.* (2003) 'Molecular mapping of QTLs for Fusarium head blight resistance in spring wheat. II. Resistance to fungal penetration and spread', *Theoretical and Applied Genetics*, 107(3), pp. 503–508. doi: 10.1007/s00122-003-1272-6.

Buerstmayr, H., Ban, T. and Anderson, J. A. (2009) 'QTL mapping and marker-assisted selection for Fusarium head blight resistance in wheat: A review', *Plant Breeding*, 128(1), pp. 1–26. doi: 10.1111/j.1439-0523.2008.01550.x.

Caglayan, M. O., Şahin, S. and Üstündağ, Z. (2022) 'Detection Strategies of Zearalenone for Food Safety: A Review', *Critical Reviews in Analytical Chemistry*, 52(2), pp. 294–313. doi: 10.1080/10408347.2020.1797468.

Choulet, F. *et al.* (2014) 'Structural and functional partitioning of bread wheat chromosome 3B', *Science (New York, N.Y.)*, 345(6194), p. 1249721. Available at: http://www.sciencemag.org/content/345/6194/1250092.abstract.

Clavijo, B. J. *et al.* (2017) 'An improved assembly and annotation of the allohexaploid wheat genome identifies complete families of agronomic genes and provides genomic evidence for chromosomal translocations', *Genome Research*, 27(5), pp. 885–896. doi: 10.1101/gr.217117.116.

Cromey, M. G. *et al.* (2001) 'Control of Fusarium head blight of wheat with fungicides', *Australasian Plant Pathology*, 30(4), pp. 301–308. doi: 10.1071/AP01065.

Dean, R. *et al.* (2012) 'The Top 10 fungal pathogens in molecular plant pathology', *Molecular Plant Pathology*. doi: 10.1111/j.1364-3703.2011.00783.x.

Delventhal, R. *et al.* (2016) 'Inoculation of Rice with Different Pathogens: Sheath Blight (Rhizoctonia solani), Damping off Disease (Pythium graminicola) and Barley Powdery Mildew (Blumeria graminis f. sp. hordei)', *Bio-Protocol*, 6(24), pp. 1–7. doi: 10.21769/bioprotoc.2070.

Doyle, J. J. and Doyle, J. L. (1987) 'Doyle_plantDNAextractCTAB_1987.pdf', *Phytochemical Bulletin*, pp. 11–15. Available at: https://webpages.uncc.edu/~jweller2/pages/BINF8350f2011/BINF8350_Readings/Doyle_plantDNAextractCTAB_1987.pdf.

Dweba, C. C. *et al.* (2017) 'Fusarium head blight of wheat: Pathogenesis and control strategies', *Crop Protection*. doi: 10.1016/j.cropro.2016.10.002.

Emara, H. M. *et al.* (2016) 'Identification of Pm24, Pm35 and Pm37 in thirteen Egyptian bread wheat cultivars using SSR markers', *Ciência e Agrotecnologia*, 40(3), pp. 279–287. doi: 10.1590/1413-70542016403036315.

Esterhuizen, D. (2022) 'Report Name : Grain and Feed Annual', *United States Department of Agriculture*, pp. 1–22.

FAO (2022) *Food Outlook*, *Global information and early warning system on food and agriculture*. Available at: http://www.fao.org/docrep/013/al969e/al969e00.pdf.

FAOSTAT (2022) *World Food and Agriculture – Statistical Yearbook 2021*, *World Food and Agriculture – Statistical Yearbook 2021*. FAO. doi: 10.4060/cb4477en.

Figlan, S. *et al.* (2020) 'Breeding Wheat for Durable Leaf Rust Resistance in Southern Africa: Variability, Distribution, Current Control Strategies, Challenges and Future Prospects', *Frontiers in Plant Science*, 11, pp. 1–12. doi: 10.3389/fpls.2020.00549.

Figueroa, M., Dodds, P. N. and Henningsen, E. C. (2020) 'Evolution of virulence in rust fungi — multiple solutions to one problem', *Current Opinion in Plant Biology*, 56, pp. 20–27. doi: 10.1016/j.pbi.2020.02.007.

Figueroa, M., Hammond-Kosack, K. E. and Solomon, P. S. (2018) 'A review of wheat diseases—a field perspective', *Molecular Plant Pathology*, 19(6), pp. 1523–1536. doi: 10.1111/mpp.12618.

Gilbert, J. and Tekauz, A. (2000) 'Review: Recent developments in research on fusarium head blight of wheat in Canada', *Canadian Journal of Plant Pathology*, 22(1), pp. 1–8. doi: 10.1080/07060660009501155.

Guttieri, M. J. (2020) 'Ms3 dominant genetic male sterility for wheat improvement with molecular breeding', *Crop Science*, 60(3), pp. 1362–1372. doi: 10.1002/csc2.20091.

Hasan, N. *et al.* (2021) 'Recent advancements in molecular marker-assisted selection and applications in plant breeding programmes', *Journal of Genetic Engineering and Biotechnology*, 19(1), pp. 1–26. doi: 10.1186/s43141-021-00231-1.

Hatta, M. A. M. *et al.* (2021) 'The wheat Sr22, Sr33, Sr35 and Sr45 genes confer resistance against stem rust in barley', *Plant Biotechnology Journal*, 19(2), pp. 273–284. doi: 10.1111/pbi.13460.

Hickey, L. T. *et al.* (2019) 'Breeding crops to feed 10 billion', *Nature Biotechnology*, 37(7), pp. 744–754. doi: 10.1038/s41587-019-0152-9.

Hyles, J. *et al.* (2020) 'Phenology and related traits for wheat adaptation', *Heredity*, 125(6), pp. 417–430. doi: 10.1038/s41437-020-0320-1.

Jamil, S. *et al.* (2020) 'Role of Genetics, Genomics, and Breeding Approaches to Combat Stripe Rust of Wheat', *Frontiers in Nutrition*, 7, pp. 1–12. doi: 10.3389/fnut.2020.580715.

Jankovics, T. *et al.* (2015) 'New insights into the life cycle of the wheat powdery mildew: Direct observation of ascosporic infection in Blumeria graminis f. sp. tritici', *Phytopathology*, 105(6), pp. 797–804. doi: 10.1094/PHYTO-10-14-0268-R.

Jha, U. C., Bohra, A. and Singh, N. P. (2014) 'Heat stress in crop plants: Its nature, impacts and integrated breeding strategies to improve heat tolerance', *Plant Breeding*, 133(6), pp. 679–701. doi: 10.1111/pbr.12217.

Joshi, R. K. and Nayak, S. (2010) 'Gene pyramiding-A broad spectrum technique for developing durable stress resistance in crops', 5(August), pp. 51–60.

Kang, Y. *et al.* (2020) 'Mechanisms of powdery mildew resistance of wheat – a review of molecular breeding', *Plant Pathology*, 69(4), pp. 601–617. doi: 10.1111/ppa.13166.

Khaneghah, A. M. *et al.* (2018) 'Deoxynivalenol and its masked forms: Characteristics, incidence, control and fate during wheat and wheat based products processing - A review', *Trends in Food Science and Technology*, 71, pp. 13–24. doi: 10.1016/j.tifs.2017.10.012.

Kloppe, T. *et al.* (2022) 'Virulence of Blumeria graminis f. sp. tritici in Brazil, South Africa, Turkey, Russia, and Australia', *Frontiers in Plant Science*, 13, pp. 1–15. doi: 10.3389/fpls.2022.954958.

Kolmer, J. (2013) 'Leaf rust of wheat: Pathogen biology, variation and host resistance', *Forests*, 4(1), pp. 70–84. doi: 10.3390/f4010070.

Leath, S. (1990) 'Identification of Powdery Mildew Resistance Genes in Cultivars of Soft Red Winter Wheat', *Plant Disease*, p. 747. doi: 10.1094/pd-74-0747.

Levy, A. A. and Feldman, M. (2022) 'Evolution and origin of bread wheat', *The Plant Cell*, pp. 2549–2567. doi: 10.1093/plcell/koac130.

Li, F. *et al.* (2019) 'Emergence of the Ug99 lineage of the wheat stem rust pathogen through somatic hybridisation', *Nature Communications*, 10(1). doi: 10.1038/s41467-019-12927-7.

Lutz, J. *et al.* (1992) 'Identification of Powdery Mildew Resistance Genes in Common Wheat (Triticum aestivum L.): I. Czechoslovakian Cultivars', *Plant Breeding*, 108(1), pp. 33–39. doi: 10.1111/j.1439-0523.1992.tb00097.x.

Ma, L. J. *et al.* (2013) 'Fusarium pathogenomics', *Annual Review of Microbiology*, 67, pp. 399–416. doi: 10.1146/annurev-micro-092412-155650.

Malbrán, I. *et al.* (2014) 'Toxigenic capacity and trichothecene production by Fusarium graminearum isolates from Argentina and their relationship with aggressiveness and fungal expansion in the wheat spike', *Phytopathology*, 104(4), pp. 357–364. doi: 10.1094/PHYTO-06-13-0172-R.

Marais, G. F., Botes, W. C. and Louw, J. H. (2000a) 'Recurrent selection using male sterility and hydroponic tiller culture in pedigree breeding of wheat', *Plant Breeding*. doi: 10.1046/j.1439-0523.2000.00529.x.

Marais, G. F., Botes, W. C. and Louw, J. H. (2000b) 'Recurrent selection using male sterility and hydroponic tiller culture in pedigree breeding of wheat', *Plant Breeding*, 119(5), pp. 440–442. doi: 10.1046/j.1439-0523.2000.00529.x.

Maree, G. J. *et al.* (2019) 'Phenotyping Kariega × Avocet S doubled haploid lines containing individual and combined adult plant stripe rust resistance loci', *Plant Pathology*, 68(4), pp. 659–668. doi: 10.1111/ppa.12985.

Matsuoka, Y. (2011) 'Evolution of polyploid triticum wheats under cultivation: The role of domestication, natural hybridization and allopolyploid speciation in their diversification', *Plant and*

Cell Physiology, 52(5), pp. 750–764. doi: 10.1093/pcp/pcr018.

Maxwell, J. J. *et al.* (2009) 'MlAG12: A Triticum timopheevii-derived powdery mildew resistance gene in common wheat on chromosome 7AL', *Theoretical and Applied Genetics*, 119(8), pp. 1489–1495. doi: 10.1007/s00122-009-1150-y.

Moore, J. W. *et al.* (2015) 'A recently evolved hexose transporter variant confers resistance to multiple pathogens in wheat', *Nature Genetics*, 47(12), pp. 1494–1498. doi: 10.1038/ng.3439.

Nhemachena, C. R. and Kirsten, J. (2017) 'A historical assessment of sources and uses of wheat varietal innovations in South Africa', *South African Journal of Science*, 113(3–4), pp. 1–8. doi: 10.17159/sajs.2017/20160008.

Olivera Firpo, P. D. *et al.* (2017) 'Characterization of Puccinia graminis f. sp. tritici isolates derived from an unusual wheat stem rust outbreak in Germany in 2013', *Plant Pathology*, 66(8), pp. 1258–1266. doi: 10.1111/ppa.12674.

Ortiz, D. *et al.* (2022) 'The stem rust effector protein AvrSr50 escapes Sr50 recognition by a substitution in a single surface-exposed residue', *New Phytologist*, 234(2), pp. 592–606. doi: 10.1111/nph.18011.

Osborne, L. E. and Stein, J. M. (2007) 'Epidemiology of Fusarium head blight on small-grain cereals', *International Journal of Food Microbiology*, 119(1–2), pp. 103–108. doi: 10.1016/j.ijfoodmicro.2007.07.032.

Palazzini, J. M., Torres, A. M. and Chulze, S. N. (2018) 'Tolerance of triazole-based fungicides by biocontrol agents used to control Fusarium head blight in wheat in Argentina', *Letters in Applied Microbiology*, 66(5), pp. 434–438. doi: 10.1111/lam.12869.

Paul, P. A. *et al.* (2018) 'Meta-Analysis of the Effects of QoI and DMI Fungicide Combinations on Fusarium Head Blight and Deoxynivalenol in Wheat', *Plant Disease*, 102(12), pp. 2602–2615. doi: 10.1094/pdis-02-18-0211-re.

Paux, E. *et al.* (2008) 'A physical map of the 1-gigabase bread wheat chromosome 3B', *Science*, 322(5898), pp. 101–104. doi: 10.1126/science.1161847.

Periyannan, S. *et al.* (2014) 'Identification of a robust molecular marker for the detection of the stem rust resistance gene Sr45 in common wheat', *Theoretical and Applied Genetics*, 127(4), pp. 947–955. doi: 10.1007/s00122-014-2270-6.

Perugini, L. D. *et al.* (2008) 'Pm37, a new broadly effective powdery mildew resistance gene from Triticum timopheevii', *Theoretical and Applied Genetics*, 116(3), pp. 417–425. doi: 10.1007/s00122-007-0679-x.

Pestka, J. J. (2007) 'Deoxynivalenol: Toxicity, mechanisms and animal health risks', *Animal Feed Science and Technology*, 137(3–4), pp. 283–298. doi: 10.1016/j.anifeedsci.2007.06.006.

Pietrusińska, A. and Tratwal, A. (2020) 'Characteristics of powdery mildew and its importance for wheat grown in Poland', *Plant Protection Science*, 56(3), pp. 141–153. doi: 10.17221/99/2019-PPS.

Pretorius, Z. A. *et al.* (2020) 'Accomplishments in wheat rust research in South Africa', *South African Journal of Science*, 116(11–12), pp. 1–8. doi: 10.17159/sajs.2020/7688.

Qadir, T. *et al.* (2019) 'Wheat Production Under Changing Climate: Consequences of Environmental Vulnerabilities on Different Abiotic and Biotic Stresses', *Journal of Global Innovations in Agricultural and Social Sciences*, 7(1), pp. 7–17. doi: 10.22194/jgiass/7.842.

Rai, A., Das, M. and Tripathi, A. (2020) 'Occurrence and toxicity of a fusarium mycotoxin, zearalenone', *Critical Reviews in Food Science and Nutrition*, 60(16), pp. 2710–2729. doi: 10.1080/10408398.2019.1655388.

Reifschneider, F. J. B., Boiteux, L. S. and Brasilia, U. De (1988) 'A Vacuum-Operated Settling Tower for Inoculation of Powdery Mildew Fungi Francisco', *Phytopathology*, 78(11), pp. 1463–1465.

Reynolds, M. P. and Braun, H.-J. (2022) *Wheat Improvement*, *Wheat Improvement*. doi: 10.1007/978-3-030-90673-3_1.

Rhoda, R. (2018) 'Improving wheat grain yield by employing an integrated biotechnology approach', *Master's dissertation, Stellenbosch Univeristy*, (March).

Röder, M. S. *et al.* (1998) 'A microsatellite map of wheat', *Genetics*, 149(4), pp. 2007–2023. doi: 10.1093/genetics/149.4.2007.

Rutkoski, J. E., Krause, M. R. and Sorrells, M. E. (2022) 'Breeding Methods: Population Improvement and Selection Methods', *Wheat Improvement*, pp. 83–96. doi: 10.1007/978-3-030-90673-3_6.

Rychlik, M. *et al.* (2014) 'Proposal of a comprehensive definition of modified and other forms of mycotoxins including "masked" mycotoxins', *Mycotoxin Research*, 30(4), pp. 197–205. doi: 10.1007/s12550-014-0203-5.

SAGIS (2021) 'Crop Estimates Committee Oesskattingskomitee', *agriculture, forestry & fisheries*, (C), pp. 2–4.

Saintenac, C. *et al.* (2013) 'Identification of wheat gene Sr35 that confers resistance to Ug99 stem rust race group', *Science*, 341(6147), pp. 783–786. doi: 10.1126/science.1239022.

Salcedo, A. *et al.* (2017) 'Variation in the AvrSr35 gene determines Sr35 resistance against wheat stem rust race Ug99', *Science*, 358(6370), pp. 1604–1606. doi: 10.1126/science.aao7294.

Santiago, J. P. and Sharkey, T. D. (2019) 'Pollen development at high temperature and role of carbon and nitrogen metabolites', *Plant Cell and Environment*, 42(10), pp. 2759–2775. doi: 10.1111/pce.13576.

Sapkota, S. *et al.* (2019) 'Genetic mapping of a major gene for leaf rust resistance in soft red winter wheat cultivar AGS 2000', *Molecular Breeding*, 39(1). doi: 10.1007/s11032-018-0909-8.

Schaarschmidt, S. and Fauhl-Hassek, C. (2018) 'The Fate of Mycotoxins During the Processing of Wheat for Human Consumption', *Comprehensive Reviews in Food Science and Food Safety*, 17(3), pp. 556–593. doi: 10.1111/1541-4337.12338.

Schiro, G. *et al.* (2018) 'Alternaria and fusarium fungi: Differences in distribution and spore deposition in a topographically heterogeneous wheat field', *Journal of Fungi*, 4(2). doi: 10.3390/jof4020063.

Selva, C. *et al.* (2020) 'Hybrid breeding in wheat: How shaping floral biology can offer new perspectives', *Functional Plant Biology*, 47(8), pp. 675–694. doi: 10.1071/FP19372.

Shi, X. and Ling, H. Q. (2018) 'Current advances in genome sequencing of common wheat and its ancestral species', *Crop Journal*, 6(1), pp. 15–21. doi: 10.1016/j.cj.2017.11.001.

Shude, S. P. N., Yobo, K. S. and Mbili, N. C. (2020) 'Progress in the management of Fusarium head blight of wheat: An overview', *South African Journal of Science*, 116(11–12), pp. 1–7. doi: 10.17159/sajs.2020/7854.

Singh, R. P. *et al.* (2015) 'Emergence and spread of new races of wheat stem rust fungus: Continued threat to food security and prospects of genetic control', *Phytopathology*, 105(7), pp. 872–884.

doi: 10.1094/PHYTO-01-15-0030-FI.

Springfield, L. (2014) 'Pyramiding of rust resistance genes in wheat utilizing male sterility mediated marker-assisted recurrent selection', *Master's dissertation, Stellenbosch Univeristy*, (December).

Steuernagel, B. *et al.* (2016) 'Rapid cloning of disease-resistance genes in plants using mutagenesis and sequence capture', *Nature Biotechnology*, 34(6), pp. 652–655. doi: 10.1038/nbt.3543.

Sukumaran, S. *et al.* (2022) 'Pre-breeding Strategies', *Wheat Improvement*, pp. 451–469.

Tadesse, W., Bishaw, Z. and Assefa, S. (2019) 'Wheat production and breeding in Sub-Saharan Africa: Challenges and opportunities in the face of climate change', *International Journal of Climate Change Strategies and Management*, 11(5), pp. 696–715. doi: 10.1108/IJCCSM-02-2018-0015.

Trail, F. (2009) 'For blighted waves of grain: Fusarium graminearum in the postgenomics era', *Plant Physiology*, 149(1), pp. 103–110. doi: 10.1104/pp.108.129684.

Van Coller, G. J. *et al.* (2022) 'The distribution and type B trichothecene chemotype of Fusarium species associated with head blight of wheat in South Africa during 2008 and 2009', *PLoS ONE*, 17(9), pp. 1–22. doi: 10.1371/journal.pone.0275084.

Wessels, E. and Botes, W. C. (2014) 'Accelerating resistance breeding in wheat by integrating marker-assisted selection and doubled haploid technology', *South African Journal of Plant and Soil*, 31(1), pp. 35–43. doi: 10.1080/02571862.2014.903434.

Worthington, M. *et al.* (2014) 'MlUM15: An Aegilops neglecta-derived powdery mildew resistance gene in common wheat', *Crop Science*, 54(4), pp. 1397–1406. doi: 10.2135/cropsci2013.09.0634.

Wu, P. *et al.* (2018) 'Development of molecular markers linked to powdery mildew resistance gene Pm4b by combining SNP discovery from transcriptome sequencing data with bulked segregant analysis (BSR-Seq) in wheat', *Frontiers in Plant Science*, 9, pp. 1–12. doi: 10.3389/fpls.2018.00095.

Xue, A. G. *et al.* (2021) 'Virulence structure of Blumeria graminis f. sp. tritici, the causal agent of wheat powdery mildew, in Ontario, Canada, in 2018 and 2019', *Canadian Journal of Plant Pathology*, 43(6), pp. 803–811. doi: 10.1080/07060661.2021.1915876.

Zeng, F. S. *et al.* (2017) 'Transcriptome analyses shed new insights into primary metabolism and regulation of Blumeria graminis f. sp. tritici during conidiation', *Frontiers in Plant Science*, 8, pp. 1–17. doi: 10.3389/fpls.2017.01146.

Zhu, T. *et al.* (2021) 'Optical maps refine the bread wheat Triticum aestivum cv. Chinese Spring genome assembly', *Plant Journal*, 107(1), pp. 303–314. doi: 10.1111/tpj.15289.

Zimin, A. V. *et al.* (2017) 'The first near-complete assembly of the hexaploid bread wheat genome, Triticum aestivum', *GigaScience*, 6(11), pp. 1–7. doi: 10.1093/gigascience/gix097.

Zingales, V., Fernández-Franzón, M. and Ruiz, M. J. (2021) 'Occurrence, mitigation and in vitro cytotoxicity of nivalenol, a type B trichothecene mycotoxin – Updates from the last decade (2010–2020)', *Food and Chemical Toxicology*, 152, p. 112182. doi: 10.1016/j.fct.2021.112182.